Chapter 2

FLUID INTERFACES AND CAPILLARITY

A. Fluid interfaces: Young's Membrane Model

1. *The thinness of interfaces*

Fluid-fluid interfaces are a good place to start because they are far simpler to describe than fluid-solid or solid-solid interfaces. The molecular mobility in fluids makes it reasonable to assume that they will be in internal mechanical and diffusional equilibrium. Thus when the composition and the required number of thermodynamic state variables are set, the system is uniquely defined. In solids, non-equilibrium structures are frozen in place over time scales of practical interest. Fluid interfaces are smooth (as opposed to generally rough), morphologically and energetically homogeneous (as opposed to heterogeneous) and free of all internal shear stresses when at rest (as opposed to supporting un-relaxed internal stresses). Consider first the simplest case of all, *viz.*, the interface between a pure liquid (water) and its equilibrium vapor at 20°C. The pressure is then the vapor pressure of water at 20°C, *i.e.,* 2.33 kPa.

As noted earlier, the interface is not a mathematical discontinuity, but rather a thin stratum of material whose intensive properties vary across it from those of the liquid phase to those of the gas phase, as suggested in Fig. 1-1. In going from the liquid phase to the gas phase in the present case, the density decreases by a factor of approximately 58,000!

It is known that, except when one is very near to the critical point, the stratum of inhomogeneity at a liquid surface is very very thin, usually of the order of a few Ångströms. The abruptness is verifiable from experimental observations of the nature of light reflected from a surface. In accord with Fresnel's Laws of reflection,[1] if the transition between a gas and a medium of refractive index n (> 1) is abrupt (*i.e.*, thickness << wavelength of light), the reflected light will be completely plane polarized when the angle of incidence is equal to $\tan^{-1}n$ (called the *polarizing angle* or Brewster's angle).[2] (An important technique for studying the structure of interfaces

---

[1] Jenkins, F. A., and White, H. E., **Fundamentals of Optics**, 3rd Ed., pp. 509ff, McGraw-Hill Co., NY, 1957.

[2] Hennon, S., and Meunier, J., *Rev. Sci. Inst.*, **62**, 936 (1991);
Hennon, S., and Meunier, *Thin Solid Films*, **234**(1-2), 471 (1993);
Hönig, D., and Möbius, D., *J. Phys. Chem.*, **95**, 4590 (1991);
Hönig, D., and Möbius, D., *Thin Solid Films*, **210, 211**, 64 (1993).

examines them when illuminated by laser light at precisely Brewster's angle ("Brewster angle microscopy" or BAM). It is the polarization of reflected light that makes it possible for sunglasses or Polaroid filters, polarized vertically, to block glare from horizontal surfaces. If the density transition through the interface is more gradual, the reflected light is *elliptically polarized*. Light reflected from most smooth solid surfaces and unclean liquid surfaces show at least some "ellipticity." Lord Rayleigh showed,[3] however, that when liquid surfaces are swept clean (by a technique to be described later), light reflected from them at Brewster's angle indeed shows virtually no ellipticity whatsoever. One monolayer of "foreign" molecules at the surface can measurably change this, and the technique of "ellipsometry"[4] (in which the extent of ellipticity is measured) is used to study the thickness and optical properties of material at surfaces.

The abruptness of a clean interface is also supported by statistical mechanical calculations, which have provided quasi-theoretical pictures of the density profile across the interfacial layer in simple systems. An example is shown in Fig. 2-1, showing density profiles for noble gases computed for various reduced temperatures. It reveals that gas-liquid interfacial layers for

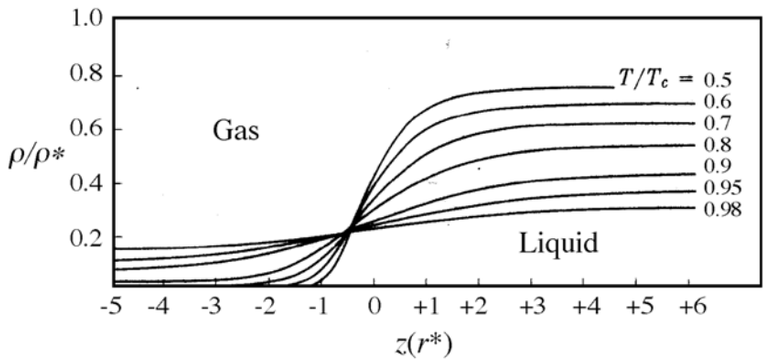

Fig. 2-1: Density profiles across the interfacial layer computed for noble gases at various reduced temperatures, T/T_c, where T_c = critical temperature. r^* is the molecular radius, and ρ^* is the maximum packing density. The point of $z = 0$ is arbitrary. After [Hill, T. L., **Introduction to Statistical Thermodynamics**, Addison-Wesley Publ., Reading, MA, 1960, p. 318.]

such systems (and by inference, for other gas-liquid systems) have thicknesses of the order of molecular dimensions, except very near to their critical points (where $T \rightarrow T_c$, and the distinction between the phases vanishes), where the interfacial layer becomes thicker and eventually envelops the entire system. Partially miscible liquid-liquid systems may also exhibit critical points. A critical solution point occurs at the temperature just below (or just above) which two liquid phases coexist. Liquid-liquid systems may have an upper critical solution temperature (UCST), a lower critical

---

[3] Lord Rayleigh (J. W. Strutt), *Phil. Mag.*, **33**, 1 (1892).

[4] Tompkins, Harlan G., **A User's Guide to Ellipsometry**, Academic Press, Boston, 1993.

solution temperature (LCST) or both. The thinness of either the gas-liquid or liquid-liquid interfacial layer (at least that associated with clean interfaces removed from their critical points) allows it to be treated, for purposes of macroscopic mechanical modeling, as a *membrane of zero thickness*.

2. *Definition of surface tension*

Everyday experience reveals that a fluid interface wants to contract in order to assume a minimum area, subject to whatever external forces or constraints are put upon it. For example, a mass of liquid undistorted by gravity, such as an oil drop of density equal to water suspended in water, or an air-filled soap bubble in air, assumes the shape of a sphere to produce the minimum area/volume. The contractile tendency of fluid interfaces can be quantified with reference to the zero-thickness-membrane model in terms of a "surface tension" or "interfacial tension" (σ) of the membrane, defined with reference to Fig. 2-2. Consider a point P on a small patch of surface (membrane). We can consider the state of tension at point P by imagining the patch to be divided into two parts by line MM′ passing through P and regarding each as a "free body." One such body exerts a pull on the other

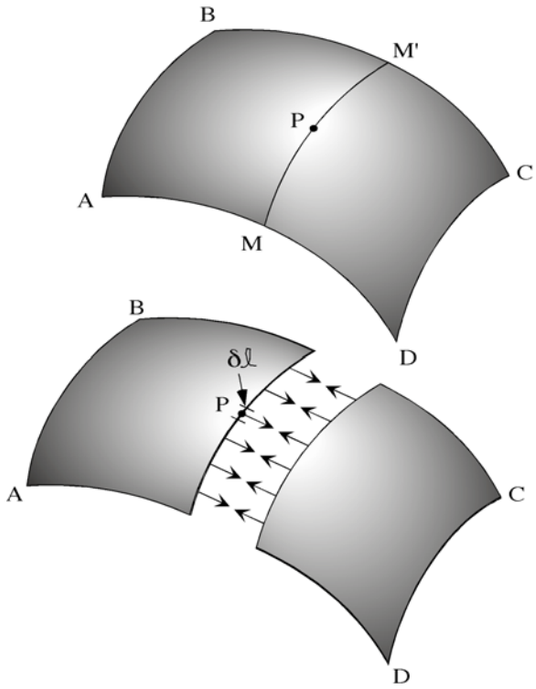

Fig. 2-2: Mechanical definition of surface or interfacial tension.

across the line MM′. The |force|/length along this line at P is the surface tension at P, *i.e.*, $d\boldsymbol{F} = \sigma\, d\ell$ or $\sigma = d\boldsymbol{F}/d\ell$, a scalar quantity with units of force/length. "σ" is the notation used for surface tension in this text, but it is also common to see the symbol "γ" used for it. For all fluid systems this force/length at P has the same value (at P) regardless of how MM′ is drawn, *i.e.* the system is *isotropic* with respect to its surface tension. Also, for uniform composition, isothermal surfaces, the surface tension is uniform. The macroscopic mechanical model of a fluid interface is thus a zero-

thickness membrane in uniform, isotropic tension, σ. This is "Young's membrane model" (after Thomas Young, who first described fluid interfaces in this way in 1805).[5] The units of surface tension, force/length, are the same as those of energy (or work) per unit area, so that surface tension can also be interpreted as the mechanical energy required to create unit new area of a *liquid* surface. (The surfaces of solids require additional considerations.)

Consideration of the *thermodynamics* of capillary systems (examined later in Chap. 3) leads to another definition of surface tension, *viz.*, $\sigma = (\partial F/\partial A)_{T,V,\mathrm{eq}}$, where F is the Helmholtz free energy of the system, A is the surface area, and the subscript "eq" refers to full internal equilibrium. If the *mechanical* definition of σ restricts itself to conditions of constant T,V and internal equilibrium, the two definitions are equivalent. It is useful for present purposes to think in terms of the mechanical model of the fluid interface and the mechanical definition of the surface or interfacial tension.

B. The surface tension of liquids

1. *Pure liquids*

Surface or interfacial tension values are usually expressed in either cgs units (dynes/cm or erg/cm^2) or SI units (mN/m or mJ/m^2). The numerical values are the same in either system, and they range from near zero to as high as nearly 2000. Literature values for the surface tension of pure liquids[6] are plentiful and usually reliable, although they are often given for only one temperature. Some specific values for pure liquids against their equilibrium vapor are shown in Table 2-1. The lowest values are those for liquefied gases. Most organic liquids (at or below their atmospheric boiling points) are in the range of 20-40 mN/m, while water has a value at 20°C of about 73 mN/m.

Essentially the only liquids having surface tensions substantially below 20 mN/m at room temperature are the lower molecular weight silicone oils and the fluorocarbons. Highest are values for molten salts and metals, being generally several hundred mN/m. The surface tensions of pure liquids are assumed to apply to liquids in contact with their equilibrium vapor when in fact, they are more often measured for the liquid against air at atmospheric pressure. The difference in surface tension between the two cases is generally negligible,[7] however, and even though it is not strictly correct to do so, we assume surface tensions of pure liquids against air to be functions of temperature only.

---

[5] Young, T., *Phil. Trans. Roy. Soc. (London)*, **95**, 55 (1805).

[6] a large database is given by: J. J. Jasper, *J. Phys. Chem. Ref. Data*, **1**, 841-1008 (1972).

[7] Defay, R., Prigogine, I., Bellemans, A., and Everett, D. H., **Surface Tension and Adsorption**, pp. 88-89, Longmans, London, 1966.

Table 2-1: Surface tension values for various liquids

Liquid	T (°C)	Surface Tension (mN/m)
Helium	-272	0.16
Hydrogen	-254	2.4
Perfluoropentane	20	9.9
Oxygen	-183	13.2
Silicone (HMDS)	25	15.9
n-Heptane	20	20.3
Ethanol	20	22.0
Benzene	20	28.9
Olive oil	18	33.1
Ammonia	-33	34.1
Nitric acid	21	41.1
Glycerol	20	63.4
Methylene iodide	20	67.0
Water	20	72.7
Sodium chloride	801	114.
Lithium	181	394.
Zinc	360	877.
Iron	1530	1700.

2. *Temperature dependence of surface tension*

The surface tension of all pure liquids decreases with temperature and goes to zero as their respective critical points are approached. Over modest ranges of temperature, the decrease is nearly linear for most liquids, as suggested by the data of Fig. 2-3, and the coefficient, $d\sigma/dT$, is approximately -0.1 mN/m-°K for most cases. This rule of thumb may be used for rough extrapolation of surface tension values in the absence of any further data. Jasper's extensive data collection provides linear expressions of the form: $\sigma = a - bT$ for many liquids. Many semi-empirical relationships have been proposed for the dependence of surface tension on temperature, one of the oldest of which is the Eötvös Law,[8]

$$\sigma v^{2/3} = \mathrm{k_E}(T_\mathrm{c} - T)\,, \tag{2.1}$$

where v is the molar volume of the liquid at the temperature of interest, T; T_c is the critical temperature, and k_E is the "Eötvös constant," equal approximately to 2.5 erg/°K (0.25 mJ/°K) for apolar, non-associating liquids (although there are many exceptions). The term $\sigma v^{2/3}$ corresponds to a molar surface free energy of the liquid, seen to decrease linearly with the approach to the critical temperature. A second semi-empirical law, based on the

[8] Eötvös, R., *Wied. Ann.*, **27**, 456 (1886).

principle of corresponding states, and valid for apolar, non-associating liquids, is that due to van der Waals (1894)[9] and Guggenheim (1945)[10] *viz.*

$$\sigma = \sigma^* \left(1 - \frac{T}{T_c}\right)^{11/9} \quad . \tag{2.2}$$

σ^* is a "characteristic surface tension," given initially in terms of the critical properties of the liquid as $\sigma^* = 4.4(T_c / v_c^{2/3})$ [=] mN/m, with T_c [=] °K and v_c the critical molar volume [=] cm^3/mol. The exponent of 11/9 in Eq. (2.2) reproduces the slight upward concavity of the σ-T curves for apolar

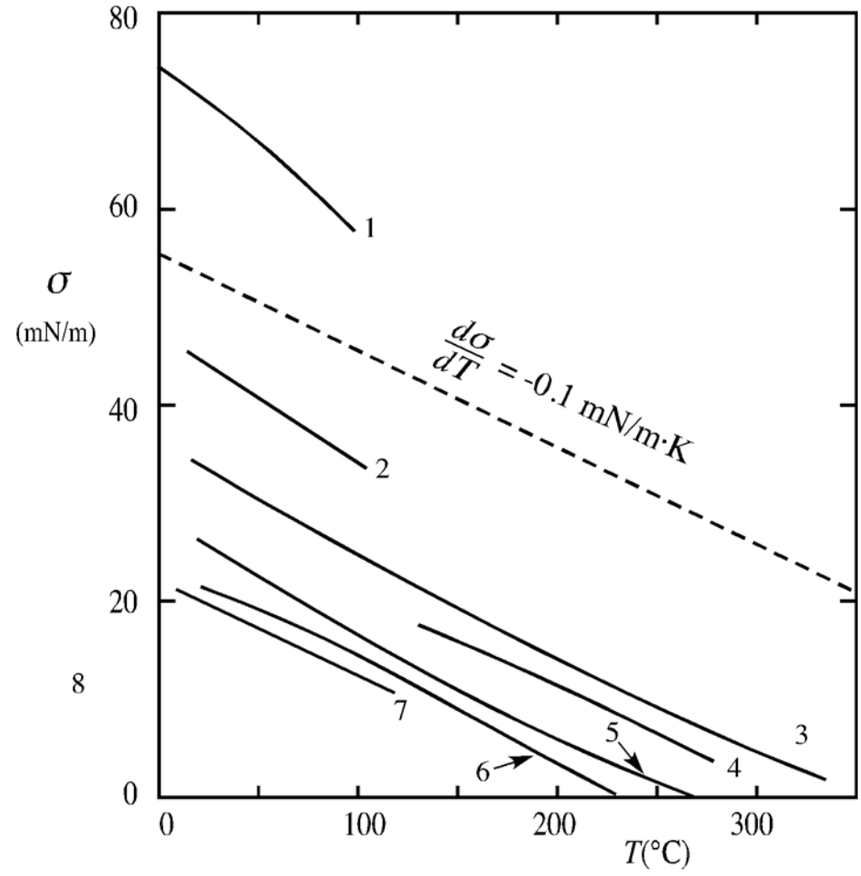

Fig. 2-3: Surface tension dependence on temperature for a variety of liquids: (1) water, (2) furfural, (3) chlorobenzene, (4) acetic acid, (5) carbon tetrachloride, (6) ethanol, (7) *n*-octane. Dashed line has slope: -0.1 mN/m·K, in reasonable agreement with that for most liquids.

liquids, and its format is excellent for generally good for interpolating σ(T) data for such systems. The equation has been much refined yielding more elaborate expressions for σ^*, usually involving a third parameter obtained

[9] van der Waals, J. D., *Z. Phys. Chem.,* **13,** 716 (1894).
[10] Guggenheim, E. A., *J. Chem. Phys.,* **13**, 253 (1945).

from vapor pressure data.[11] It has also been extended to include polar or self-associating liquids, but this requires more general expressions for the exponent as well.

3. *Surface tension of solutions*

The surface tension of solutions depends on both temperature and composition. Some representative data for binary systems at 20°C are shown in Fig. 2-4, and an extensive bibliography for binary solutions has been compiled by McClure *et al.*[12] A more nearly complete discussion of the surface tension dependence on composition must await the discussion of capillary thermodynamics, but the figure suggests a few generalizations:

i) The surface tension of binary solutions is usually intermediate to those of the pure components, but less than the mole-fraction-average value. Some systems show extrema (minima or maxima) at intermediate values of the composition. The pronounced maximum in the water-sulfuric system is thought to be associated with the formation of the hydration complex: $H_2SO_4 \cdot 4H_2O$.

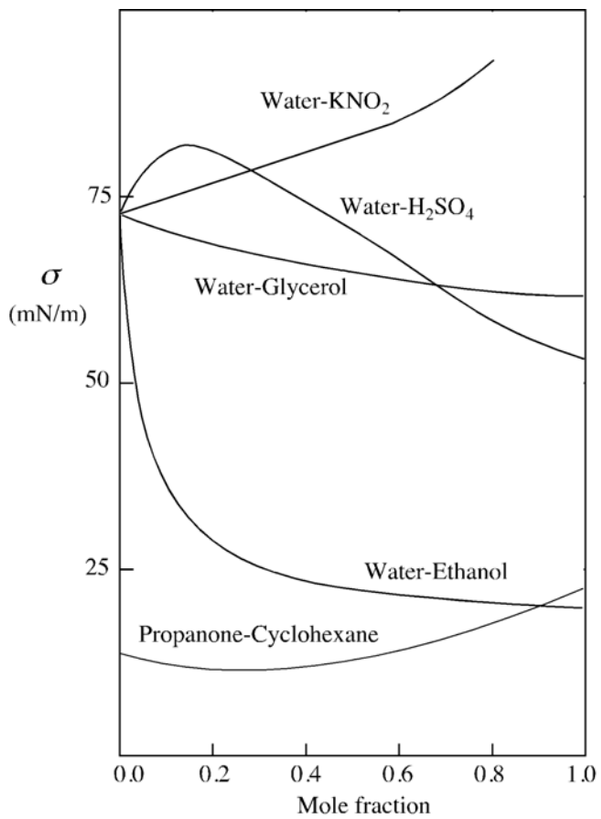

Fig. 2-4: Surface tension dependence on composition for several binary solutions at 20°C.

---

[11] Reid, R.C., Prausnitz, J.M., and Sherwood, T.K., **The Properties of Gases and Liquids**, 3rd Ed., Chap. 12, McGraw-Hill, New York, 1977.

[12] McClure, I. A., Pegg, I. A., and Soares, V. A. M., "A Bibliography of Gas-Liquid Surface Tensions for Binary Liquid Mixtures," in **Colloid Science (A Specialist Periodical Report)**, Vol. 4, D. H. Everett (Ed.), The Royal Society of Chemistry, London, 1983.

ii) The surface tension of water is increased approximately linearly by dissolved salts, although the increases are small for low concentrations.

iii) The surface tension of water is usually decreased sharply by organic solutes.

The surface tension of water may be reduced *very* sharply at low concentrations of certain solutes (termed "surface active agents" or "surfactants") as shown in Fig. 2-5. These will be discussed in more detail later. To classify as a surface active agent, a solute must generally reduce the surface tension of water by 30 mN/m or more at a concentration of 0.01M or less. Although "surface activity" may also be identified in non-aqueous media, the reductions in surface tension involved are generally much less.

Certain surfactants are but vanishingly soluble in water, as well as being nonvolatile, and monomolecular films of these compounds at the water-air interface represent an important class of systems. Their surface activity may be represented by plots of surface tension against *surface* concentration, Γ, [=] moles/cm^2, or more conveniently μmole/m^2, as shown in Fig. 2-5(b). Surfactant solutions have a monomolecular layer at the surface that is highly enriched in the solute (called an "adsorbed" or "Gibbs" monolayer), whereas insoluble surfactants form such a monolayer (called a "spread" or "Langmuir" monolayer) by direct spreading of the surfactant at

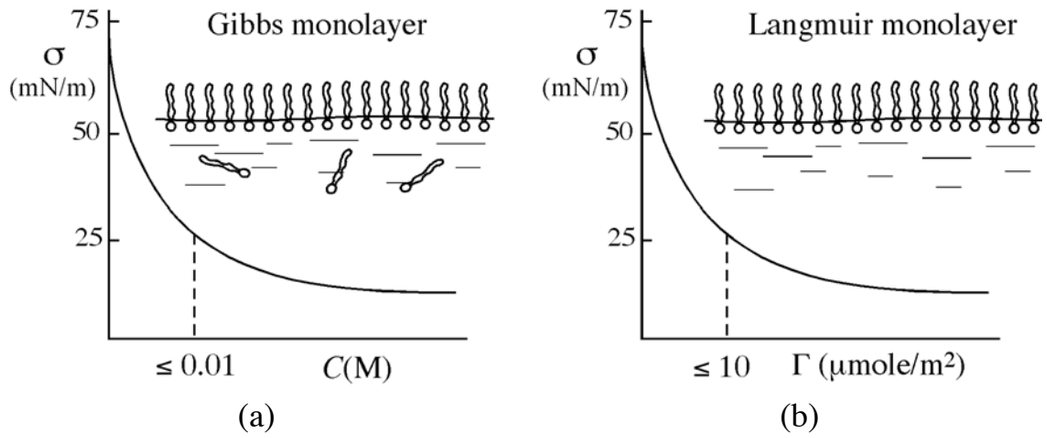

Fig. 2-5: Surface tension dependence on composition for surfactant monolayers (a) adsorbed or "Gibbs monolayer," or (b) spread or insoluble "Langmuir monolayer." Insert shows schematic of surfactant monolayer for either case.

the surface. In either case, the surfactant molecules consist of segregated hydrophilic and hydrophobic portions which orient themselves at the interface with their hydrophilic portions dissolved in the water and their hydrophobic portions directed outward, as shown. One of the most powerful of all insoluble surfactants is that which lines the moist inner lining of the *alveoli* of the mammalian lung. This surfactant mixture is primarily dipalmitoyl lecithin (DPL), pictured in Fig. 2-6. It consists of a glycerol molecule with an adjacent pair of its hydroxyl groups esterified with

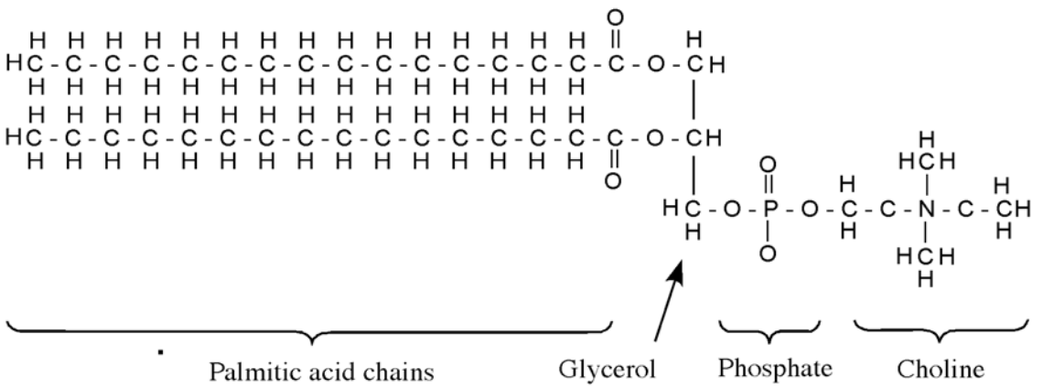

Fig. 2-6: Stylized diagram of a lung surfactant molecule: L-a, dipalmitoyl lecithin.

palmitic (C_{15}) acid, and the remaining group with phosphoric acid. The opposite hydrogen atom of the phosphoric acid is substituted with a choline group. A monolayer of these molecules is capable, upon compression, of reducing the tension of water to less than one mN/m.

C. Intermolecular forces and the origin of surface tension

1. *Van der Waals forces*

The existence of surface tension, and all of its manifestations, derives ultimately from the forces that exist between molecules.[13] These may be purely physical in nature or they may involve chemical complexation (association), such as that due to hydrogen bonding. If liquid metals are involved, metallic bonding exists, in which a cationic matrix of metal atoms is held together in part by a "sea" of free (conductance) electrons. Media containing ions introduce net electrostatic (Coulombic) interactions.

The purely physical interactions between neutral molecules are referred to as "van der Waals interactions." One type is that which exists between permanent molecular charge distributions, such as dipoles or quadrupoles. The interaction is obtained through vectorial summation of the Coulombic interactions between the various charge centers of the molecules, and is mutual-orientation dependent. Boltzmann-averaging over all possible mutual orientations of a pair of permanent dipoles yields the result (due to Keesom) for the potential energy of interaction Φ as a function of their distance of separation, r:

$$\Phi_{\text{dip-dip}} = -\frac{B_{\text{polar}}}{r^6}, \tag{2.3}$$

where B_{polar} varies as the square of the dipole moments of the molecules and inversely with the dielectric constant, ε, and with absolute temperature. The

[13] A comprehensive account is given by: Israelachvili, J. N., **Intermolecular and Surface Forces**, 2nd Ed., Academic Press, London, 1991.

potential function Φ is defined as the reversible work required to bring the two molecules, initially at infinite separation, to a distance r from one another.

A second type of van der Waals interaction results when a molecule with a permanent dipole induces a dipole in a neighboring molecule, with which it then interacts. The resulting pair interaction energy function (due to Debye) takes the form:

$$\Phi_{\text{ind}} = -\frac{B_{\text{ind}}}{r^6}, \tag{2.4}$$

where B_{ind} depends on the permanent dipole moment of the first molecule and the molecular polarizability of the second molecule. Of course both molecules may possess permanent dipoles so that two such terms may be involved.

A final type of van der Waals force results from the oscillations of the electron clouds of all molecules, which produce strong *temporary* dipole moments. These induce strong temporary dipole moments in neighboring molecules with which they then interact in accord with the relationship (due to London):

$$\Phi_{\text{disp}} = -\frac{B_{\text{disp}}}{r^6}, \tag{2.5}$$

where B_{disp} depends on the ground-state energies of the molecular oscillations, which in turn are closely proportional to the first ionization potentials of the molecules and their molecular polarizabilities.[14] (The close analogy of the effects described by London to that of light impinging on a medium has led to their being termed "dispersion" interactions, and hence the notation above.) For the interaction between a molecule i and a molecule j, to good approximation:

$$B_{\text{disp(ij)}} \approx \frac{3}{2}\alpha_{\text{i}}\alpha_{\text{j}}\left(\frac{I_{\text{i}}I_{\text{j}}}{I_{\text{i}} + I_{\text{j}}}\right) \approx \frac{3}{4}\alpha_{\text{i}}\alpha_{\text{j}}I = \sqrt{B_{\text{ii}}B_{\text{jj}}}, \tag{2.6}$$

where I_{i} and I_{j}, and α_{i} and α_{j} are the first ionization potentials and the molecular polarizabilities of molecules i and j, respectively. The second approximate equality derives from the fact that the first ionization potentials seldom differ by more than a factor of two between molecules, so that it is

---

[14] It should be appreciated that this is a simplified picture. Attractive interactions may also arise from other than the ground state oscillation frequencies, as well as from fluctuating quadrupole and higher multipole interactions. Also, as the distance between molecules increases, the induced molecular oscillations become increasingly out of phase with the inducing oscillations, due to the finite speed of electromagnetic radiation. This effect, called *retardation*, generally begins at separations of about 50 nm or so, and by 100 nm the interaction energy approaches a $-1/r^7$ dependence. Retardation will be addressed again in the discussion of interactions between colloid particles in Chap. 7.

generally reasonable to put $I_i \approx I_j = I$. This gives the important result, used later, that *when dispersion forces predominate*, the interaction between unlike molecules is given by the geometric mean of the interactions between the like molecules (Berthelot's Principle).

An important observation related to the Φ-functions for all the principal van der Waals interactions is that they vary as $1/r^6$, so that they may be combined to give:

$$\Phi_{vdW} = -\frac{B_{vdW}}{r^6}. \tag{2.7}$$

The content of B_{vdW} is discussed with somewhat more sophistication in Chap. 7. The above relationship holds only so long as the electron clouds of the interacting molecules do not overlap. Under such conditions, strong repulsive forces arise. While the exact functional form of the r-dependence of these repulsive interactions has not been established, they are known to be very steep and can reasonably be represented by:

$$\Phi_{rep} = \frac{B_{rep}}{r^{12}}. \tag{2.8}$$

The net (or total) physical interaction between a pair of molecules is given by the sum of the van der Waals and repulsive interactions, and takes the form shown in Fig. 2-7.

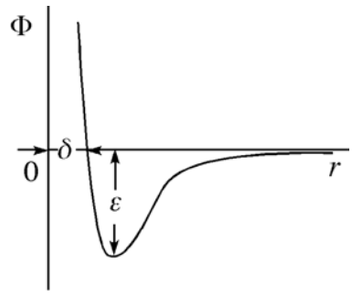

Fig. 2-7: Schematic of Lennard-Jones potential function.

Defining δ as the distance of separation for which $\Phi = 0$ (representative of the molecular diameter) and ε as the depth of the "potential well," Lennard-Jones derived expressions for B_{vdW} and B_{rep} leading to what is now termed the "Lennard-Jones potential:"

$$\Phi = 4\varepsilon\left[\left(\frac{\delta}{r}\right)^{12} - \left(\frac{\delta}{r}\right)^{6}\right]. \tag{2.9}$$

Its application is restricted to approximately spherical, apolar or weakly polar molecules.

The *attractive force* of interaction between two molecules is the slope of the potential energy function, *viz.*

$$F_{\text{att}} = \frac{d\Phi}{dr} = -\frac{24\varepsilon}{r}\left[2\left(\frac{\delta}{r}\right)^{12} - \left(\frac{\delta}{r}\right)^{6}\right]. \qquad (2.10)$$

Both Φ and F_{att} are shown in Fig. 2-8, computed for carbon tetrachloride (for which δ = 5.881 Å, and ε = 4.514 x 10^{-14} erg).[15] It is to be noted that at the average distance of molecular separation in the gas at standard conditions, both Φ and the intermolecular force are effectively zero. In the liquid, due to thermal motion, the average molecular separation lies not at the potential minimum, but just to the right of it, and the attractive intermolecular force at this point has a finite positive value.

The intermolecular forces and energies associated with chemical complexation, such as hydrogen bonding, require essentially direct molecular contact, and are thus shorter-ranged than attractive van der Waals forces. They are not generally represented in terms of an r-dependence, but it is clear that such dependence would be very steep and would produce a deep potential energy minimum. Metallic "bonding" is very strong at close range, and ionic interaction energies are both very strong and long-ranged, varying as $1/r$, as compared with $1/r^6$ for van der Waals energies.

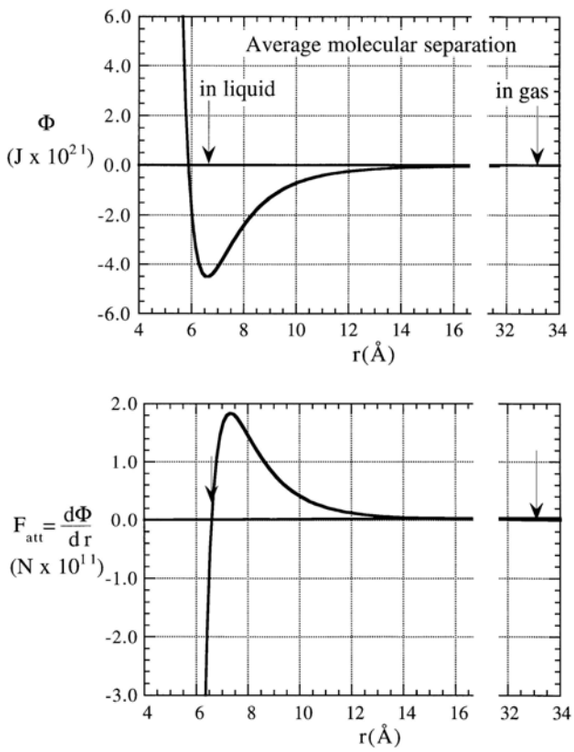

Fig. 2-8: Pair interaction curves for CCl_4.

[15] Bird, R. B., Stewart, W. E., and Lightfoot, E. N., **Transport Phenomena**, 2nd Ed., p. 865, Wiley, New York, 2007.

2. *Surface tension as "unbalanced" intermolecular forces; the Hamaker constant*

Surface tension may be interpreted directly in terms of intermolecular forces. The simplest picture, suggested by Fig. 2-9, contrasts the intermolecular forces acting on a molecule at the surface of a liquid with those acting on a molecule in the interior. The latter is acted upon equally in all

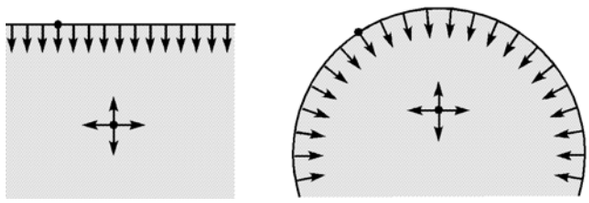

Fig. 2-9: Unbalanced intermolecular forces on molecules at a liquid surface.

directions, while a molecule at the surface experiences intermolecular forces directed only inward towards the interior. The net inward attraction tends to draw surface molecules toward the interior, causing the surface to seek minimum area (subject to whatever additional forces and constraints act on the system). The stronger the intermolecular attractions are, the greater the expected surface tension. This may be made somewhat more quantitative as follows.

Consider a body of liquid conceptually divided into an upper and a lower half extending to infinity away from the imaginary interface dividing them. We may compute the total energy of interaction between the molecules above the interface with those beneath it, on a per unit area basis. If the two liquid half-spaces were conceptually separated (to infinity), the work required to do so can be identified with (the negative of) this energy, and may be equated to twice the energy/area of the new surface created, *i.e.*, 2σ, because two new interfaces would be produced by the process. Begin by considering the interaction of a single molecule in the upper layer a distance D above the interface with the lower layer, as shown in Fig. 2-10. First we compute the energy of the molecule's interaction with a ring of diameter x of molecules in the lower half-space a vertical distance z away from it. The volume of the ring is $2\pi x dx dz$; and the number of molecules in it is $\rho_{\mathrm{m}} 2\pi x dx dz$, all a distance $r = \sqrt{x^2 + z^2}$ from the subject molecule in the upper half-space. ρ_{m} here is the *molecular* density. The energy of interaction between the subject molecule and the entire ring, assuming a van der Waals fluid, Eq. (2.7), and pairwise additivity of the molecular interactions, is $-\frac{B_{\mathrm{vdW}}}{r^6} \cdot \rho_{\mathrm{m}} 2\pi x dx dz = -2\pi B_{\mathrm{vdW}} \rho_{\mathrm{m}} \frac{x dx dz}{\left(x^2 + z^2\right)^3}$. Integration then gives the interaction between that molecule and the entire lower half-space:

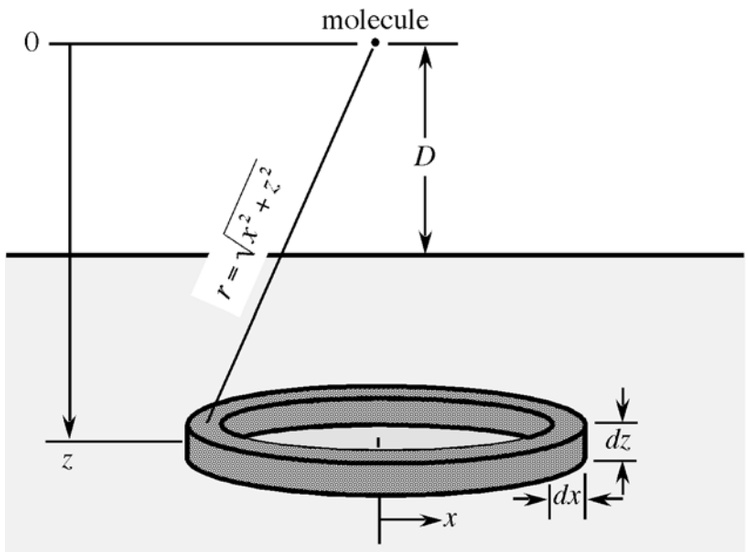

Fig. 2-10: Computation of the interaction of a single molecule with a semi-infinite half-space of the same molecules.

$$\Phi_{\text{molec-half-space}} = -2\pi B_{\text{vdW}}\rho_{\text{m}} \int_D^\infty dz \int_0^\infty \frac{x}{(x^2+z^2)^3}\,dx \qquad \left(\text{inner integral} = 1/4z^4\right)$$

$$= -\frac{\pi}{2} B_{\text{vdW}}\rho_{\text{m}} \int_D^\infty \frac{1}{z^4}\,dz = -\frac{\pi B_{\text{vdW}}\rho_{\text{m}}}{6D^3}. \qquad \left(\text{outer integral} = 1/3D^3\right) \tag{2.11}$$

Next we compute the interaction of a thin sheet (of thickness dD and unit area) of molecules in the upper half space at a distance D from the interface with the lower half-space. The number of molecules in this thin sheet of unit area is $\rho_{\text{m}}dD$, so the interaction of the sheet with the lower half-space is $-\frac{\pi B_{\text{vdW}}\rho_{\text{m}}^2 \text{d}D}{6D^3}$, and the total interaction energy of a unit area (signified by the superscript $^{\sigma}$) of infinite depth[16] with the lower half-space is

$$\Phi^{\sigma} = -\frac{\pi B_{\text{vdW}}\rho_{\text{m}}^2}{6} \int_{D_0}^\infty \frac{dD}{D^3} = -\frac{\pi B_{\text{vdW}}\rho_{\text{m}}^2}{12D_0^2}, \tag{2.12}$$

where D_0 is the closest distance of molecular approach. It is common to put

$$(\pi\rho_{\text{m}})^2 B_{\text{vdW}} = A, \tag{2.13}$$

[16] A simplification is made here in that the effects of "retardation" are neglected.

where A is called the Hamaker constant,[17] embodying the integrated molecular interactions. This is discussed in more detail in Chap. 7. Then

$$\sigma = -\frac{1}{2}\Phi^{\sigma} = \frac{A}{24\pi D_0^2}. \tag{2.14}$$

D_0 may be estimated from the molecular size and packing density in the liquid and is usually of the order of 1-2 Å. The accepted value of D_0 is 1.65 Å.[18] The important point that has been demonstrated here, however, is the direct relationship between the surface tension and the strength of the intermolecular interactions in the liquid.

3. *Pressure deficit in the interfacial layer; Bakker's Equation*

A somewhat different picture focuses upon intermolecular forces within the zone of inhomogeneity that constitutes the interfacial layer. Consider a pure liquid at rest in the absence of external force fields and facing its own vapor across the interfacial layer, and divided into two parts by a plane AB drawn normal to the interface,[19] as shown in Fig. 2-11. One may consider the forces acting across the plane AB by one part on the other. Out in the bulk of each phase, the forces acting on the plane are those of the hydrostatic pressure, which, in the absence of flow in the bulk material and external force fields such as gravity, is uniform and isotropic. In general, the net pressure force exerted on a plane drawn in the fluid depends on the following two factors:

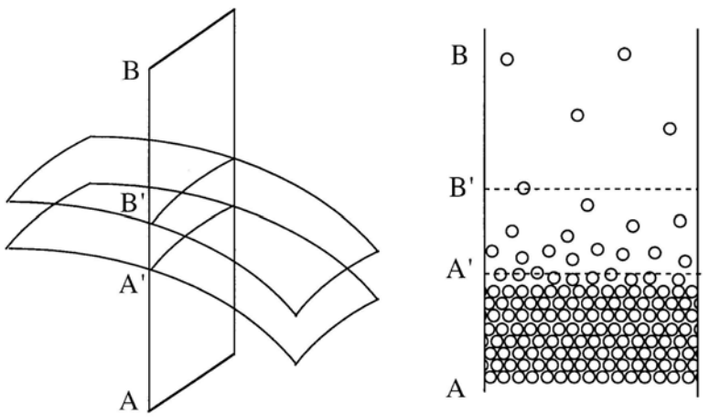

Fig. 2-11: Molecular interpretation of surface tension.

1) The kinetic energy (thermal agitation) of the molecules: Pressure is manifest at the (real or conceptual) confining boundaries of the phase through the change in momentum of the molecules colliding with them, per

---

[17] Hamaker, H. C., *Physica*, **4**, 1058 (1937), who was one of the first to perform such integrations.

[18] Israelachvili, J. N., **Intermolecular & Surface Forces**, 2nd Ed., p. 203, Academic Press, London, 1991.

[19] "Normal to the interface" is defined as the direction of the density gradient, $\nabla\rho$.

unit area, and this pressure is transmitted throughout the bulk of the phase. This is the only factor at play in ideal gases.

2) Configurational potential energy, due to intermolecular forces: This is expressed as the sum of interaction energies between pairs of molecules, per unit area of the conceptual interface between them, and is a function of the distance of their separation, as shown in the preceding paragraphs. The *forces* between the molecules are generally attractive and thus *subtract* from the pressure effect that would be attributable to thermal agitation alone.

Out in the bulk phases on either side of the interfacial layer, the net effect of these two contributions is a pressure that is uniform (neglecting external field effects) and isotropic. As detailed below, this condition does *not* exist within the interfacial layer, between A′ and B′ in Fig. 2-11.

Since density is presumed to vary continuously from that of the liquid to that of the gas as one moves upward through the interfacial layer, intermediate molecular separations are forced to exist, and for these, the lateral attractive forces will be much greater than they are in either the bulk liquid or gas. This is suggested by Fig. 2-8, in which it is seen that the forces between molecules at the average spacing in either bulk liquids or gases are quite small relative to those at intermediate spacings. Thus the net local pressure forces in the lateral direction, p_T, *i.e.*, the difference between the pressure forces due to thermal motion and those due to the attractive intermolecular forces, are substantially reduced in the interfacial region relative to the bulk regions, as shown schematically in Fig. 2-12. They may even become negative, producing a net local tension. The lateral pressure component becoming negative, however, is not a requirement for the occurrence of surface tension; merely the reduction in the pressure component is sufficient.

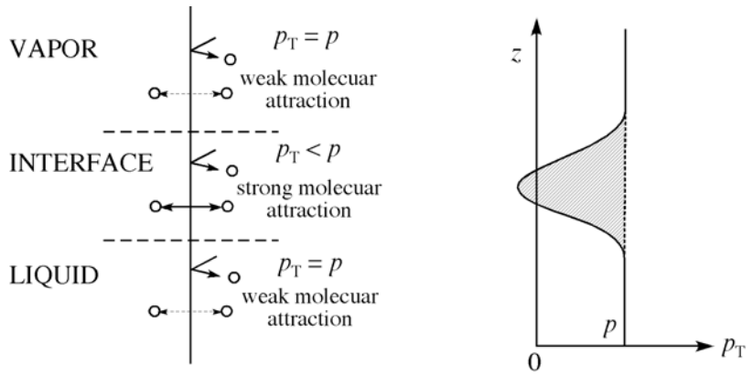

Fig. 2-12: Deficit in the tangential component of pressure in the interfacial layer.

One can be more specific about the “pressure” quantities being discussed. In general the state of (compressive) stress in a fluid is given by the tensor $\underline{\underline{p}}$. In a bulk fluid at rest this tensor reduces to

$$\underline{\underline{p}} = \begin{bmatrix} p & 0 & 0 \\ 0 & p & 0 \\ 0 & 0 & p \end{bmatrix}. \tag{2.15}$$

The off-diagonal elements must be zero because they represent shear stresses, which a fluid cannot support in equilibrium at rest. The three normal components of stress must furthermore be equal since a bulk fluid phase (in the absence of external force fields) is uniform in all intensive variables. One can still balance the forces even when the pressure components are different, *i.e.*, if the requirement of isotropy is relaxed, so that

$$\underline{\underline{p}} = \begin{bmatrix} p_{xx} & 0 & 0 \\ 0 & p_{yy} & 0 \\ 0 & 0 & p_{zz} \end{bmatrix}, \tag{2.16}$$

with $p_{xx} \neq p_{yy} \neq p_{zz}$. In the interfacial layer, these pressure components *will* be different, as full isotropy with respect to the pressure can no longer exist. In particular, one must have two different pressure components, one normal and one tangential to the interface, $p_N(z)$ and $p_T(z)$, respectively. Mechanical stability requires that the gradient of the pressure tensor be everywhere equal to zero[20], and symmetry requires isotropy in the plane tangent to the surface ("lateral" or "transverse" isotropy) so that $p_{xx}(z) = p_{yy}(z) = p_T(z)$, where z is the coordinate normal to the surface. The pressure component normal to the surface is $p_{zz}(z) = p_N(z) \neq p_T(z)$. The pressure component being discussed in terms of intermolecular forces is p_T.

Knowledge of the pressure tensor across the interfacial layer (which can be expressed only to the extent that one has detailed knowledge of the intermolecular potential functions and the molecular distribution functions) and application of Young's membrane model thus permits, in principle, a computation of the surface tension. The result is:

$$\sigma = \int_{z_a}^{z_b} (p_N - p_T) \mathrm{d}z, \tag{2.17}$$

where z is the coordinate normal to the interface, and the gap $z_a \Leftrightarrow z_b$ defines the region of molecular inhomogeneity constituting the interfacial layer. If the interface is flat, $p_N(z) = p$ = constant, and one may replace the finite limits with $\pm\infty$, since the regions outside the zone $z_a \Leftrightarrow z_b$ contribute nothing to the integral:

$$\sigma^{\text{flat surf.}} = \int_{-\infty}^{+\infty} (p - p_T) \mathrm{d}z. \tag{2.18}$$

---

[20] Ono, S., and Kondo, S., "Molecular Theory of Surface Tension in Liquids," pp. 134-304 in **Handbuch der Physik, Vol. 10**, E. Flügge (Ed.), Springer-Verlag, Berlin, 1960.

The above result is due to Bakker.[21] Using an assumed *local* equation of state similar to that describing the bulk phase, together with an expression for free energy minimization in the interfacial layer, van der Waals made computations of the interfacial density profiles and the resulting surface or interfacial tension. Others[22] have since refined these arguments and have applied statistical mechanics to the problem.[23,24]

What has been done using Bakker's Equation is to project the integrated excess lateral stress (or alternatively, the compressive stress deficit), as shown in Fig. 2-12, onto the mathematical surface defined as the interface. The mathematical surface of the model is termed the "surface of tension," and for a flat interfacial layer, its exact location is immaterial, *i.e.*, its location in no way impacts the unambiguous and physically measurable surface tension. For an interface that is not flat, it is useful to distinguish between weak curvature and strong curvature. (A more detailed discussion of surface curvature is given later.) Weakly curved surfaces are those whose mean radius of curvature is large relative to the thickness of the zone of inhomogeneity, whereas strongly curved surfaces are those whose radius of curvature is comparable to that of the interfacial layer thickness. In the latter case, since interfacial layers are of the order of only a few Å in thickness, one might expect the continuum concept of surface tension to break down, or alternatively, to require that the surface tension be regarded as a *function* of the curvature. For the moment, we shall consider only weakly curved surfaces. As will be proved later, curved fluid surfaces (whether strongly or weakly curved) require a difference in the equilibrium bulk pressures, with the pressure on the concave side larger than the pressure on the convex side.

The molecular picture of the interfacial layer, particularly with respect to the interpretation of the states of stress that exist within it, gives one the idea of why fluid interfacial layers should exhibit a tension. It also explains qualitatively why there should be a difference in the surface tension from one pure liquid to the next in terms of the type and strength of the intermolecular forces that prevail. Intermolecular forces such as those of ionic bonds, metallic bonds, or hydrogen bonds, which yield very strong attractions, lead to much higher boundary tensions than those for liquids with only van der Waals interactions. Thus it is that molten salts and liquid metals have very high surface tensions and that water's surface tension is high relative to that of organic liquids. One may also explain the nature of the temperature dependence of surface tension. The portion of the pressure component due to kinetic energy increases linearly with temperature, while

---

[21] Bakker, G., **Kapillarität u. Oberflächenspannung**, Vol. 6 of **Handb. d. Experimentalphysik**, W. Wien, F. Harms and H. Lenz (Eds.), Akad. Verlags., Leipzig, 1928.

[22] Cahn, J. W., and Hilliard, J. E., *J. Chem. Phys.*, **28**, 258 (1958).

[23] Rowlinson, J. S., and Widom, B., **Molecular Theory of Capillarity**, Clarendon Press, Oxford, 1982.

[24] Davis, H. T., **Statistical Mechanics of Phases, Interfaces and Thin Films**, VCH, New York, 1996.

that due to intermolecular attractive forces remains essentially constant. Thus, as temperature increases, the difference between p and p_T diminishes, and σ decreases in approximately linear fashion. The reason for the effectiveness of surface active agents in reducing surface tension can also be understood. These molecules orient themselves in the interface so that in both the upper and the lower portions of the layer, *portions* of molecules are present which interact favorably with the predominant component of the respective bulk phases. This reduces the impact of the lateral intermolecular forces, *i.e.*, the magnitude of $p - p_N$, in passing from one phase to the other. The high-energy clean water surface is effectively replaced by the lower energy hydrocarbon moieties of the surfactant. Finally, the molecular picture of the interfacial layer makes clear the reason for its thinness. The zone of inhomogeneity constituting the interfacial layer is necessarily limited by the range of the intermolecular forces. Van der Waals forces, for example, seldom are significant beyond the second- or third- nearest neighbors. Intermolecular forces leading to hydrogen bonding are even shorter-ranged. Ionic interactions are longer ranged, and interfacial layers involving these types of forces may be somewhat thicker.

4. *Components of the surface tension*

The direct dependence of surface tension on the intermolecular forces in the fluid has led Fowkes and others to divide the contributions to surface tension into the various contributions to the intermolecular forces that may exist. Specifically, Fowkes[25] first wrote

$$\sigma = \sigma^d + \sigma^p + \sigma^i + \sigma^H + \sigma^m + ..., \tag{2.19}$$

where “d” refers to dispersion forces, “p” to forces between permanent dipoles, “i” to induced dipoles, “H” to hydrogen bonds, “m” to metallic bonds, *etc*. It is now known from the theory of intermolecular forces in condensed-phase media[26] that the contributions of dipole-dipole (Keesom) and dipole-induced dipole (Debye) interactions to the surface energy are essentially negligible, as a result of the self-cancellation that occurs when multiple dipoles interact. This is in contrast to the situation in gases, where dipoles interact predominantly in pairwise fashion. The portion of the 72 mN/m surface energy of water at room temperature that is attributable to such polar effects, for example, has been computed to be only 1.4 mN/m.[27] In addition to dispersion force interactions, the major contributor to σ is that due to donor-acceptor interactions, *i.e*. Lewis acid-base association. A donor (base) donates a pair of electrons in an adduct-forming complexation with an acceptor (acid). This picture can be made to include hydrogen bonding.[28]

---

[25] Fowkes, F. M., *A.C.S. Advances in Chemistry Series,* **43**, 99-111 (1964).

[26] Israelachvili, J. N., **Intermolecular and Surfaces Forces,** 2nd Ed., Academic Press, London, 1992.

[27] van Oss, C. J., Chaudhury, M. K., and Good, R. J., *J. Colloid Interface Sci*., **111**, 378 (1986).

[28] Fowkes, F. M., *J. Adhesion Sci. Tech.*, **1**, 7 (1987).

Thus σ^H is replaced with the more general σ^{ab}. Many liquids (most notably water) may act as both acids *and* bases, and thus *self*-associate. For most liquids then, Eq. (2.19) reduces to: $\sigma = \sigma^d + \sigma^{ab}$, where σ^{ab} refers to the contribution of acid-base self-association. In molten metals, metallic bonding is important, so in those cases: $\sigma = \sigma^d + \sigma^m$.

As will be seen later, the components of surface tension for a given liquid may be determined experimentally from interfacial tension measurements between that liquid and an immiscible, non-associating reference liquid, or from the measurement of contact angles against reference solids (see Chap. 4). Of particular importance, for water at 20°C: σ = 72.8 mN/m, with σ^d = 21.2±0.7 mN/m. For mercury, σ = 485 mN/m and σ^d = 200 mN/m. A list of values for various liquids is given in Table 2-2.

Table 2-2: Components of surface tension (in mN/m at 23.±0.5°C). From [Fowkes, F. M., Riddle, F. L., Pastore, W. E., and Webber, A. A., *Colloids Surfaces,* **43**, 367 (1990)].

Liquid	σ	σ^d	σ^{ab}	Type
Water	72.4	21.1	51.3	both
Glycerol	63.4	37.0	26.4	both
Formamide	57.3	28.0	29.3	both
Methyl iodide	50.8	50.8	0	Neither
a-Bromonaphthalene	44.5	44.5	0	Neither
Nitrobenzene	43.8	38.7	5.1	Both
Dimethylsulfoxide	43.5	29.0	14.5	Both
Aniline	42.5	37.3	5.1	Both
Benzaldehyde	38.3	37.0	1.3	Both
Pyridine	38.0	38.0	0	Basic
Formic acid	37.4	18.0	19.4	Both
Pyrrole	37.4	32.6	4.8	Both
Dimethylformamide	36.8	30.2	6.6	Both
1,4-Dioxane	33.5	33.5	0	Basic
cis-Decaline	32.2	32.3	0	Neither
Squalane	29.2	29.2	0	Neither
Acetic acid	27.6	22.8	4.8	Both
Chloroform	27.1	27.1	0	Acidic
Methylene chloride	26.6	26.6	0	Acidic
Tetrahydrofuran	26.5	26.5	0	Basic
Ethyl acetate	25.2	25.2	0	Basic
Acetone	23.7	22.7	1.0	Both
Ethanol	22.2	20.3	1.9	Both
Triethylamine	20.7	20.7	0	Basic
Ethyl ether	17.0	17.0	0	Basic

D. Interfacial tension

1. *Experimental interfacial tension*

As stated earlier, the terminology "surface tension" is usually reserved for the tension observed at a liquid-vapor interface, whereas "interfacial" tension is used in reference to fluid interfaces of all kinds, but in the present context to liquid-liquid interfaces. The same molecular picture developed earlier explains the existence of interfacial tension between liquids. If the liquids are dissimilar enough to form an interface, then the molecules of each bulk phase prefer to stay together rather than mix. They resist the enforced molecular separation between like species that must exist throughout the interfacial layer, where intermediate compositions prevail, and manifest this resistance as interfacial tension. For example, at the water-oil interface, the hydrogen bonds between the water molecules are disrupted.

Values for liquid-liquid interfacial tensions are less plentiful in the literature than those of surface tension and are generally less reliable, due to uncertainty as to the extent of mutual saturation of the liquid phases during the measurement. Some representative experimental values for interfacial tensions between water and various liquids are shown in Table 2-3.

Table 2-3: Interfacial tension values

Liquids	T(°C)	Interfacial tension (mN/m)
Water/Butanol	20	1.8
Water/Ethyl Acetate	20	6.8
Water/Benzene	20	35.0
Water/HMDS (Silicone)	20	44.3
Water/Perfluorokerosene	25	57.0
Water/Mercury	20	415
Water/Oil (with surfactant)	20	as low as < 0.001

The effect of temperature on interfacial tension is somewhat more complex than that for surface tension, because changes in temperature may strongly change the extent of mutual solubility of the liquids. For systems having an upper critical solution temperature (UCST), σ decreases with temperature, but for those with a lower critical solution temperature (LCST), σ increases with T. For systems with both a UCST and an LCST, σ passes through a maximum at an intermediate temperature.

2. *Combining rules for interfacial tension*

Effort has been put into developing semi-empirical equations allowing interfacial tension to be calculated in terms of known values for the surface tensions of the two liquids forming the interface. Some are based on the simple picture of the molecular origin of surface tension displayed in Fig. 2-9. If surface tension represents the "unbalanced" inward-pulling

intermolecular forces, then interfacial tension should represent the *net* inward force, directed toward the liquid of greater surface tension, as suggested in Fig. 2-13. This is the basis for Antanow's Law,[29] which states that the interfacial tension between two liquids is the absolute value of the difference between their surface tensions:

$$\sigma_{AB} = \left|\sigma_{A(B)} - \sigma_{B(A)}\right|. \tag{2.20}$$

It often does well if the surface tension values used correspond to mutually saturated liquids, as suggested by the subscripts in the equation. Table 2-4 shows data for several mutually saturated, water–organic systems in comparison with calculations based on Antanow's Law.

Table 2-4: Interfacial tensions of mutually saturated water-organic liquid systems. From [Voyutsky, S., **Colloid Chemistry**, p. 129, Mir. Pub., Moscow, 1978.]

Liquid T (°C)	Surface tension, against air (mN/m)		Interfacial tension (mN/m)	
	Water layer	Organic layer	Antanow's Law	Experimental
Benzene (19°)	63.2	28.8	34.4	34.4
Aniline (26°)	46.4	42.2	4.2	4.8
Chloroform (18°)	59.8	26.4	33.4	33.8
Carbon tetrachloride (17°)	70.2	26.7	43.5	43.8
Amyl alcohol (18°)	26.3	21.5	4.8	4.8
Cresol (18°)	37.8	34.3	3.5	3.9

Another equivalent approach to estimating interfacial tensions also derives from their direct computation in terms of intermolecular forces. Consider two immiscible liquids A and B as semi-infinite half-spaces

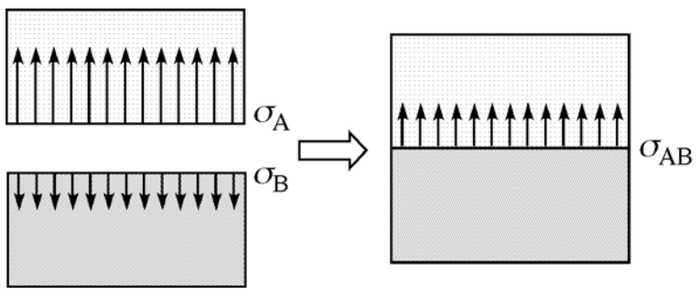

Fig. 2-13: Model for evaluating interfacial tension in terms of surface tensions.

meeting at their common interface. The work required to separate the two phases (to infinity, *in vacuo*) is the energy required to form the surfaces of A and B, minus the energy recovered by the destruction of the AB interface, *viz.*

[29] Antanow, G., *J. Chem. Phys.*, **5**, 372 (1907).

$$W_{\text{separation}} = \sigma_{\text{A}} + \sigma_{\text{B}} - \sigma_{\text{AB}}. \tag{2.21}$$

This work of separation can be computed as the sum of the intermolecular forces between the molecules of phase A with those of phase B, by analogy with Eqs. (2.12)-(2.14):

$$W_{\text{separation}} = -\Phi^{\sigma}_{\text{AB}} = \frac{\pi B_{\text{AB}} \rho_{\text{A}} \rho_{\text{B}}}{12 D_0^2} = \frac{A_{\text{AB}}}{12\pi D_0^2}, \tag{2.22}$$

where B_{AB} is the cross van der Waals molecular interaction constant between molecules A and B, ρ_{A} and ρ_{B} are molecular densities, and A_{AB} is the cross Hamaker constant. Applying the geometric mean rule, Eq. (2.6), for B_{AB} (assuming the dominance of dispersion forces), we see that the cross Hamaker constant is given by

$$A_{\text{AB}} = \pi^2 \rho_{\text{A}} \rho_{\text{B}} \sqrt{B_{\text{AA}} B_{\text{BB}}} = \sqrt{A_{\text{AA}} A_{\text{BB}}}. \tag{2.23}$$

Then relating the Hamaker constant to surface tension, Eq. (2.14):

$$W_{\text{separation}} = \Phi^{\sigma}_{\text{AB}} = 2\sqrt{\sigma_{\text{A}} \sigma_{\text{B}}}, \tag{2.24}$$

so that finally, substituting in Eq. (2.21):

$$\sigma_{\text{AB}} = \sigma_{\text{A}} + \sigma_{\text{B}} - 2\sqrt{\sigma_{\text{A}} \sigma_{\text{B}}}. \tag{2.25}$$

Girifalco and Good[30] wrote Eq. (2.25) in the form:

$$\sigma_{\text{AB}} = \sigma_{\text{A}} + \sigma_{\text{B}} - 2\Phi\sqrt{\sigma_{\text{A}} \sigma_{\text{B}}}, \tag{2.26}$$

with the factor Φ (presumably ≤ 1) accounting for the fact that not all of the molecular interactions across the interface may be of the dispersion force type.

An alternative formulation was given by Fowkes,[31] who argued that, in the absence of acid-base interactions (or metallic bonding), only dispersion forces were operative *across* the interface. The result was thus:

$$\sigma_{\text{AB}} = \sigma_{\text{A}} + \sigma_{\text{B}} - 2\sqrt{\sigma_{\text{A}}^{\text{d}} \sigma_{\text{B}}^{\text{d}}}, \tag{2.27}$$

To use Eq. (2.27) one needs to know the dispersion force contributions to the surface tension values, such as given in Table 2-2. The interpretation of the Girifalco-Good Φ-factor becomes rather awkward (and quite different from its original interpretation, which involved presumed polar interactions). The Fowkes equation is easily extended, at least in a formal way, to include the possibility of acid-base interactions *across* the interface, I^{ab}:

$$\sigma_{\text{AB}} = \sigma_{\text{A}} + \sigma_{\text{B}} - 2\sqrt{\sigma_{\text{A}}^{\text{d}} \sigma_{\text{B}}^{\text{d}}} - I^{\text{ab}}. \tag{2.28}$$

---

[30] Girifalco, L.A., and Good, R.J., *J. Phys. Chem.,* **67**, 904 (1957).

[31] Fowkes, F. M., *A.C.S. Advances in Chemistry Series,* **43**, 99-111 (1964).

Situations in which I^{ab} is significant may lead to $\sigma_{AB} \leq 0$, suggesting miscibility between liquids A and B. While strictly applicable only in the case of total immiscibility, the Fowkes Equation may be applicable to partially miscible systems if the values of surface tension correspond to those of mutual saturation, *i.e.* $\sigma_{A(B)}$, $\sigma^{d}_{A(B)}$, *etc.* This idea, however, seems not to have been tested.

A word of caution must be raised concerning the use of equations for interfacial tension employing Berthelot's principle. The mixing rule applies to energy quantities (such as internal energy or enthalpy), whereas surface and interfacial tensions are *free* energies.[32] Thus equations such as those of Girifalco and Good or Fowkes ignores the entropy effect associated with bringing together or disjoining the phases.

E. Dynamic surface tension

The surface and interfacial tensions referred to in the foregoing are assumed to be *equilibrium* values. Before exploring further the mechanical consequences of capillarity for equilibrium systems, a word should be said about systems which may *not* be in equilibrium, and which exhibit a time-dependent, or *dynamic* surface or interfacial tension $\sigma(t)$. Examples would include "fresh" surfaces created in coating operations, for liquids emerging from orifices or spray nozzles, or when bubbles are formed within liquids. Practical situations exist, such as in ink-jet printing, in which surface ages as low as fractions of a millisecond are important. The time required for molecular re-orientation at fresh interfaces of non-macromolecular *pure* liquids is less than one *micro*-second, so that dynamic surface tension behavior of pure liquids is of little practical significance, but for solutions, particularly dilute solutions of surface active agents, surface tension may be found to vary from its value at $t \rightarrow 0$ (when σ is presumably close to that corresponding to the pure solvent) to its equilibrium value over times from less than one millisecond to several hours. As has been noted, such solutes reduce surface tension as they accumulate at the interface, and to do so requires at least the time for diffusion. Additional time may be required for the solute molecules to enter the surface and possibly to re-orient themselves. Further discussion of dynamic surface tension is deferred to Chap. 3, following discussion of surfactant adsorption.

F. Capillary hydrostatics: the Young-Laplace Equation

1. *Capillary pressure: pressure jump across a curved fluid interface*

Consider next the problem of determining the shape and location of fluid interfaces, the fundamental problem of capillary hydrostatics. The solution to this problem is the basis for most of the methods of measuring

---

[32] Lyklema, J., *Colloids Surfaces A*, **156**, 413 (1999).

surface or interfacial tension and has important consequences for the formation of adhesive bonds, for the motion of liquids in porous media, for the thermodynamic properties of small drops or bubbles, and for the process of phase change by nucleation. For the fluid interface, nothing more complicated than Young's membrane model is needed.

It is a matter of experience that when an elastic membrane is deformed, as when air is blowing on a soap film suspended on a frame as shown in Fig. 2-14, the pressure on the concave side (p'') must be greater than the pressure on the convex side (p'). The pressure difference is found

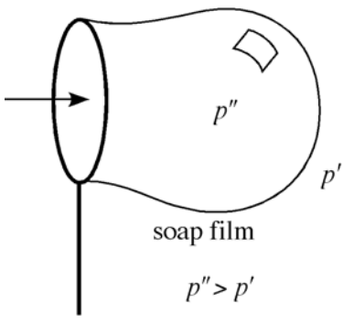

Fig. 2-14: Pressure applied to a soap film.

to be directly proportional to the *curvature* of the soap film, as demonstrated by the example shown in Fig. 2-15. When two bubbles of different sizes are connected by a tube, the larger one will grow at the expense of the smaller one since the curvature of the smaller bubble is greater (has a higher pressure inside) than the larger one. Flow continues until the curvatures are equal, as shown, with the smaller bubble eventually becoming a spherical cap with the same radius as the larger bubble.

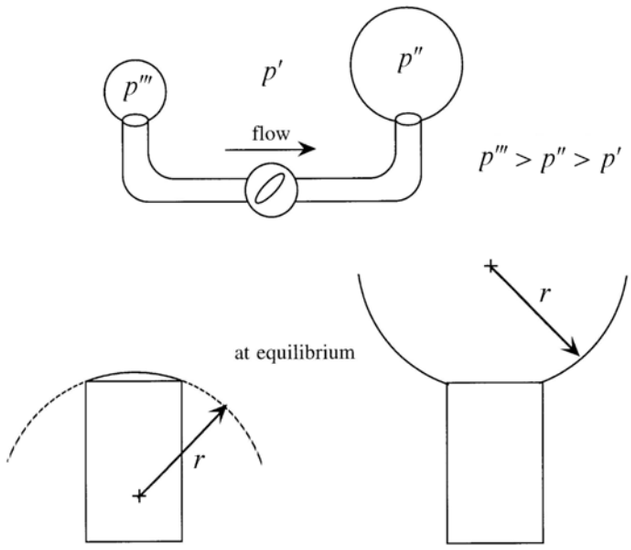

Fig. 2-15: Spontaneous flow occurs from the smaller bubble (higher curvature) to the larger bubble until the spherical cap at the location where the smaller bubble started has the same radius of curvature as the final larger bubble.

Thomas Young (in 1805, *loc. cit.*) and P. S. Laplace (in 1806)[33] derived the exact relationship which must hold between the pressure jump across a fluid interface, $\Delta p = p'' - p'$, and its local curvature, κ, *viz.*,

$$\Delta p = \sigma\kappa, \tag{2.29}$$

with pressure on the concave side higher. This is the *Young-Laplace Equation*, and is derived below. In order to understand and use Eq. (2.29), the curvature κ, of a surface in space (at a point) must be defined.

2. *The curvature of a surface*

One may first recall the definition of the curvature of a *plane* curve, with reference to Fig. 2-16. The curvature of a plane curve C at P is its rate of change of direction with arc length *S*, at P, measured along the curve, *i.e.*, $\kappa = d\phi/dS$, where ϕ is the angle made between the tangent to the curve at the

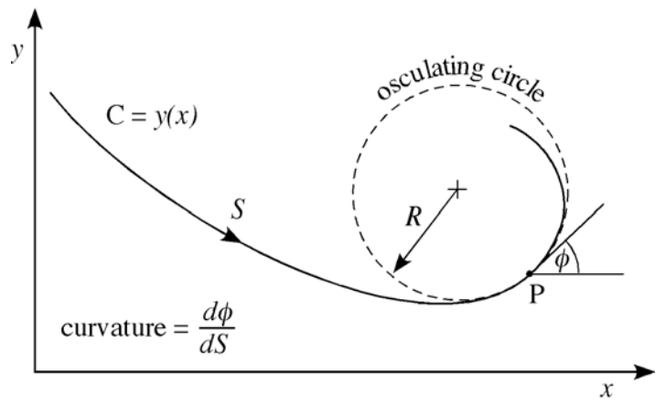

Fig. 2-16: Construction for defining plane curvature.

point of interest and some arbitrary direction (say, the *x*-direction, as shown in the figure). Its units are length^{-1}, and its sign is ambiguous. In terms of the equation of the curve $y(x)$:

$$\kappa = \pm \frac{d^2y}{dx^2}\left[1+\left(\frac{dy}{dx}\right)^2\right]^{-3/2}. \tag{2.30}$$

The curvature of a circle is computed from its equation: $x^2 + y^2 = R^2$ (for a circle of radius R centered at the origin) and is seen to be $\pm 1/R$. It is thus possible to define a *circle of curvature* (or "osculating circle") for any point P along any curve C, as the circle passing through point P and having the same curvature as C at P. The radius of the circle of curvature at P is referred to as the *radius of curvature* of C at P.

It is next possible to define the curvature of a *surface* in space, with reference to Fig. 2-17, in the following way. We first erect a normal, n, at the point of interest and pass a pair of orthogonal planes through it. These

---

[33] De Laplace, P. S., **Traité méchanique céleste, supplement au Livre X**, 1806.

cut the surface in two plane curves. The curvature of the surface is the *sum* of the curvatures of these two plane curves:

$$\kappa = \pm\left(\frac{1}{R_1} + \frac{1}{R_2}\right) = \pm\frac{2}{R_m}, \tag{2.31}$$

where R_m is the mean radius of curvature of the surface. It may be identified as the radius of the osculating *sphere*. The sum is invariant as one rotates the planes about the normal. The R_1-value that is maximum, and the corresponding R_2-value which is minimum, are referred to as the *principal*

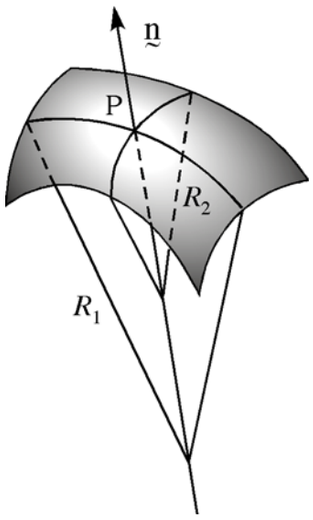

Fig. 2-17: General surface in Cartesian space.

radii of curvature. The sign of the curvature of the surface is ambiguous until a physical context is specified.

Recalling the expression for the curvature of a plane curve, it is easy to appreciate that the general expression for the curvature of a surface is quite complex. For the general case shown in Fig. 2-18, where the surface is

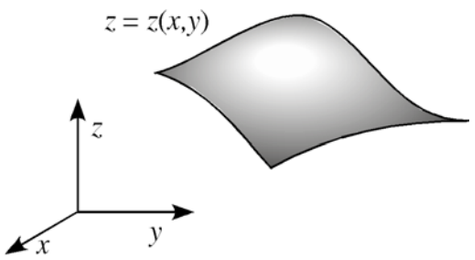

Fig. 2-18: General surface in Cartesian space.

given as the elevation z as a function of the planform variables x and y, *viz.* $z = z(x,y)$, the general expression for the curvature becomes:

$$\kappa = \pm\frac{\left(\frac{\partial^2 z}{\partial x^2}\right)\left[1+\left(\frac{\partial z}{\partial y}\right)^2\right] - 2\left(\frac{\partial z}{\partial x}\right)\left(\frac{\partial z}{\partial y}\right)\left(\frac{\partial^2 z}{\partial x \partial y}\right) + \left(\frac{\partial^2 z}{\partial y^2}\right)\left[1+\left(\frac{\partial z}{\partial x}\right)^2\right]}{\left[1+\left(\frac{\partial z}{\partial x}\right)^2 + \left(\frac{\partial z}{\partial y}\right)^2\right]^{3/2}}. \tag{2.32}$$

Many of the cases of special interest, however, possess certain symmetries that simplify the expressions considerably. Some examples of special cases are discussed below.

For spheres or segments of spherical surfaces, as might be created by soap films, it is evident, as shown in Fig. 2-19, that any normal to the surface will pass through the center of the sphere, and any plane containing this line will cut the sphere to yield a great circle. The radius of this circle, R_1, is the radius of the sphere, R. The plane containing the normal and orthogonal to the first plane will also cut the surface of the sphere in a great circle, so we see that the curvature of the spherical surface is

$$\kappa = \frac{1}{R_1} + \frac{1}{R_2} = \frac{1}{R} + \frac{1}{R} \equiv \frac{2}{R}. \tag{2.33}$$

Right cylindrical surfaces (or portions of such surfaces) may be similarly analyzed. Any normal to the surface will pass through and be orthogonal to the axis of the cylinder, as shown in Fig. 2-20. One convenient

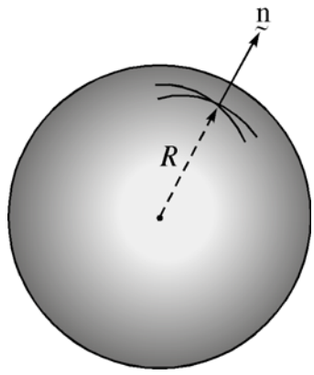

Fig. 2-19: Curvature of a spherical surface.

plane passing through the normal will be perpendicular to the axis of the cylinder, and cut the cylindrical surface in a circle whose radius, R_1, is the radius of the cylinder. Then the plane perpendicular to this circle and cutting the surface of the cylinder will be a rectangle. The "radius" of this curve = ∞. Thus for the circular cylinder,

$$\kappa = \frac{1}{R_1} + \frac{1}{\infty} = \frac{1}{R}. \tag{2.34}$$

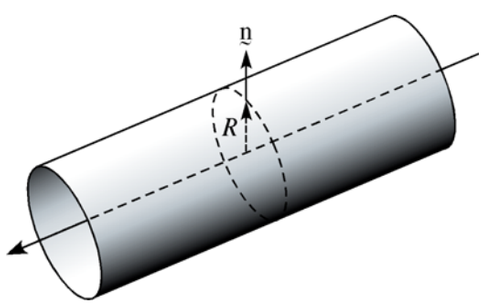

Fig. 2-20: Curvature of a right circular cylinder

Cylindrical surfaces in general are those swept out by moving a straight line (the *generatrix*) normal to itself, as shown in Fig. 2-21. It is evident that the curvature of any general cylindrical surface will be the

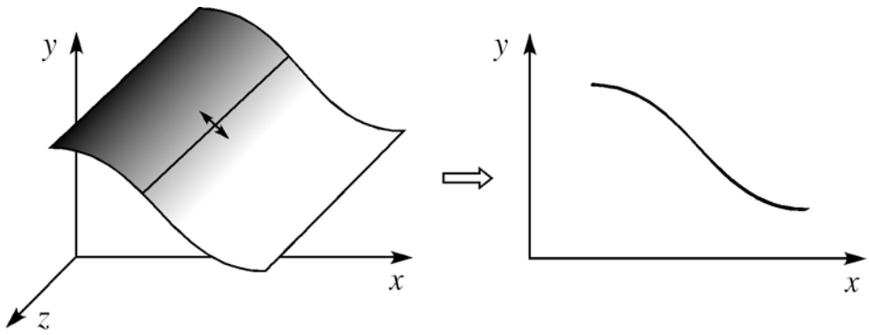

Fig. 2-21: A general cylindrical surface.

curvature of a plane curve in the plane perpendicular to the generatrix, *i.e.*,

$$\kappa = \frac{1}{R_1} + \frac{1}{\infty} = \pm \frac{y''}{\left[1 + (y')^2\right]^{3/2}} . \tag{2.35}$$

Some practical situations yielding this type of surface are shown in Fig. 2-22 and include menisci against flat walls contacting a liquid, and menisci between flat plates or between cylinders and plates.

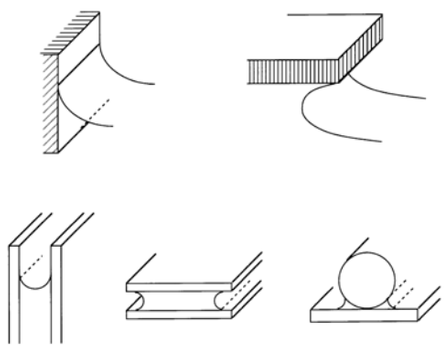

Fig. 2-22: Examples of cylindrical liquid surfaces.

Finally, there are surfaces of axial symmetry, some examples of which are shown in Fig. 2-23. The first three are closed surfaces, *i.e.*, cut by the axis of symmetry. Case (d) is a soap film suspended between opposing open

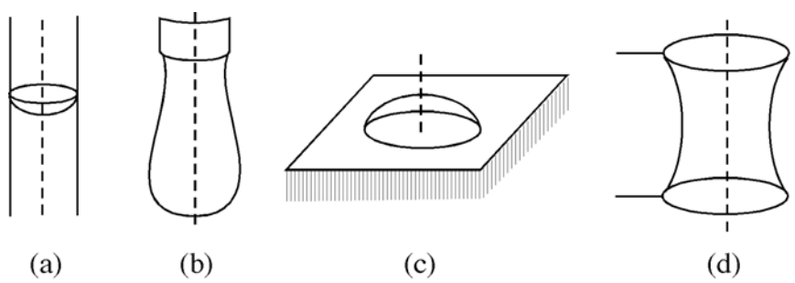

Fig. 2-23: Examples of surfaces of axial symmetry. The meniscus in a round tube (a), the pendant drop (b) and the sessile drop (c) are cut by the axis of symmetry, whereas the soap film suspended between circular rings (c) is not.

wire loops, and is an example of an axisymmetric surface that is not closed. One may derive the expression for the curvature of closed surfaces of axial symmetry by considering that any normal to such a surface, when extended, will intersect the axis of symmetry, and the plane established by the normal and the axis of symmetry will cut surface yielding its profile, as shown in Fig. 2-24. The profile may be given the equation $y(x)$, defining the origin as the point where the surface is cut by its axis of symmetry, y as the coordinate along the axis of symmetry, and x the distance measured away from it. One of the two principal radii of curvature, R_1, at the point of interest, will be the

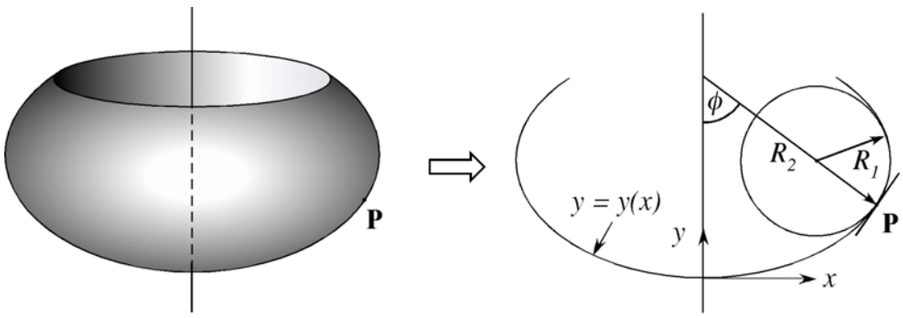

Fig. 2-24: Axisymmetric interface; profile view in plane passing through axis of symmetry.

plane curvature of $y(x)$ at that point. A little examination of the figure reveals that the second principal radius of curvature, R_2, must be the distance measured from the point of interest on the surface back to the axis of symmetry along a line perpendicular to the tangent of the curve $y(x)$. It is evident that as such a radius swings around the axis of symmetry, it will trace out a circle on the surface. R_1 thus swings in the plane of the figure, while R_2 swings around the axis as shown. R_1 is given by the usual expression for plane curvature. R_2 is x divided by $\sin\phi$, where ϕ is the angle whose tangent is dy/dx, *i.e.* y'. This works out to be:

$$R_2 = \pm \frac{x\left[1 + (y')^2\right]^{1/2}}{y'}. \tag{2.36}$$

Thus for an axisymmetric surface (which is cut by the axis of symmetry) the expression for the curvature becomes:

$$\kappa = \frac{1}{R_1} + \frac{1}{R_2} = \pm\left\{\frac{y''}{\left[1 + (y')^2\right]^{3/2}} + \frac{y'}{x\left[1 + (y')^2\right]^{1/2}}\right\}. \tag{2.37}$$

Fluid interfaces that are cylindrical or axially symmetric represent perhaps the majority of cases of practical interest.

3. *Derivation of the Young-Laplace Equation*

The Young-Laplace Equation, Eq. (2.29), which takes the general form:

$$\Delta p = \sigma\left(\frac{1}{R_1} + \frac{1}{R_2}\right), \tag{2.38}$$

may be derived with reference to Fig. 2-25. Consider a small patch of surface centered at P and enclosed by a curve drawn in the surface everywhere a distance ρ (measured along the surface) from P. ρ is taken to be very small. Phase ($''$) is on the lower, concave side of the patch, while phase ($'$) is above it. Construct orthogonal lines AB and CD as shown, as lines made by a pair of orthogonal planes passing through a normal to the surface at P, *viz*., $\underline{n}$. A normal force balance, *i.e*., in the direction of $\underline{n}$, on the patch, requires:

$$\begin{bmatrix}\text{net pressure force}\\ \text{on patch}\end{bmatrix} = \begin{bmatrix}\text{normal component of surface tension}\\ \text{force acting on patch perimeter}\end{bmatrix}.$$

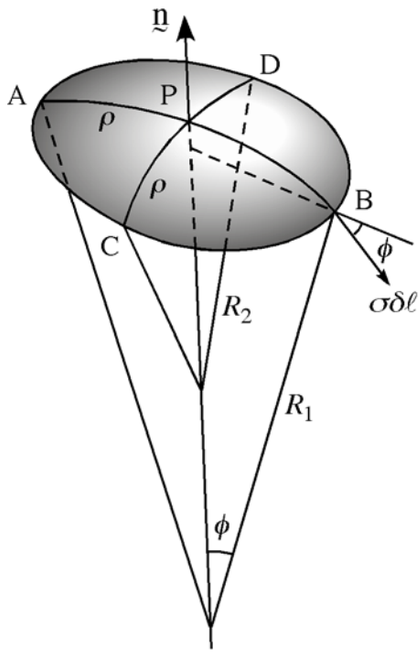

Fig. 2-25: Figure for derivation of the Young-Laplace Equation.

The net upward (+$\underline{n}$ direction) force on the patch is

$$F\uparrow = (p'' - p')\pi\rho^2 \tag{2.39}$$

to any desired degree of accuracy by making ρ sufficiently small. To compute the downward force, consider first the force on an element of perimeter, $\delta\ell$, at point B, as shown. The force pulling downward (-$\underline{n}$ direction) on the element of perimeter is $\delta F\downarrow = -\sigma\delta\ell\sin\phi$. Since ϕ is very small (because ρ is small), $\sin\phi \approx \tan\phi \approx \rho/R_1$, and this component of force is $-\sigma(\rho/R_1)d\ell$. At point A, the component of force is the same. At points C

and D, the force is $-\sigma(\rho/R_2)d\ell$. Adding these gives $-2\sigma\rho(1/R_1 + 1/R_2)d\ell$. To obtain the total downward force acting on the perimeter, the above expression is integrated around one-fourth the perimeter, *i.e.*, a distance of $1/4(2\pi\rho) = 1/2(\pi\rho)$, to get:

$$F\downarrow = -\int_0^{\pi\rho/2} 2\sigma\rho\left(\frac{1}{R_1}+\frac{1}{R_2}\right)\delta\ell = -\sigma\pi\rho^2\left(\frac{1}{R_1}+\frac{1}{R_2}\right). \tag{2.40}$$

Equating $F\uparrow = F\downarrow$, and canceling $\pi\rho^2$ from both sides yields Eq. (2.38).

The general expression for curvature renders the result a second-order, non-linear partial differential equation, whose solution will give the shape of a fluid interface under given conditions.

Next the Young-Laplace Equation requires the appropriate expression for Δp. For a static system, such as that of the meniscus against a vertical plate shown in Fig. 2-26, in the absence of force fields other than gravity, the local pressure *on each side* of the interface at a point P is given by the hydrostatic equation written in the appropriate phase at the elevation h of point P above the datum plane[34] *i.e.*,

$$p'' = p_0'' - \rho''gh, \text{ and } p' = p_0' - \rho'gh. \tag{2.41}$$

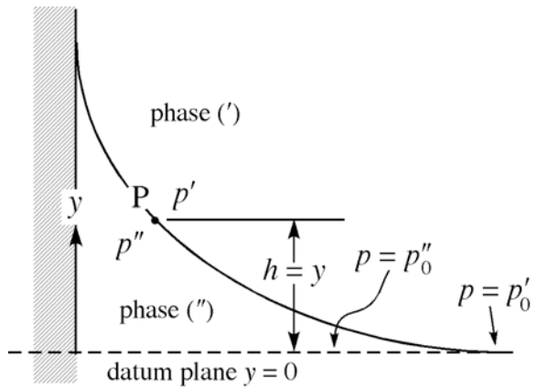

Fig. 2-26: Hydrostatic pressure difference across a curved fluid interface.

Note that both pressures must be referenced to the location of the datum plane *in the appropriate phase*, whether or not either or both the actual phases exists at the datum plane. Δp is then the difference between the hydrostatic pressures of Eq. (2.41):

$$\Delta p = \Delta p_0 - (\rho'' - \rho')gh. \tag{2.42}$$

If $y = 0$ is located at the datum plane, then $h = y$, and

$$\Delta p = \Delta p_0 - (\rho'' - \rho')gy. \tag{2.43}$$

If, as in Fig. 2-26, the datum plane is located at an elevation where the surface happens to be flat (one cannot always do this, as for example, in any

[34] Under more general conditions, stagnation flows and/or rigid body rotation may also contribute to the local value of p at a given point on either side of the interface.

of the cases of Fig. 2-23), $p_0' = p_0''$, and $\Delta p = -(\Delta\rho)gy$. Using expressions of the above type for Δp, the Young-Laplace Equation for the special cases of curvature discussed earlier may be written as follows:

1. Sphere: $\Delta p = \Delta p_0 = \dfrac{2\sigma}{R}$. (2.44)

2. Circular cylinder: $\Delta p = \Delta p_0 = \dfrac{\sigma}{R}$. (2.45)

3. General cylindrical surface:

$$\Delta p = \Delta p_0 - (\Delta\rho)gy = \pm\sigma \frac{y''}{\left[1 + (y')^2\right]^{3/2}} \tag{2.46}$$

4. Axisymmetric (closed) surface:

$$\Delta p = \Delta p_0 - (\Delta\rho)gy = \pm\sigma \left\{ \frac{y''}{\left[1 + (y')^2\right]^{3/2}} + \frac{y'}{x\left[1 + (y')^2\right]^{1/2}} \right\} \tag{2.47}$$

A quick calculation of the pressure jump Δp between the inside and the outside of a soap bubble of radius 5 mm, using Eq. (2.44), reveals that it is quite small for curvatures of this magnitude. Taking the surface tension of the soap solution as 35 mN/m, and noting that the soap film has both an inside and an outside surface, gives $\Delta p \approx 2.8 \cdot 10^{-4}$ atm.

4. *Boundary conditions for the Young-Laplace Equation*

In order to obtain solutions to the Young-Laplace Equation in general, one must provide information equivalent to two boundary conditions. If the surface has an edge, there are two types of conditions that may prevail there (as pictured in Fig. 2-27): 1) the "fixed edge location" condition, and 2) the "fixed contact angle" condition. The latter condition states that a given fluid interface must meet a given solid surface at some specified angle. When a fluid interface terminates on a solid surface, the angle drawn in one of the fluid phases (which must be specified) is termed the "contact angle."

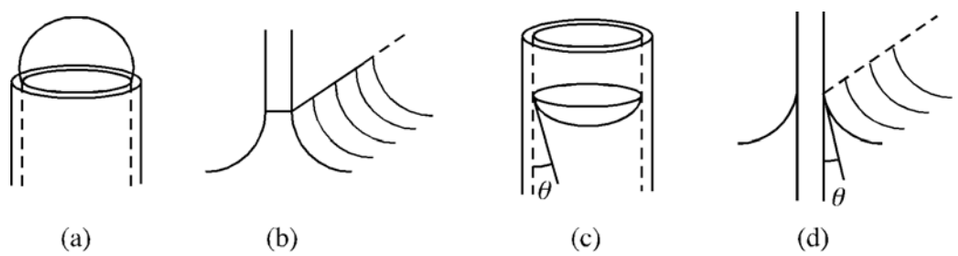

Fig. 2-27: Boundary conditions for Young-Laplace Equation: (a) and (b) are examples of "fixed-edge" conditions, and (c) and (d) are "fixed-angle" conditions.

When a fluid interface terminates at another fluid interface, as when a liquid drop rests upon another immiscible liquid (as shown in Fig. 2-28), the angles between the three interfaces meeting at the interline must be such as to satisfy the vectorial equation

$$\underset{\sim}{\sigma}_{AB} + \underset{\sim}{\sigma}_{BC} + \underset{\sim}{\sigma}_{AC} = 0 \,. \tag{2.48}$$

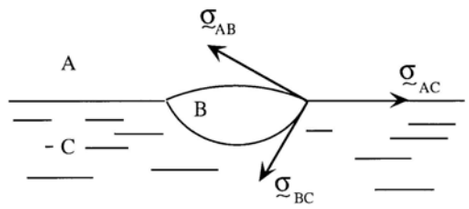

Fig. 2-28: Boundary tension forces at a tri-fluid interline.

Equation (2.48) is referred to as "Neumann's triangle of forces,"[35] and it fixes the angles between the surfaces. For the intersection of soap film lamellae in a foam (as shown in Fig. 2-29), the σ's are all equal, and the films must thus intersect at 120° angles. One might inquire about an intrinsic tension associated with the fluid interline itself, *i.e.* a "line tension" τ_ℓ (which would presumably tend to contract the interline). Such a property would have units of force, or energy/length, and estimates for its magnitude range from -10^{-9} to $+10^{-9}$ N[36] (from which it is seen that it may take on negative values).[37] If the value of the line tension is positive, it will contribute a radially inward force on the interline of magnitude τ_ℓ/R, where R is the radius of the lens. For a lens of radius 1 mm, and a line tension of 10^{-9} N, this would contribute a tension of only 10^{-3} mN/m, quite negligible in comparison with typical surface or interfacial tensions. Line tension may play an important role, however, for micro or nano lenses.

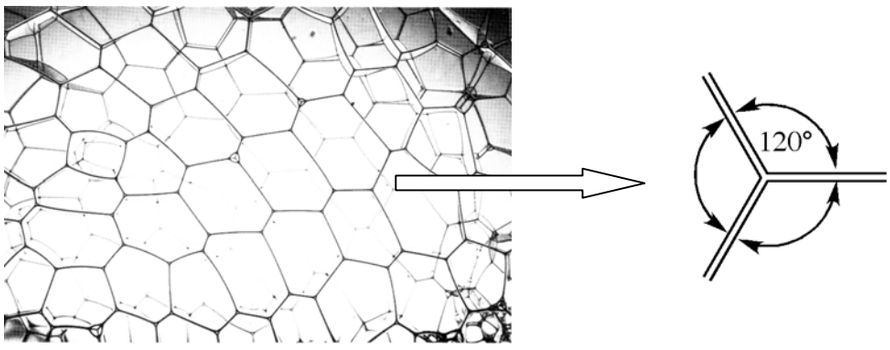

Fig. 2-29: Photograph of a typical foam structure. After [Everett, D. H., **Basic Principles of Colloid Science**, p. 178, Roy. Soc. of Chem., Letchworth (1988).]

With reference to Fig. 2-28, consider the possibility that $\sigma_{AC} > \sigma_{AB} + \sigma_{BC}$, *i.e.*, the force pulling the interline to the right is larger than the maximum possible force pulling it to the left. Under such circumstances it

---

[35] Neumann, F., **Vorlesungen über die Theorie de Capillarität**, B. G. Teubner, Leipzig, 1894.
[36] Toshev, B. V., Platinakov, D., and Sheludko, A., *Langmuir*, **4**, 489 (1988).
[37] Kerins, J., and Widom, B., *J. Chem. Phys.*, **77**, 2061 (1982).

would be impossible to satisfy Neumann's equilibrium condition. The droplet of liquid B would have no recourse but to spread indefinitely as a thin liquid film, possibly all the way to becoming a monolayer. The driving force for the spreading of liquid B at the A-C interface is the *spreading coefficient*, defined as

$$S_{B/AC} = \sigma_{AC} - (\sigma_{AB} + \sigma_{BC}). \tag{2.49}$$

If the spreading coefficient is positive, one may expect to see the spontaneous spreading of the liquid at the interface. Spreading of this type may also be observed at a solid-fluid interface, discussed further in Chap. 4.

G. Some solutions to the Young-Laplace Equation

1. *Cylindrical surfaces; meniscus against a flat plate*

One solution to the Young-Laplace Equation that can be obtained analytically is that for the shape of the meniscus formed by a flat plate dipping into a liquid pool, as shown in Fig. 2-30. This is an example of a general cylindrical surface and satisfies the differential equation given for this case for interfaces of liquids at rest in a gravitational field, acting in the -*y* direction, *viz.*

$$\sigma \frac{y''}{\left[1 + (y')^2\right]^{3/2}} - \rho g y = 0, \tag{2.50}$$

where the datum plane of $y = 0$ has been chosen as the elevation where the surface is flat. The derivatives y' and y'' are taken with respect x, the horizontal coordinate measured away from the location where the interface is (or would be) vertical. The analytical solution in dimensionless form[38] is explicit in x, specifically:

$$(x/a) = \frac{1}{\sqrt{2}} \ln \left[\frac{\sqrt{2} + \left[2 - (y/a)^2\right]^{1/2}}{(y/a)} \right] - \left[2 - (y/a)^2\right]^{1/2} + C, \tag{2.51}$$

where "a" is the "capillary length," defined as: $a = \sqrt{2\sigma/\rho g}$.[39] It is a useful yardstick characterizing the size of a meniscus. The constant of integration, C, is determined by the value of x corresponding to the location of the solid-liquid-gas interline. The curve (c) in Fig. 2-30 includes all possible situations, with the relevant piece of that curve being determined by the angle made by the meniscus at the interline with the vertical axis. This angle is the difference η btween the contact angle θ and the tilt angle of the plate α, *i.e.* $\eta = \theta - \alpha$. C is given by:

---

[38] Princen, H.M., in **Surface and Colloid Science, Vol. 2**, E. Matijevic (Ed.), pp. 1-84, Wiley-Interscience, New York,1969.

[39] It must be noted that some authors define the capillary length as: $\sqrt{\sigma/\rho g}$.

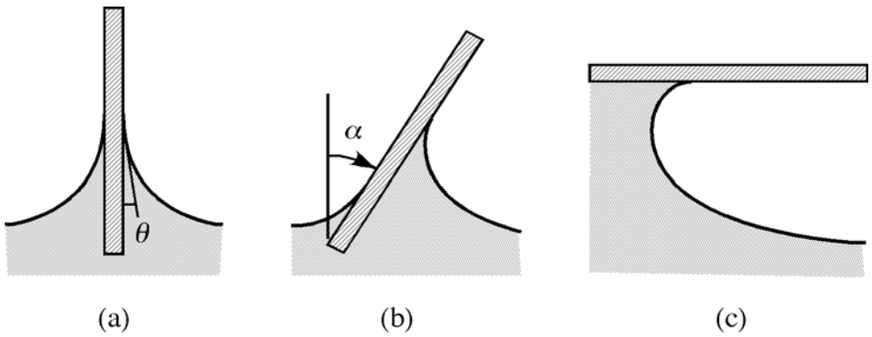

Fig. 2-30: Meniscus against a flat plate dipping into a liquid at various angles.

$$C = \left(1+\sin\eta\right)^{1/2} + \frac{1}{\sqrt{2}}\ln\left[\frac{\left(1-\sin\eta\right)^{1/2}}{\sqrt{2}+\left(1+\sin\eta\right)^{1/2}}\right]. \qquad (2.52)$$

Figure 2-31 shows the complete solution. The value of C corresponding to $\eta = 0°$ is 0.3768... Under these conditions, the meniscus against a vertical wall

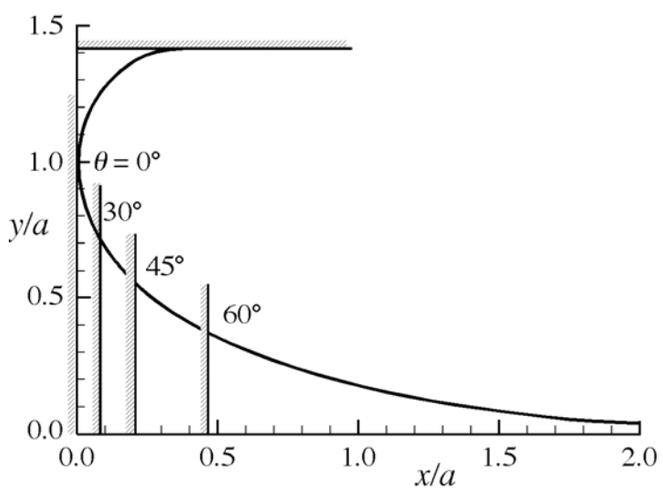

Fig. 2-31: Meniscus profile against a flat plate.

with $\theta = 0°$ rises to a height of precisely the capillary length, a. Other values of the contact angle θ yield other values of C, shifting the location of the wall, *i.e.*, where $(x/a) = 0$, but not altering the shape of the curve. The locations of the wall corresponding to contact angles of 30°, 45° and 60° are shown. A useful result that can readily be derived is that for the maximum height, h_m, of a meniscus against a vertical flat wall, *viz.*

$$\left(\frac{h_m}{a}\right)^2 = 1-\sin\theta. \qquad (2.53)$$

2. *Axisymmetric and other surfaces*

Figure 2-32 shows the solution for the axisymmetric surface of sessile drops (or captive bubbles, when inverted.) Problems of this type, *i.e.*,

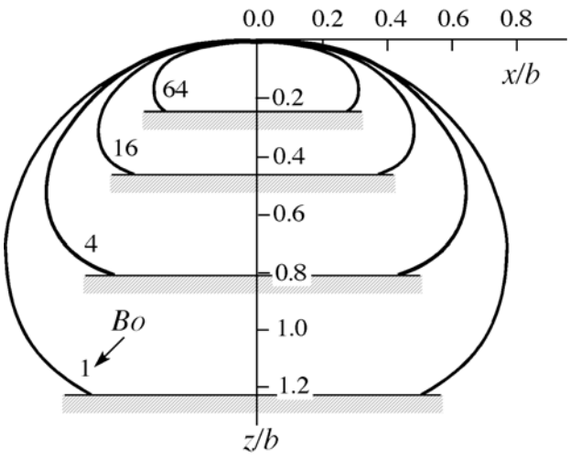

Fig. 2-32: Sessile drop (or if inverted, captive bubble) profiles.

axisymmetric interfaces cut by the axis of symmetry and described by Eq. (2.47), were solved numerically by Bashforth and Adams.[40] Over a twenty year period, these authors compiled solutions for closely-spaced values of the dimensionless parameter $\beta = (\Delta\rho)gb^2/\sigma$ using seven-place tables of logarithms. (The parameter β is now known as the Bond Number,[41] *Bo*.) This achievement was of great importance because it yielded solutions for most of the cases encountered in measuring surface tension.

Computer solutions have been obtained for meniscus shapes in which simplifying symmetries do not exist, and examples are shown in Figs. 2-33 and 2-34. The first shows the profile of a drop on an inclined surface, and the second shows the meniscus about a rectangular object immersed at an angle into a liquid surface.

3. *Non-dimensionalization of the Young-Laplace Equation; the Bond Number*

It is useful to consider limiting cases where the Young-Laplace Equation and its solution take on especially simplified forms. The most important way of delineating these is in terms of the relative importance of surface tension and gravity forces in determining the interface shape. This can be done in a systematic way by nondimensionalization, requiring only the specification of an appropriate characteristic length L for the system. Some examples are shown in Fig. 2-35. If one is interested in the shape of

---

[40] Bashforth, F., and Adams, J.C., **An Attempt to Test the Theories of Capillary Action**, Univ. Press, Cambridge, UK, 1883.

[41] Following: Bond, W. N., and Newton, D. A., *Phil. Mag.*, **5**, 794 (1928), in which the group was used in describing the rise of bubbles in liquids.

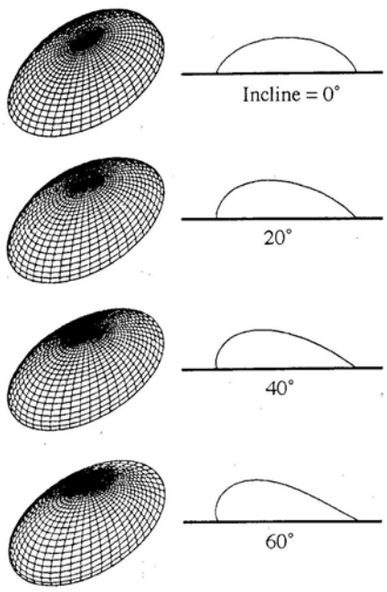

Fig. 2-33: Drop shape on an inclined plane. From [Brown, R.A., Orr, F.M., and Scriven, L.E., *J. Colloid Interface Sci.*, **73**, 76 (1980).]

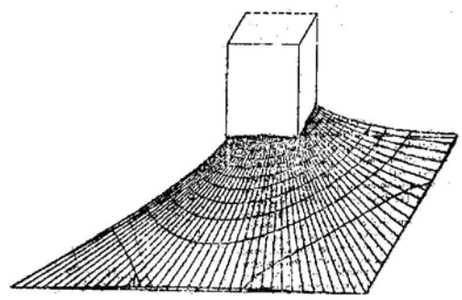

Fig. 2-34: Meniscus around a square pin. From [Orr, F.M., Scriven, L.E., and Chu, Y.T., *J. Colloid Interface Sci.*, **60**, 402 (1977).]

the liquid surface in a large container, such as that in a laboratory beaker shown at the right, the characteristic length depends on what aspects of the shape are sought. If the entire surface is of interest, the diameter of the beaker, D, is appropriate, but for only the meniscus near the wall, the characteristic length is usually chosen as the capillary length, *i.e.* $L = a$.

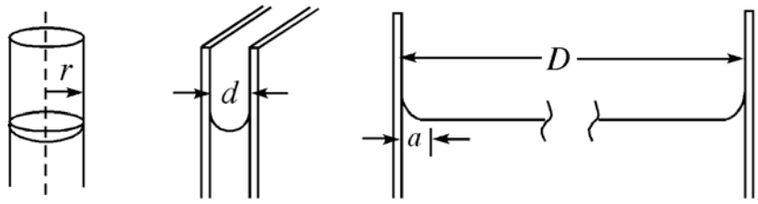

Fig. 2-35: Characteristic lengths for various systems.

Non-dimensionalization of the Young-Laplace Equation in the form:

$$\Delta p_0 + (\Delta\rho) g y = \sigma\left(\frac{1}{R_1} + \frac{1}{R_2}\right) \tag{2.54}$$

proceeds from the definition of the dimensionless length variables: $\hat{y} = y/L$; $\hat{x} = x/L$, *etc.* , and gives

$$\left[\frac{(\Delta p_0)L}{\sigma}\right] + \left[\frac{(\Delta\rho)gL^2}{\sigma}\right]\hat{y} = \left(\frac{1}{\hat{R}_1} + \frac{1}{\hat{R}_2}\right). \tag{2.55}$$

It is seen to yield two dimensionless groups. The first, $(\Delta p_0)L/\sigma$, is a dimensionless reference curvature. The second is the Bond Number, *Bo*:

$$Bo = \frac{(\Delta\rho)gL^2}{\sigma} = \frac{\text{(gravity forces)}}{\text{(surface tension forces)}}, \tag{2.56}$$

which is seen to be the ratio of the gravity forces to the surface tension forces that are responsible for determining the shape of a fluid interface.

When the Bond Number is sufficiently small (< 0.01), gravity is unimportant in determining the shape of the interface, and under such circumstances, the second term of the equation drops out, giving *surfaces of constant curvature*. All confined cylindrical surfaces become portions of right circular cylinders, and all closed surfaces of revolution become portions of spherical surfaces (spherical caps, *etc*.). For example, for a spherical cap of radius *R*, $L = R$, and $\hat{R}_1 = \hat{R}_2 = R/R = 1$, so that:

$$\left[\frac{(\Delta p_0)R}{\sigma}\right] + 0 = \left(\frac{1}{\hat{R}_1} + \frac{1}{\hat{R}_2}\right) = 2, \text{ or } \Delta p_0 = \frac{2\sigma}{R}. \tag{2.57}$$

On the other hand, if *Bo* is very large (> 100), surface tension forces will be unimportant relative to gravity in determining the interface shape. The interface (at rest) will be just a flat surface perpendicular to the *g*-vector. This would be the case considering the *entire* surface of liquid in a large beaker (large $L = D$), as opposed to the shape of the meniscus near the wall. Low-to-moderate *Bo* cases are thus of importance in capillary hydrostatics. Various ways in which very low Bond Numbers can be achieved might be:

- Characteristic length (L) is small.
- Density difference between phases ($\Delta\rho$) is small.
- Gravitational acceleration (g) is low.
- Surface tension (σ) is large.

When fluid systems are small, low *Bo* conditions often exist; for liquids of ordinary surface tension, this is usually the case when $L \leq 1$ mm. Thus menisci in small tubes, small liquid bridges between solid particles, *etc*. will have surfaces strongly affected (and sometimes totally determined) by capillary forces. Surface tension forces are also dominant in determining the shape of interfaces across which the density difference is small. An oil drop suspended in a liquid of nearly the same density will assume the shape of a sphere, undistorted by gravity, which would flatten the drop if it were denser than the medium, and distend it, if it were lighter. A soap bubble, with air inside and outside at nearly the same pressure, is also a sphere. A soap bubble deposited on a flat surface pre-moistened with the soap solution, will be a perfect hemisphere.

Another situation leading to very low Bond Numbers is that of low-to-zero *g*, as realized on board spacecraft, and many capillary hydrodynamics experiments have been performed on space flights (as well as in zero-*g* maneuvers in ordinary aircraft). When gravity is no longer operative to contain or transport liquids, they behave in ways that are often counter-intuitive to one's experience on Earth. Wetting liquids, for example, when

let loose in the capsule, do not fall to the "floor," but may contact and spread out over the entire solid inner surface of the capsule and all the equipment, *etc*., contained in it.[42]

The condition of high σ may yield a small Bond Number. Surface tension values are not large enough to render very large fluid interfaces free of gravitational influence, but it is a matter of experience that a droplet of mercury (with a very high surface tension) will be more nearly spherical than a drop of water or organic liquid of comparable size.

4. ***Saddle-shaped surfaces***

A soap film open to the same pressure on both sides, as in the case of Fig. 2-23(d) is interesting. The surface must be one of zero mean curvature everywhere because Δp is zero, yet the film is clearly "curved." This does not mean that the surface must be flat, but may be saddle-shaped, as shown in Fig. 2-36. The two plane curvatures must be equal in magnitude and opposite in sign so that the *sum*: $(1/R_1 + 1/R_2)$ is zero. The problem of determining the surface satisfying the condition of zero mean curvature and passing through a given closed (non-planar) curve (or set of curves) in space is known as "Plateau's problem," after the blind Belgian physicist, J. Plateau, who published work on capillary hydrostatics in the late 1800's[43].

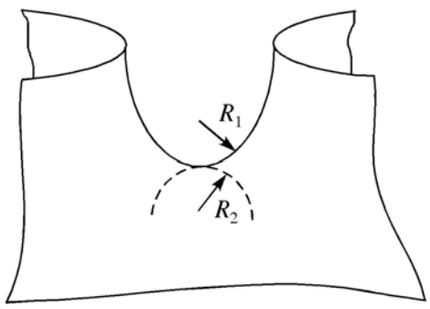

Fig. 2-36: Saddled-shaped surface (surface of zero mean curvature).

It can be proven that this is also the surface of minimum area passing through the given closed curve(s). A number of fascinating experiments with Plateau's problem can be done with a soap solution and wire frames of various shapes, as suggested by Fig. 2-37. A delightful account of experiments that can be done with soap films has been written by C.V. Boys[44]. It is the substance of a series of lectures delivered to juvenile and

---

[42] A delightful 47-minute suite of zero-*g* experiments conducted by NASA on board the Space Station can be viewed at: http://www.youtube.com/watch?v=jXYlrw2JQwo

[43] Plateau, J. A. F., **Statique expérimentale et théorique des liquides soumis aux seules forces moléculaires,** Gauthier-Villars, Trubner et cie, F. Clemm, 2 Vols., 1873.

[44] Boys, C.V., **Soap Bubbles: Their Colors and the Forces Which Mold Them**, Dover, New York, 1959.

popular audiences in 1889-1890. A more detailed description of much of its contents is given by Isenberg.[45]

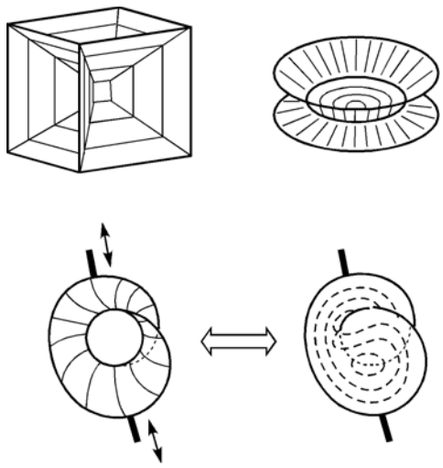

Fig. 2-37: Some soap-films suspended on wire frames. Many interesting saddle-shaped surfaces may be created by selectively puncturing different panels (using an alcohol-dipped pencil point) on the cubical frame. Puncturing the center panel on the structure between circular loops leads to a film as shown in Fig. 2-23(d). The film on the spiral wire may jump between two shapes as the spiral is squeezed or distended.

The apparent mechanical equivalence between a flat surface and a saddle-shaped surface of zero mean curvature belies the assumption that an interface shape may be specified completely in terms of a single variable, such as κ or R_m. The interface shape in fact requires *two* variables for its specification. These may be chosen as the two principal radii of curvature, R_1 and R_2, defined earlier, but more commonly one uses the curvature κ, defined by Eq. (2.31), as the first variable, and

$$\lambda + = \frac{1}{R_1 R_2}, \tag{2.58}$$

termed the *Gaussian* curvature, as the second. Different nomenclature and notation are sometimes used. The *mean* curvature, defined as $H = 1/2\ \kappa$, is termed the "Hermitian curvature." Gaussian curvature is generally important in those cases when the interfacial layer has a highly organized structure, as might be the case for close-packed surfactant monolayers or bilayers. Such interfaces may resist bending deformations in accord with the relationship given by Helfrich:[46]

$$F^{\sigma}(\text{bending}) = \frac{1}{2} k_1 \left(\kappa - \kappa_o\right)^2 + k_2 \lambda, \tag{2.59}$$

where $F\sigma$(bending) is the Helmholtz free energy/area of an interface attributable to its state of bending, and k_1 and k_2 are the "mean bending modulus" and the "saddle splay modulus," respectively. These constants have units of energy and magnitudes of order kT. κ_0 is the "spontaneous curvature," taken as zero for interfacial layers of symmetrical structure (Critical Packing Parameter $\approx$ 1, *cf.* Chap. 3.I), but non-zero otherwise. The spontaneous Gaussian curvature is taken as zero in all cases. A second

---

[45] Isenberg, C., **The Science of Soap Films and Soap Bubbles**, Dover Publ., New York, 1992.
[46] Helfrich, W., *Z. Naturforsch.*, **28c**, 693 (1973); **33a**, 305 (1978).

Helfrich Equation expresses the interfacial tension in such systems as a function of curvature:

$$\sigma_{\text{curved}} = \sigma_{\text{flat}} + \frac{1}{2} k_1 \kappa^2 - k_1 \kappa_o \kappa + k_2 \lambda . \qquad (2.60)$$

The magnitudes of k_1 and k_2 are such that even for these structured interfaces, the interfacial tension is effectively independent of curvature for radii of curvature in excess of a few tens of nanometers.

H. The measurement of surface and interfacial tension

1. *Geometric vs. force methods*

A large number of methods and devices for measuring surface or interfacial tension in the laboratory have been proposed, and many are now represented by commercial instrumentation. A few examples are listed in Table 2-5. Solutions to the Young-Laplace Equation, one way or another, provide the basis for their use. Some, termed geometric methods, are based

Table 2-5: Some methods for measuring surface or interfacial tension.

Geometric methods

- Capillary rise
- Sessile drop (captive bubble)
- Pendant drop (pendant bubble)
- Spinning drop
- Oscillating jet
- Contracting circular jet

Force methods

- Du Nüoy ring detachment
- Wilhelmy slide (or rod)
- Langmuir barrier
- Drop weight (volume)
- Maximum bubble pressure

on a direct determination of an interface shape or position. In these cases, the boundary tension is determined by finding the value for it that produces the best match between a measured interfacial profile or location and the appropriate solution to the Young-Laplace Equation. Force methods, on the other hand, are based on the measurement of a force or its equivalent, such as a mass, volume or pressure, and its comparison with the value computed using the Young-Laplace Equation. In the latter case, one most often deals with a solid object suspended in or detached from a fluid interface or a liquid drop detached from an orifice. Since the geometry of the experimental situation can be designed to be convenient, one is essentially always dealing with interfaces of a high degree of symmetry. The interfaces are usually

closed-axisymmetric or cylindrical (in the general sense). A few of the methods that are important historically or are commonly used in present-day laboratories are described briefly below.

2. *Capillary rise*

One of the oldest methods for measuring surface tension is based on determining the position of the meniscus of the liquid in a capillary tube. If the liquid wets the tube wall, which is generally glass, its surface is constrained to meet the wall at a contact angle less than 90°. The meniscus is thus concave upward, requiring that at equilibrium, the pressure above it be greater than the pressure beneath. To achieve equilibrium, the meniscus rises in the tube, as shown in Fig. 2-38, until the hydrostatic pressure beneath the surface (p_0 -ρgh) is sufficiently below atmospheric (p_0) to support the

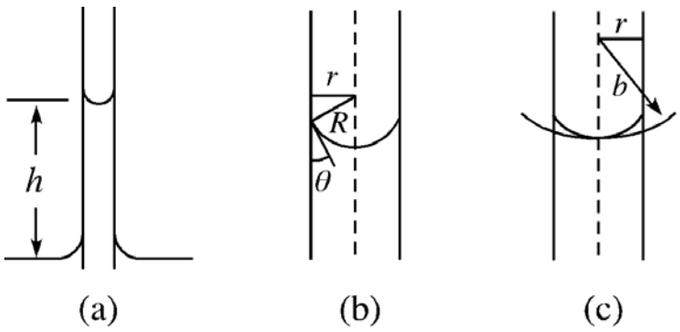

Fig. 2-38: The capillary rise method for measuring surface tension. (a) h is the equilibrium rise height, (b) If the meniscus is spherical, but the contact angle is > 0°, the radius of the meniscus is $R = r/\cos\theta$, where r is the radius of the capillary, and θ is the contact angle, (c) if the meniscus is flattened by gravity, the radius of the curvature at its apex is $b > r$.

curvature of the meniscus. The simplest situation arises when $Bo = (\Delta\rho)gr^2/\sigma << 1$ (where r = capillary radius) so that gravity will not flatten the meniscus, and it will be a segment of a sphere. If the contact angle is 0°, the meniscus will be a hemisphere of radius r, so that:

$$\Delta p = \rho gh = \sigma\left(\frac{1}{R_1} + \frac{1}{R_2}\right) = \frac{2\sigma}{r}\ , \tag{2.61}$$

where ρ is the density of the liquid (the density of the overlying gas has been neglected) and h is the height of rise from the flat surface in the vessel to the bottom of the meniscus. (In order to assure a flat surface in the vessel, it should be at least five cm wide, so that for the vessel, $Bo > 100$.) The above formula simplifies to:

$$\sigma = \frac{1}{2}\rho grh\,. \tag{2.62}$$

Parenthetically, it was noted by early investigators (including Leonardo da Vinci) that for a given capillary tube and liquid, the product rh was a constant. It is evident now that

$$rh = \frac{2\sigma}{\rho g} = \text{constant}, \tag{2.63}$$

from which one obtains the original (da Vinci) definition of the capillary constant:

$$a^2 = \frac{2\sigma}{\rho g} = \text{the capillary constant, [=] length}^2. \tag{2.64}$$

The capillary length, a, has been defined earlier and is seen to be the square root of the capillary constant. If the contact angle is different from 0°, (but $Bo << 1$) one would still have a spherical segment as the meniscus, but the radius of curvature would be $R = r/\cos\theta$, as shown in Fig. 2-38(b), and the amount of capillary rise would be correspondingly less. As a practical matter, however, it is necessary that $\theta = 0°$, as this is the only condition which is reliably reproducible. The condition is generally satisfied for most liquids against glass (with the notable exception of mercury, for which $\theta > 90°$, resulting in capillary *depression*) if the glass is scrupulously clean and has been put in contact with the liquid for a sufficient period of time (*i.e.*, "seasoned"). The liquid is generally brought to a level above the equilibrium rise height and allowed to recede to the equilibrium position. It is thus the receded angle that must be 0°. Also, one usually uses a device with two tubes of different radius with a precision cathetometer to measure the difference in capillary rise between them.

The radius of the capillary required to achieve $Bo < 0.01$ is generally less than 0.2 mm, often impracticably small. For larger tubes, the meniscus must be treated as a general surface of revolution, flattened to some extent by gravity. The surface tension in this case can be expressed in terms of the rise height and the radius of curvature, b, of the meniscus at its apex, as shown in Fig. 2-38. But determining b amounts to solving for the entire meniscus configuration using the Bashforth-Adams tables. This is extremely inconvenient since the unknown (σ) is buried in β and b, and tedious trial and error is required. Thus Sugden[47] derived tables from those of Bashforth and Adams for use with the capillary rise method. They give values of (r/b) *vs.* (r/a) (where a = the capillary length) for the case of $\theta = 0°$, as shown in Table 2-6. The procedure for using the tables is one of successive approximation.

---

[47] Sudgden, S., *J. Chem. Soc.*, **1921**, 1483.

Table 2-6: Sugden's tables for capillary-rise corrections.

Values of r/b for values of r/a

r/a	0.00	0.01	0.02	0.03	0.04	0.05	0.06	0.07	0.08	0.09
0.00	1.0000	9999	9998	9997	9995	9992	9988	9983	9979	9974
0.10	0.9968	9960	9952	9944	9935	9925	9915	9904	9893	9881
0.20	9869	9856	9842	9827	9812	9796	9780	9763	9746	9728
0.30	9710	9691	9672	9652	9631	9610	9589	9567	9545	9522
0.40	9498	9474	9449	9424	9398	9372	9346	9320	9293	9265
0.50	9236	9208	9179	9150	9120	9090	9060	9030	8999	8968
0.60	8936	8905	8873	8840	8807	8774	8741	8708	8674	8640
0.70	8606	8571	8536	8501	8466	8430	8394	8358	8322	8286
0.80	8249	8212	8175	8138	8101	8064	8026	7988	7950	7913
0.90	7875	7837	7798	7759	7721	7683	7644	7606	7568	7529
1.00	7490	7451	7412	7373	7334	7295	7255	7216	7177	7137
1.10	7098	7059	7020	6980	6941	6901	6862	6823	6783	6744
1.20	6704	6655	6625	6586	6547	6508	6469	6431	6393	6354
1.30	6315	6276	6237	6198	6160	6122	6083	6045	6006	5968
1.40	5929	5890	5851	5812	5774	5736	5697	5659	5621	5583
1.50	5545	5508	5471	5435	5398	5362	5326	5289	5252	5216
1.60	5179	5142	5106	5070	5034	4998	4963	4927	4892	4857
1.70	4822	4787	4753	4719	4686	4652	4618	4584	4549	4514
1.80	4480	4446	4413	4380	4347	4315	4283	4250	4217	4184
1.90	4152	4120	4089	4058	4027	3996	3965	3934	3903	3873
2.00	3843	3813	3783	3753	3723	3683	3663	3633	3603	3574
2.10	3546	3517	3489	3461	3432	3403	3375	3348	3321	3294
2.20	3267	3240	3213	3186	3160	3134	3108	3082	3056	3030

The first estimate is $a \approx \sqrt{rh}$. Then r/a is computed and r/b is obtained from the table, giving an estimate of b. The next estimate of a is: $a \approx \sqrt{bh}$, from which r/a is computed, *etc*., to convergence. It seldom requires more than three rounds.

Lord Rayleigh[48] proposed a convenient approximate solution, valid for $Bo \leq 0.04$, in the form:

$$a^2 = r\left(h + \frac{r}{3} - \frac{0.1288r^2}{h} + \frac{0.1312r^3}{h^2} \ldots\right). \tag{2.65}$$

For wide tubes ($Bo > 10$), he proposed the approximate formula:

$$\ln\left(\frac{h}{a}\right) = 0.6648 + 0.1978\left(\frac{a}{r}\right) - \sqrt{2}\left(\frac{r}{a}\right) + \frac{1}{2}\ln\left(\frac{r}{a}\right). \tag{2.66}$$

[48] Lord Rayleigh (J. W. Strutt), *Proc. Roy. Soc*., **A92**, 184 (1915).

3. ***Sessile drop and pendant drop***

Among the most commonly used methods for measuring boundary tension are those in which the shape profiles of drops or bubbles are determined and compared with solutions of Bashforth and Adams with the value of σ chosen that produces the best fit. The most common methods of this type are those of the sessile drop (or captive bubble) and the pendant drop (or bubble) as pictured in Fig. 2-39. An expedited method obtains the fit in terms of a pair of descriptive parameters, commonly the maximum diameter, and the height above it (or below it). Tables derived from the Bashforth-Adams calculations can then be used to estimate surface tension.

At present it is more common to use a commercially available axisymmetric drop shape analysis (ADSA) system, as shown schematically in Fig. 4-22 (where it is discussed in the context of determining contact angle). An accurate drop or bubble profile is obtained using a precision CCD camera, and the full profile match is effected using a computer.

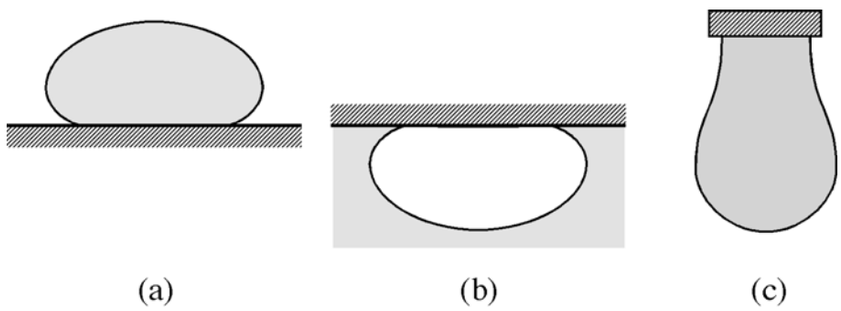

Fig. 2-39: Axisymmetric drop profiles: (a) sessile drop, (b) captive bubble, (c) pendant drop.

4. ***Du Noüy ring detachment***

In this method, pictured in Fig. 2-40, one measures the force required to detach a ring (usually of platinum) from a surface. A schematic plot is shown of the measured downward force as a function of the height of the ring above the undisturbed surface of the liquid. It is the maximum in the measured force that is used to determine the boundary tension. After the maximum is reached, the meniscus beneath the ring begins to contract before final detachment occurs. Since the maximum force is what is needed, most current instrumentation does not actually detach the ring. The maximum downward force on the ring is given by

$$(\text{Force})\downarrow \; = \frac{4\pi R\sigma}{F_c}, \tag{2.67}$$

where R is the radius of the ring and F_c is a correction factor for which there are tables[49] or empirical fitting formulas.[50-51] It represents the weight of the

[49] Harkins, W. D., and Jordan, H. F., *J. Amer. Chem. Soc.*, **52**, 1751 (1930).

subtended liquid at the point of maximum force. The needed correction factor is generally automatically implemented in current commercial instrumentation. The method is generally suitable for interracial as well as surface tension measurements. Other objects of known wetted perimeter (*e.g.*, plates, cylinders, *etc.*) can also be detached from surfaces and the appropriate forces measured and analyzed to give the boundary tension.

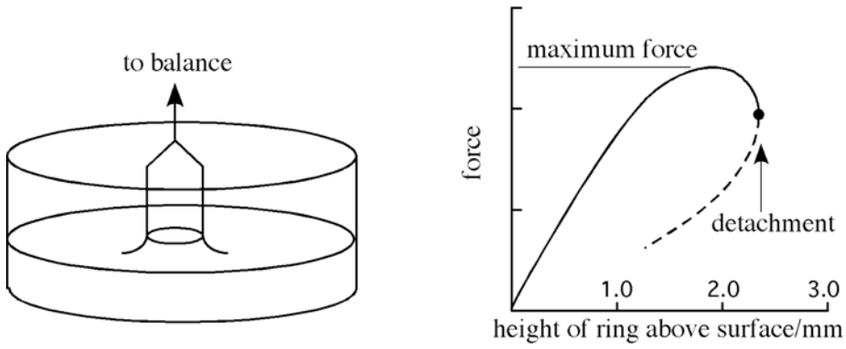

Fig. 2-40: du Nüoy ring detachment method.

5. *Wilhelmy slide*

In a simple but powerful method one measures the downward force on an object partially immersed in the liquid. The usual configuration is a dipping slide, as shown in Fig. 2-41 (left), known as a Wilhelmy slide. In some cases a rod is convenient to use rather than a slide, as shown at the right. It is assumed that the contact angle of the liquid against the solid surface is 0°, in which case the downward force on it consists of its weight

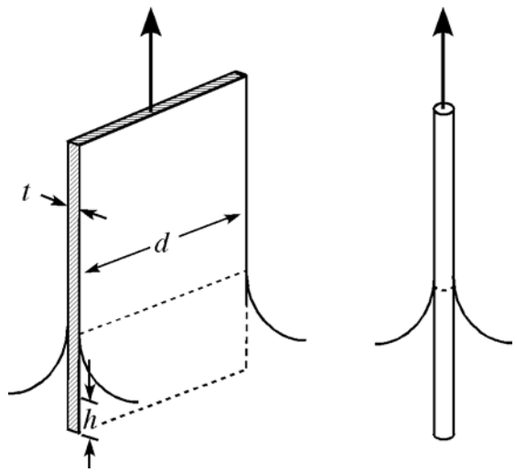

Fig. 2-41: Wilhelmy slide (or rod).

in air, plus the downward-pulling interline force of surface tension acting around its wetted perimeter, minus the buoyancy force due any protrusion of the plate (or rod) beneath the level of the undisturbed liquid surface. The weight in air is usually zeroed out, so the net downward force is given by:

---

[50] Freud, B. B., and Freud, H. Z., *J. Amer. Chem. Soc.*, **52**, 1772 (1930).
[51] Zuidema, H. H., and Waters, G. W., *Ind. Eng. Chem.*, **13**, 312 (1941).

$$F_{\text{net}} = \sigma \cdot (\text{wetted perimeter}) - (\text{buoyancy}) . \tag{2.68}$$

For a rectangular plate of width d and thickness t, extending a distance h beneath the flat, undisturbed surface of the liquid:

$$F_{\text{net}} = \sigma \cdot (2d + 2t) - \rho ghtd . \tag{2.69}$$

Since the plates used are usually thin ($t << d$), and measurements are made at the point where $h = 0$, σ is evaluated from:

$$\sigma = \frac{F_{\text{net}}}{2d} . \tag{2.70}$$

The Wilhelmy technique is often used for measurement of the surface tension, σ, of water in a rectangular trough, covered with an insoluble (Langmuir) surfactant monolayer. In a method pioneered by Agnes Pockels,[52] and shown schematically in Fig. 2-42, one compresses or expands the surfactant film by means of a movable barrier that seals the liquid surface on one side from that on the other. Surface tension is monitored during compression or expansion by measuring the force on the plate held in null position.

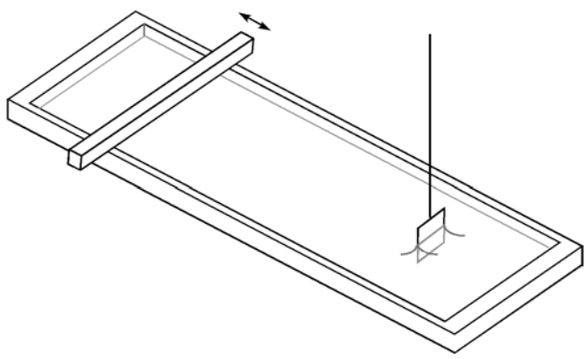

Fig. 2-42: Schematic of Pockels' trough, with Wilhelmy slide.

6. *Langmuir film balance*

Another method for measuring the surface tension of monolayer-covered liquid surfaces is to divide the trough surface into two parts by a movable boom, as shown in Fig. 2-43. The boom is connected to the trough edges by flexible hydrophobic threads that seal the parts of the surface from one another. The film is deposited on one side, while the other side presents a clean water surface. A force equal to σW, where W is the boom length, pulls on the film side of the boom, while the force $\sigma_0 W$, where σ_0 is the surface tension of pure water, pulls in the opposite direction. The net force on the boom, $F_{\text{net}} = (\sigma_0 - \sigma)W$, is measurable by means of rigid connection to a calibrated torsion wire. When the monolayer is soluble to some extent, the subphase portions between the two parts of the surface may be kept apart by

---

[52] Pockels, A., *Nature*, **43**, 437 (1891).

a flexible membrane connecting the boom and its tethers to the bottom of the trough.

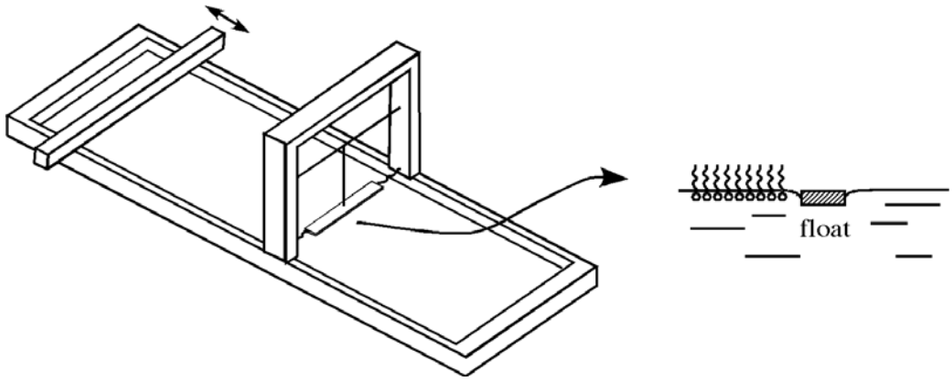

Fig. 2-43: Langmuir film balance.

7. *Drop weight (or volume)*

In this method, drops are formed, as shown in Fig. 2-39(c), and made to grow until they break away by gravity. The collective volume (or weight) of several drops is measured. Despite the complexity of the break-off event, as shown in the rapid sequence photographs of Fig. 2-44, the size at break-off is a reproducible function of σ for a given nozzle radius, and fluid density difference.[53] To a rough approximation, the weight of the drop is given by $2\pi r\sigma$, where r is wetted tube radius, assuming the surface is vertical around the perimeter at the time of rupture, and that no liquid is retained on tip when detachment occurs. Actual results may be conveniently expressed as

$$mg = r\sigma \frac{1}{F_c}, \tag{2.71}$$

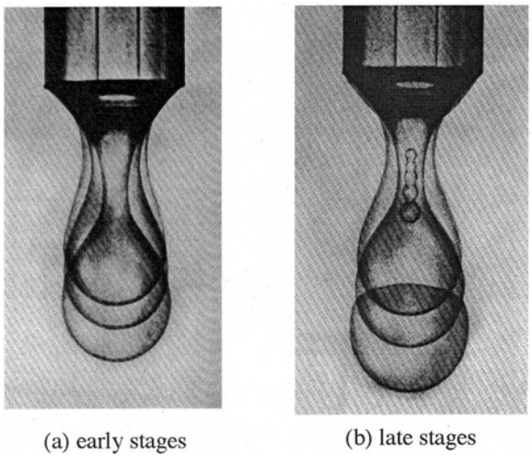

Fig. 2-44: Break-off of water drops in air. From [Pierson, F. W., and Whitaker, S., *J. Colloid Interface Sci.*, **54**, 219 (1976).]

where m is the drop mass and the correction factor F_c is a universal function of (V/r^3), where V is the drop volume. F_c accounts primarily for liquid

[53] Harkins, W. D., and Brown, F. E., *J. Amer. Chem. Soc.*, **41** 499 (1919).

retained on the tip after detachment and has been given in tabular form,[54] and fit analytically by[55]:

$$F_c = 0.14782 + 0.27896\left(\frac{r}{V^{1/3}}\right) - 0.1662\left(\frac{r}{V^{1/3}}\right)^2, \qquad (2.72)$$

valid for $0.3 < (r/V^{1/3}) < 1.2$. The drop weight method may be used for interfacial as well as surface tension measurement. In the latter case, the drop mass m is replaced by $V|\rho'' - \rho'|$, where ρ' and ρ'' are the densities of the two liquids involved. Instruments are available commercially,[56] but a home-built setup for interfacial tension measurement is shown schematically in Fig. 2-45. Oil drops are formed in an inverted water-filled vessel with a side arm. The mass of water displaced by the formation of a given number of oil drops is used to determine the oil drop size.

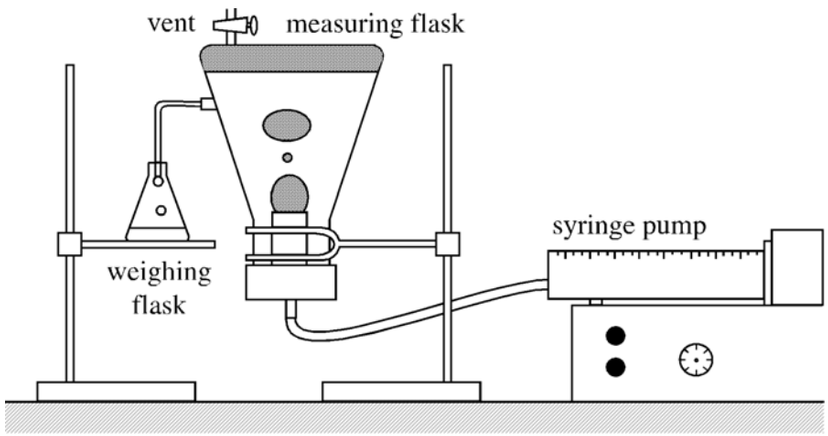

Fig. 2-45: Drop weight method for interfacial tension measurement.

8. *Maximum bubble pressure and dynamic surface tension*

In the formation of a bubble from a nozzle tip, as shown in Fig. 2-46, maximum pressure is required when the radius of curvature of the bubble is minimum (for $Bo << 1$), and under these conditions the surface is a hemisphere, with $p_{max} - p_{liq} = 2\sigma/r$, where r is the radius of the capillary. For larger capillaries, the appropriate corrections can be worked out for the bubble flattening using the Bashforth and Adams tabulations, as in the capillary rise method. A useful approximate formula (with reference to Fig. 2-46) is:

$$\sigma = \frac{r}{2}p_{max} - \frac{1}{3}\rho g r^2 - \frac{1}{2}\rho g r h - \frac{\rho g^2 r^2}{12\left(p_{max} - \rho g h\right)}, \qquad (2.73)$$

---

[54] Lando, J. L., and Oakley, H. T., *J. Colloid Interface Sci.*, **25**, 526 (1967).

[55] Heertjes, P.M., De Nie, L.H., and De Vrie, H.J., *Chem. Eng. Sci.*, **26**, 441 (1961).

[56] Gilman, L. B.,(Krüss USA) "A Review of Instruments for Static and Dynamic Surface and Interfacial Tension Measurement," presented at 84th AOCS Ann. Mtg. and Expo, Anaheim, CA Apr. 27, 1993.

where h is the depth of the capillary tip beneath the surface of the liquid. For very small tubes (giving $Bo < 0.01$), the final three terms of Eq. (2.73) are negligible. The maximum bubble pressure method has the advantage of being very rapid, and the surface formed is fresh. The method is good for difficult-to-access liquids, such as molten metals, polymer melts, *etc*., and for rapid "on-line" determinations of surface tension in general.

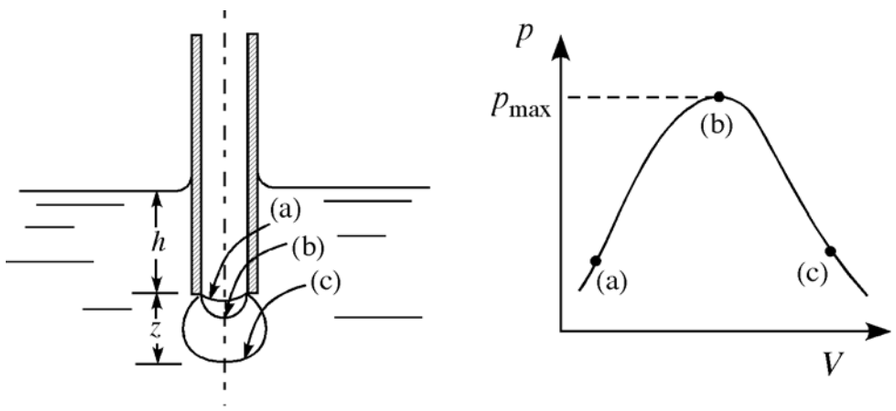

Fig. 2-46: Maximum bubble pressure method.

One of the most important advantages of the maximum bubble pressure method is that it is amenable to dynamic surface tension measurement, usually down to surface ages of a few milliseconds or less. Surface tension is often time dependent as a result of slow solute diffusion to the interface, kinetic barriers to adsorption or desorption, surface chemical reaction rates, including denaturation, *etc*., as mentioned earlier and discussed further in Chap. 3. Many of these processes, such as spray coating, pesticide or herbicide spray applications and ink-jet printing, produce changes over time scales of practical interest. Structural changes accompanying the formation of fresh surfaces of pure liquids occur over time scales of *micro*seconds or less, and are not of practical interest. While the methods of drop (or bubble) shape analysis, Wilhelmy tensiometry and drop weight determination are useful for surface ages of the order of one second or greater, they are not applicable for the much shorter times that are often of practical interest. In commercial maximum bubble pressure devices, the bubbling rate may be varied so that the surface tension corresponding to a range of surface ages may be obtained. A bubble tensiometer currently available from Lauda Instruments (Model MPT-2)[57] is capable of measurements for surface ages from about three seconds down into the sub-millisecond time range.

9. *The pulsating bubble "surfactometer"*

A useful variation on the maximum bubble pressure method employs a single small bubble suspended at the end of a capillary and made to pulsate and therefore produce sinusoidal time variations in the bubble surface area.

---

[57] Munsinger, R. A., *Amer. Lab. News*, Jan. (1997).

The device is termed commercially a "surfactometer,"[58] and is shown schematically in Fig. 2-47. The bubble radius is made to oscillate between 0.40 and 0.55 mm at frequencies from 1 to 100 cycles/min. The sample chamber contains 25 μL, usually of a surfactant solution, that communicates with ambient air through a capillary, which also serves as the airway for bubble formation. The liquid sample is pulsed by means of a volume displacement piston to produce the desired radius variation, while the pressure inside the chamber is monitored using a sensitive pressure transducer. Assuming the bubble to be spherical, knowledge of its size and the chamber pressure suffices to calculate the surface tension.[59] The method is especially applicable to the study of the dynamics of surfactant monolayers, in particular lung surfactant, and has the advantage of producing wider ranges of surface compression/expansion rates and requiring much smaller sample sizes than the Langmuir trough.

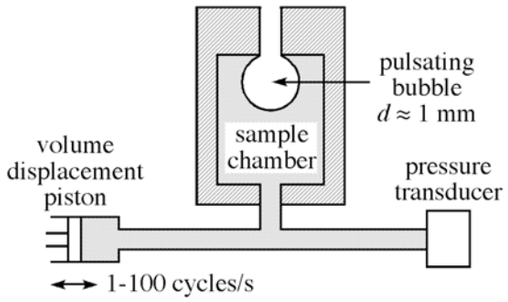

Fig. 2-47: Schematic of the pulsating bubble "surfactometer."

10. ***Elliptical (vibrating) jet***

One of the earliest devices for measurements of dynamic surface tension in the millisecond range was the elliptical (oscillating) jet. In this method, now primarily of historical interest, a liquid is forced through an elliptical orifice at a sufficient rate to form a jet. The jet attempts to "correct" its noncircular cross-section, and in so doing overshoots and oscillates about a circular shape, as shown in Fig. 2-48. The value of the surface tension can be computed from knowledge of the jet parameters, fluid density and the measured wavelength of the oscillations, as originally shown by Nils Bohr, but in simplified form for liquids of low viscosity by Sutherland:[60]

$$\sigma \approx \frac{2\rho Q^2\left(1+37a^2/24b^2\right)}{3a\lambda^2\left(1+5\pi^2a^2/3\lambda^2\right)}, \tag{2.74}$$

where Q = volumetric flow rate; $a = r_{max} + r_{min}$, and $b = r_{max} - r_{min}$. When σ is changing with time (surface age), as by the adsorption of a solute that must first diffuse to the surface, λ will vary with distance along the jet (*i.e.*, time).

---

[58] Enhorning, G., *J. Appl. Physiol.*, **43**, 198 (1977).

[59] This assumption has been relaxed: Seurynck, S.L., *et al., J. Appl. Physiol.*, **99**, 624 (2005).

[60] Sutherland, K. L., Aust. *J. Chem.*, **7**, 319 (1954).

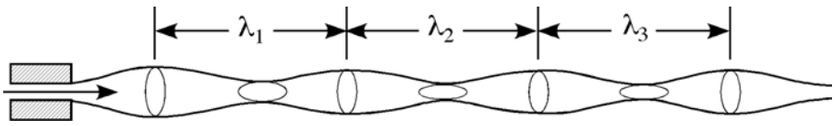

Fig. 2-48: Elliptical oscillating jet.

Since the flow rate is known, one can measure the wavelength λ as a function of position and, knowing the rate of jet flow, extract the time variation of the surface tension. Usually up to seven or eight wavelengths can be realized before the jet disintegrates. It is generally not a good method for interfacial tension, because the jet breaks up too quickly. A number of practical difficulties have precluded the method from being realized commercially, but its use in earlier studies was indispensable in the study of dynamic processes at interfaces.

11. *Contracting circular jet*

For surface or interface lifetimes in the hundredths of a second range, the elliptical jet is not practical, but the contracting circular jet method may be used, in particular for oil-water interfacial tensions.[61] The extent of contraction in a given distance for a given set of jet parameters and fluid properties can be related directly to the interfacial tension.

12. *Problems with interfacial tension measurement*

There are sometimes difficulties in the measurement of interfacial tension that do not arise in the measurement of surface tension. While the drop shape analysis, the ring detachment method and drop weight methods are all in principle adaptable to interfacial tension measurements, their use is limited to systems with an adequate density difference between the liquids and/or a sufficiently high value of the interfacial tension itself. From a practical point of view, a density difference of at least 0.10 specific gravity units is required. Otherwise, the drop shape will be too close to spherical for accurate matching with the Bashforth-Adams computed profiles, and for the drop weight method, drops of impractically large size are obtained. In the ring detachment method, very large displacements of the ring above the surface are required for the maximum force to be attained. The recommended method for handling the problem is to carefully equilibrate the two liquids (with respect to any mutual solubility), as in a separatory funnel, remove samples of each liquid and measure their respective surface tensions. The needed interfacial tension can then be computed using Antanow's Law, Eq. (2-20).

Another problem arises if the interfacial tension between the liquids is extremely small (< 0.1 mN/m). It is then difficult to adequately pin a drop for profile determination, *i.e.*, either one liquid or the other will wet out the

---

[61] England, D. C., and Berg, J. C., *AIChE J.*, **17**, 313 (1970).

surface, producing contact angles either approaching 0° or 180°. The detachment method requires such small forces and displacements that accurate determination of the low interfacial tension is difficult. The problem is addressed by the spinning drop method described below.

13. *Spinning drop method*

The spinning drop method[62], shown in Fig. 2-49, is especially useful for determining ultra-low interfacial tensions of the type encountered in the polymer-surfactant flooding strategies for tertiary oil recovery. A drop of the less dense liquid is injected into a capillary tube containing the denser fluid. The tube is spun on its axis until the suspended drop is elongated into a cylindrical shape with hemispherical caps. The lower the interfacial tension, the greater will be the elongation. When the drop length is much greater than the radius, r_m, the result is:

$$\sigma = \frac{(\Delta\rho)\omega^2 r_m^3}{4}, \tag{2.75}$$

where $\Delta\rho$ is the density difference between the liquids, and ω is the angular velocity of rotation about the tube axis.

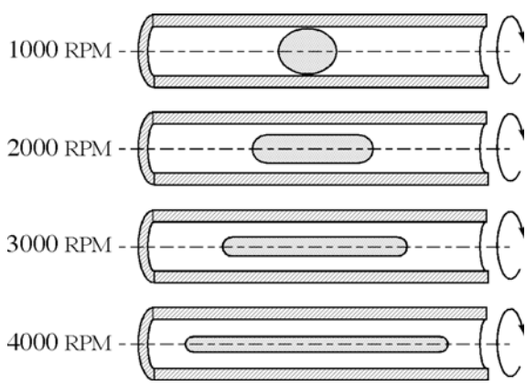

Fig. 2-49: Spinning drop method. Drawing taken from photographs showing a heptane drop (0.156 cm^3) in glycerol rotating at various speeds about a horizontal tube axis. Redrawn from [Princen, H. M., Zia, I., and Mason, S. G., *J. Colloid Interface Sci.*, **23**, 99 (1967).]

I. Forces on solids in contact with liquids: capillary interactions

1. *Liquid bridges*

Recall that liquids exert forces on solids in contact with them through the action of boundary tension. When two or more solid objects are in contact with the same liquid mass, such that they share a meniscus there are effective forces (referred to as capillary forces) acting between the solid bodies, tending either to draw them together or to push them apart. It is convenient to distinguish between two categories of systems, *viz.*, liquid bridges and shared menisci, as shown in Fig. 2-50.

---

[62] Vonnegut, B., *Rev. Sci. Inst.*, **13**, 6 (1942).

When a finite liquid mass separates two solids, it is referred to as a "liquid bridge." A similar configuration (a "vapor bridge") is created when a bubble joins two particles immersed in a liquid medium. Consider as an example, a drop of liquid between a pair of horizontal flat plates wet by the

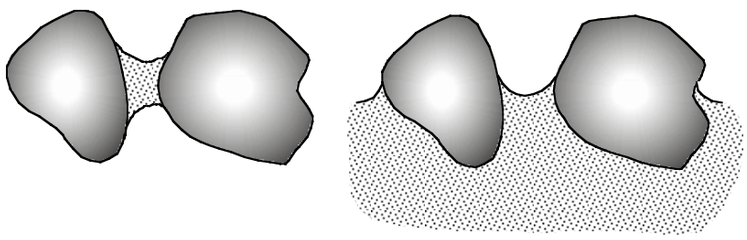

(a) (b)

Fig. 2-50: (a) Liquid bridge, (b) shared meniscus.

liquid as shown in side view in Fig. 2-51. The volume of the drop is small, but since the plate spacing, h, is also considered very small, the diameter of the drop D (as would be observed in a top view) may be large. Focusing on the upper plate, one may note that there are two types of forces (apart from gravity) drawing it toward the lower plate. The first of these is the downward component of the *interline force* acting around the perimeter of the drop, *viz.* $\pi D\sigma \sin\theta$, where θ is the contact angle of the liquid against the

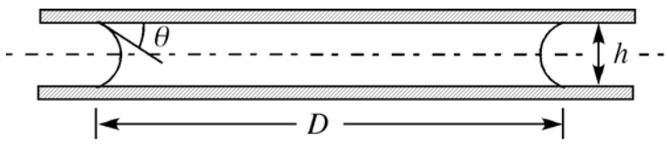

Fig. 2-51: Liquid bridge between horizontal flat plates.
Not in perspective, since $h << D$.

glass plate. The second contribution is the *capillary pressure force*, *i.e.*, the force pulling down on the upper plate because the liquid is on the convex side of the fluid interface, rendering the pressure inside the liquid lower than that outside by an amount Δp, the Young-Laplace pressure jump. This produces a pressure force acting to hold the plates together equal to Δp times the area which is wetted ($\pi D^2/4$). The capillary pressure force, which can be considerable if θ is low and the plate spacing is small, is often much larger than the interline force, which may then be neglected.

Δp is given by the Young-Laplace Equation: $\Delta p = \sigma(1/R_1 + 1/R_2)$. The meniscus is a saddle with $R_2 = -D/2$ (the minus sign being used to account for the fact that this curvature is opposite in sign to that of the profile of the figure). Since $h << D$, one may neglect $1/R_2$, and treat the meniscus as effectively a cylindrical surface, and if it is assumed further that h is sufficiently small that $Bo << 1$, it is a right circular cylindrical surface, whose radius is $R_1 = (h/2)/\cos\theta$. Thus:

$$F\downarrow = \Delta p\frac{\pi D^2}{4} = \sigma\frac{\cos\theta}{(h/2)}\frac{\pi D^2}{4} \equiv \frac{\sigma\pi D^2\cos\theta}{2h}. \tag{2.76}$$

For the case of perfect wetting, $\theta = 0°$, and

$$F\downarrow = \frac{\sigma\pi D^2}{2h}. \tag{2.77}$$

This "adhesive" force must be overcome if the plates are to be separated, and the formation of a liquid bridge is the first step in the formation of an adhesive bond. It is clear that it becomes very large as $h \rightarrow 0$. It is also seen to go to zero as θ approaches 90°, and becomes negative (*i.e.*, a force pushing the plates apart) if $\theta > 90°$, *i.e.*, the plates are unwet.

Liquid bridges, as described above, can be formed between solids of various shapes. For example, Fig. 2-52 shows the establishment of a liquid bridge between a cylinder and a plane. The total force acting to hold the objects together consists of three terms. The first two are capillary forces of

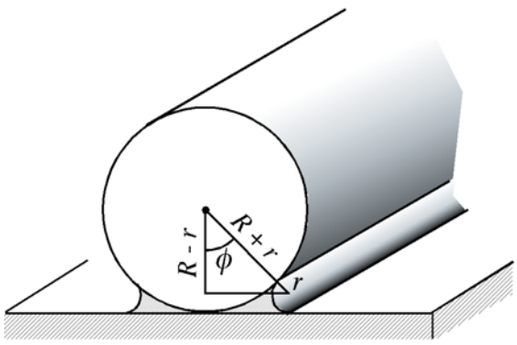

Fig. 2-52: Liquid bridge between a cylinder and a flat plate.

the same type as those described above for the flat plates, *viz.*, the downward force of the liquid surface tension acting along the cylinder-liquid interline and the force due to the Young-Laplace pressure deficit within the liquid. A third term may arise because the solids in this system are in direct contact, leading to a solid-solid adhesion term, as described later in Chap. 4. This last effect can often be neglected because the presence of even small degrees of roughness precludes significant direct solid-solid contact (unless the solids are soft and subject to flattening). If the liquid masses are sufficiently small that $Bo << 1$, and that the contact angle θ is 0°, the downward capillary forces per unit length acting on the cylinder are given by:

$$(F/L)\downarrow = 2\sigma\sin\phi + \Delta p(2R\sin\phi). \tag{2.78}$$

Thus with a circular meniscus, $\Delta p = \sigma/r$, and with reference to Fig. 2-52, it can be seen that the cylinder radius R, the meniscus radius r and the filling angle ϕ are related to one another in accord with

$$\frac{(R-r)}{(R+r)} = \cos\phi, \quad \text{or} \quad r = R\frac{(1-\cos\phi)}{(1+\cos\phi)}, \tag{2.79}$$

and $\Delta p = \dfrac{\sigma}{R}\dfrac{(1+\cos\phi)}{(1-\cos\phi)}$. Substituting into Eq. (2.78):

$$\frac{F}{L} = 2\sigma\sin\phi + \frac{\sigma}{R}\left[\frac{1+\cos\phi}{1-\cos\phi}\right](2R\sin\phi) = 4\sigma\left[\frac{\sin\phi}{1-\cos\phi}\right] \quad . \qquad (2.80)$$

It is to be noted that as $\phi \rightarrow 0$, $F/L \rightarrow \infty$. Thus the adhesive force is maximized when the amount of liquid is *very* small. Anyone who has glued together the parts of model airplanes knows this. Equation (2.80) is not valid, of course, when $\phi \approx 0$, since the continuum concept of surface tension breaks down as the meniscus approaches molecular dimensions, although there is evidence that this does not occur until r is less than a few nm.[63]

The adhesive force of a liquid bridge between two cylinders also approaches infinity as the bridge size approaches zero. For equal-sized cylinders,

$$\frac{F}{L} = \frac{2\sigma\sin\phi}{1-\cos\phi} \quad \text{(half the cylinder-plane value).} \qquad (2.81)$$

The expression for the adhesive force between a sphere and a plane is:

$$F = \pi R\sigma(1+\cos\phi)(3-\cos\phi), \qquad (2.82)$$

which approaches a *finite* constant as $\phi \rightarrow 0$, *viz.*,

$$F_{\lim} \rightarrow 4\pi R\sigma. \qquad (2.83)$$

a result confirmed by experiment.[64] The corresponding results for equal-sized spheres are:

$$F = \frac{1}{2}\pi R\sigma(1+\cos\phi)(3-\cos\phi), \text{ with} \qquad (2.84)$$

$$F_{\lim} \rightarrow 2\pi R\sigma. \qquad (2.85)$$

The physically important case of a liquid bridge between *crossed* circular cylinders of geometric mean radius R, shown in Fig. 2-53, yields a

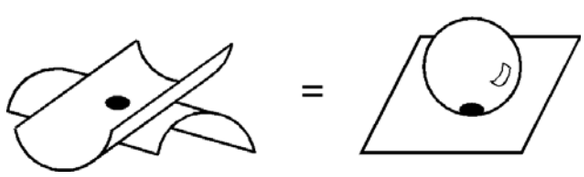

Fig. 2-53: Equivalence of small liquid bridges between crossed cylinders and a sphere and plane.

---

[63] Fisher, L. R., and Israelachvili, J. N., *Colloids Surfaces*, **3**, 303 (1981).
[64] McFarlane, J. S., and Tabor, D., *Proc. Roy. Soc. A,* **202**, 224 (1950).

force the same as that given for the bridge between a sphere of radius R and a flat plate, as long the condition of $r << R$ holds.[67] It should be recalled that all of the formulae developed above refer to the case in which the contact angle is 0°. They may all be modified to accommodate the case in which θ is finite, or is different against the two solid surfaces.[65] It should also be noted that the results above assume either a perfect line or point of direct contact between the solid surfaces subtending the liquid bridge. If these solid surfaces are held even a very small distance (a few nm) apart, as by intervening particles or asperities, the relationship between the bridge strength and bridge size is very different. Instead of rising monotonically as ϕ decreases, the inter-particle force rises to a maximum at some finite ϕ and then falls abruptly to zero as $\phi \rightarrow 0$.

Liquid bridge formation underlies the important process for the size-enlargement of fine powders or particulates known as *spherical agglomeration*. The bridging liquid is immiscible with the dispersion medium and must preferentially wet the particles. The process is used in granulation, balling, pelletization, tabletting and sintering to produce, *e.g.*, ceramic powders, carbon blacks, catalysts, commercial fertilizers, pesticides and pharmaceutical products.[66] It is especially useful for the *selective* collection of one dispersed phase from among many, such as may be desired in mineral beneficiation. The process agglomerates the more hydrophobic particles to a size that can be easily separated from an aqueous dispersion by screening or other mechanical means.

2. *Shared menisci*

Shared menisci refer to fluid interfaces between neighboring solids partially immersed in a common liquid pool. This configuration also leads to apparent forces acting between the solid objects in the direction parallel to the undisturbed interface, tending either to draw them together or push them apart. Solid objects, such as those shown in Fig. 2-50(b), find themselves located in fluid interfaces in the first place by virtue of forces on them *normal* to the undisturbed fluid interface. Aside from the interline forces that act around their wetted perimeters to hold them in the interface, the objects may be floating, *i.e.*, trapped at the interface by gravity. This occurs whenever the object is intermediate in density between the lower and upper fluids. If the objects are denser than the lower fluid, they may be supported by a rigid surface from below (or conversely, if they are lighter than the upper phase, they may be supported from above). In some cases, the interline forces are sufficient to retain the objects in the interface under such conditions (*e.g.*, the "floating" needle or paperclip mentioned in Chap. 1).

The concern here is with forces acting parallel to the interface. To fix ideas, consider the parallel dipping plates held or supported in the interface

---

[65] Orr, F. M., Scriven, L. E., and Rivas, A. P., *J. Fluid Mech.*, **67**, 723, 1975.
[66] Pietsch, W., **Size Enlargement by Agglomeration**, Wiley, New York, 1991.

as shown in Fig. 2-54. It is assumed that liquid may flow between the region between the plates and the outer pool. If the contact angle θ is less than 90°, liquid will rise to some level h required to satisfy the Young-Laplace pressure jump across the curved meniscus. Focusing on the left plate, it is seen to be acted upon by interline forces and hydrostatic (Δp) forces. The interline forces have equal and opposite horizontal components in the amount of $L\sigma\sin\theta$.[67] The capillary rise between the plates (to the level h)

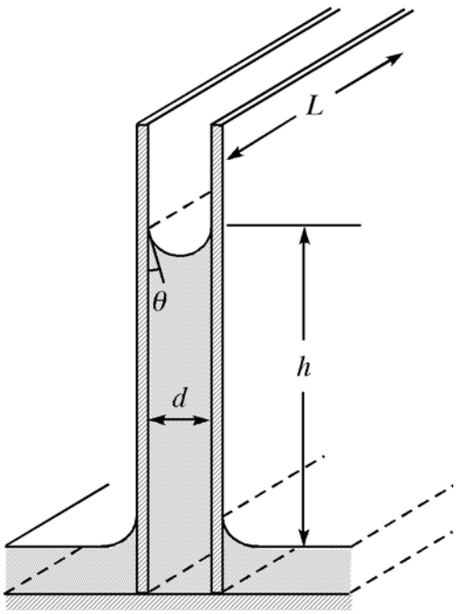

Fig. 2-54: Capillary rise between vertical flat plates. Example of a shared meniscus, with the plates held in vertical position by a supporting surface from below.

creates a pressure deficit on the right side of the free body, yielding a force

$$F = L\int_0^h \rho g y dy = \frac{1}{2}\rho g h^2 L, \tag{2.86}$$

tending to pull the plates together. Assuming the plate spacing d is very small, so that $Bo = (\rho g d^2/\sigma) << 1$, the meniscus will be a portion of a right circular cylindrical surface of radius $R_1 = d/2\cos\theta$. R_2, in the plane perpendicular to the figure, is infinite. Therefore:

$$\rho g h = \sigma\left(\frac{1}{R_1} + 0\right) = \frac{2\sigma\cos\theta}{d}, \tag{2.87}$$

so that $h = \dfrac{2\sigma\cos\theta}{\rho g d}$, and

$$\frac{F}{L} = \frac{1}{2}\rho g h^2 = \frac{2\sigma^2\cos^2\theta}{\rho g d^2}. \tag{2.88}$$

---

[67] These forces are applied at different elevations, imparting a clockwise torque to the plate, causing it to tip toward the opposite plate at the top.

If neither plate is wet by the liquid, there will be a *depression* of the liquid between them, and examination of the diagram shows that there will be a net force tending to *push* them together. In this case h is *negative*, but h^2 of course remains positive, and Eq. (2.88) is still valid.

The case in which one of the plates is wet by the liquid, while the other is not, is shown in Fig. 2-55. In this event, the meniscus has a point of inflection, which must occur at an elevation of $h = 0$ (since the surface has no curvature there). The equation of this inflected meniscus cannot be obtained in closed form, but it can be expressed in terms of elliptic integrals. The solution[68] shows that the curvature of the meniscus at the interline on

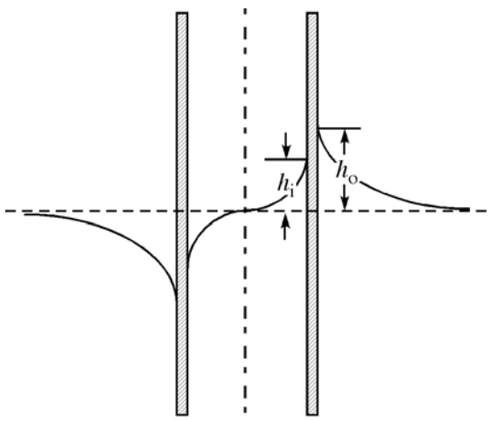

Fig. 2-55: Meniscus formed against vertical walls of opposite wettability.

the *inside* is always less than that on the outside. Thus the interline location will be further away from $h = 0$ on the outside than the inside, *i.e.*, $h_0 > h_i$, as shown. The pressure will be greater on the inside than on the outside, and the plates will be seen to *repel* each other.

The qualitative conclusions concerning the forces acting between neighboring flat plates in contact with a liquid pool also apply of course to objects of other shapes. Thus if two solid particles of the same material are floating on a liquid and happen to approach one another, a meniscus forms between them, and since the wetting is the same on both (whether it be wetting *or* non-wetting) will attract them together, leading to surface flocculation. On the other hand, if particles of two *different* materials are floating on the surface, they will be attracted if $\theta > 90°$ for both or $\theta < 90°$ for both, but if they have contact angles on opposite sides of 90°, they will be mutually repelled. If particles that are wet by the liquid come near to the edge of the containing vessel whose walls are also wet by the liquid, they will be drawn into the meniscus at the wall and accumulate there, as shown in Fig. 2-56(a). Particles un-wet by the liquid ($\theta > 90°$) will shun the edge meniscus. When the meniscus at the edge is reversed, it is the unwet particles that will be drawn to it, as shown in (b). Capillary forces are thus seen to be responsible for the clumping together of particulate materials at

---

[68] Princen, H.M., "The Equilibrium Shape of Interfaces, ...," in **Surface and Colloid Science, Vol. 2**, E. Matijevic (Ed.), pp. 1-84, Wiley-Interscience, New York, 1969.

fluid interfaces, as in the formation of “rafts” or “rags” of solid contaminants at liquid-liquid interfaces in extraction equipment, and they also explain the collection of particulates at the meniscus around the containing vessel, if the vessel walls and the particles are of like wettability.

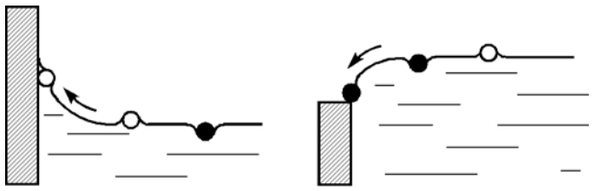

Fig. 2-56: (a) Wetted particles (○) are drawn to a wetting meniscus at the container wall while non-wetted particles (●) shun the meniscus. (b) Non-wetted particles are drawn to a non-wetting meniscus at the edge.

The action of shared menisci is also responsible for the coherence of the fibers in a paintbrush, as shown in Fig. 2-57. Immersed in either the paint or in air, the bristles are separated from one another, but when a liquid meniscus is formed between them, they are drawn together in a coherent bundle.

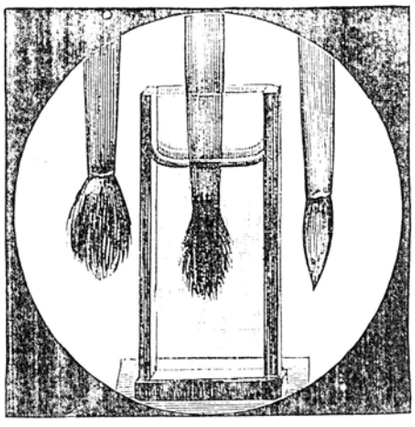

Fig. 2-57: Paint brush in air, in water and in air after being dipped in water. From [Boys, C.C., **Soap Bubbles and the Forces which Mould Them**, Doubleday Anchor Books, Garden City, NY, p. 22, 1959.]

The consequences of the forces of the type described above are widespread. The formation of liquid bridges or shared menisci is not only an important first step in the action of liquid adhesives, but also plays a vital role in the consolidation of wet-formed non-woven fibrous materials (such as paper). The enormous capillary forces developed between adjacent fibers during dry-down are believed to be sufficient to produce inter-fiber hydrogen bonding. These large capillary forces also pose a serious problem for the drying of porous media whose structural integrity one seeks to preserve. Waterlogged specimens of archeological interest, as an example, will implode if they are simply dried in air. Strategies for addressing this problem include the successive exchange of the water with volatile liquids of lower surface tension, or freezing the specimen followed by freeze- drying. One of the most successful methods, however, is the exchange of the water with supercritical carbon dioxide, followed by its drying without the

presence of a liquid interface at all. Capillary interactions between particles bound to interfaces are discussed further in Chap. 4, and more detailed descriptions, with additional references, are given by Kralchevsky and Nagayama.[69]

J. Effect of curvature on the equilibrium properties of bulk liquids: the Kelvin Effect

1. *The vapor pressure of small droplets and liquids in pores*

When a liquid is bounded at least in part by a strongly curved interface against another fluid, the phase equilibrium properties of the system are not the same as in the case when the phases are divided by a flat interface. This is a direct consequence of the required *pressure* difference that must exist across a strongly curved fluid interface. For example, the vapor pressure of a tiny droplet of radius r, p_r^s is higher than that associated with a flat surface of the same liquid, p_∞^s, the "handbook" value. Similarly, the vapor pressures of liquids in finely porous solids are different from those over flat surfaces, leading to the phenomenon of capillary condensation described below. Analogously, the solubility of tiny droplets, bubbles or solid particulates in a liquid will be different from the solubility of their larger counterparts.

Consider here a small droplet of radius r of a pure liquid. The dependence of its vapor pressure on its radius is derived as follows. At equilibrium, the fugacities of the vapor and liquid are equal, *i.e.*, $f^V = f^L$. If it is assumed that the vapor phase behaves as an ideal gas, its fugacity is equal to its vapor pressure, *i.e.*, $f^V = p_r^s$. The fugacity of the liquid, $(f^L)_{drop}$, is to be evaluated at the pressure: $p_r^s + 2\sigma/r$. It is computed by referencing it to the fugacity of the pure liquid beneath a flat interface. Recall from thermodynamics that, at constant T:

$$RTd\ln f^L = v^L dp. \tag{2.89}$$

Thus the change in fugacity of a liquid in going from its pressure when the surface is flat (p_∞^s) to the pressure inside a droplet of radius r ($p_r^s + 2\sigma/r$) is

$$\ln\frac{(f^L)_{drop}}{(f^L)_{ref}} = \int_{p_\infty^s}^{p_r^s + 2\sigma/r} \frac{v^L}{RT} dp. \tag{2.90}$$

Assuming 1) the vapor above the flat surface is also an ideal gas, so that $(f^L)_{ref} = p_\infty^s$; 2) that the liquid is incompressible, *i.e.*, v^L = constant, and 3) that $2\sigma/r >> p_\infty^s$, Eq. (2.90) becomes

---

[69] Kralchevsky, P. A., and Nagayama, K., *Adv. Colloid Interface Sci.*, **85**, 145 (2000).

$$(f^L)_{\text{drop}} = p_\infty^{\text{s}} \exp\left(\frac{2\sigma v^L}{rRT}\right). \tag{2.91}$$

Finally, equating $(f^L)_{\text{drop}}$ to the fugacity in the vapor phase around the droplet:

$$p_{\text{r}}^{\text{s}} = p_\infty^{\text{s}} \exp\left(\frac{2\sigma v^{\text{L}}}{rRT}\right), \tag{2.92}$$

known as the *Kelvin Equation*. The vapor pressure is seen to increase as droplet size decreases, as shown in Fig. 2-58, in which values for water and mercury at room temperature (20°C) are plotted. One-micron radius water

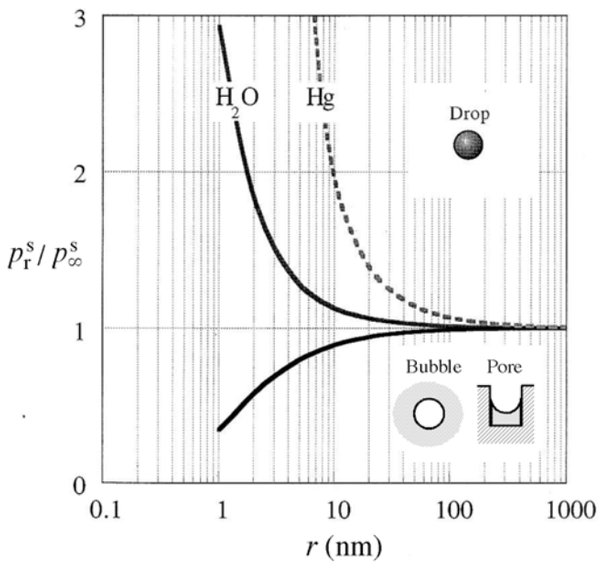

Fig. 2-58: Vapor pressure dependence for water drops or inside bubbles as a function of drop or bubble size, vapor pressure of mercury as a function of drop size.

droplets show a vapor pressure enhancement of approximately 0.1%, while those of radius one nm are increased by about a factor of three. One would not expect smaller droplets to be described by the Kelvin Equation due to the continuum assumption inherent in it. Mercury droplets of a given size show much larger vapor pressure enhancements than water since the surface tension of mercury is much larger, with a one-nm droplet of mercury showing a vapor pressure nearly 300 times its handbook value. Figure 2-58 also shows the vapor pressure of water surrounding small bubbles or inside small wetted capillaries or pores. In this case the liquid is on the con*vex* rather than the concave side of the surface, so that the vapor pressure should be *reduced* rather than increased. The Kelvin Equation is the same, but the sign of the argument of the exponential is negative. The vapor pressure of water inside a one-nm radius bubble is only about 1/3 its handbook value.

The Kelvin effect has many important consequences. In a mixture of droplets at the conditions (T, p_r^s), droplets smaller than radius r evaporate, while larger ones grow. As the small drops shrink, the driving force for their evaporation increases until they disappear. Thus raindrops "condense" out of fog, or fog evaporates, *i.e.*, "lifts." The equilibrium of a droplet of radius r to which the conditions (T, p_r^s) refer is thus an *unstable* equilibrium. The slightest addition or subtraction of material from such a drop will lead to further condensation or evaporation, respectively, until the drop has either grown to a very large size or disappeared.

2. *The effect of curvature on boiling point*

One might also consider the effect of curvature on the equilibrium temperature (boiling point) of a droplet at constant pressure, *i.e.*, constant vapor pressure p_r^s. This requires evaluation and integration of the coefficient: $\left(\frac{\partial T_r^s}{\partial r}\right)_{p_r^s}$. Using ordinary partial derivative reductions, together with the Kelvin and the Clausius-Clapeyron Equations, one obtains:

$$\left(\frac{\partial T_r^s}{\partial r}\right)_{p_r^s} = -\left(\frac{\partial p_r^s}{\partial r}\right)_{T_r^s} \Bigg/ \left(\frac{\partial p_r^s}{\partial T_r^s}\right)_r = \frac{2\sigma v^L T_r^s}{r^2 \lambda^{vap}}, \tag{2.93}$$

in which, in the last step, it has been assumed that the heat of vaporization λ^{vap} and the liquid molar volume v^L are constant and that $v^L << RT/p_r^s$. Integration of the above equation leads to:

$$T_r^s = T_\infty^s \exp\left(-\frac{2\sigma v^L}{r\lambda^{vap}}\right), \tag{2.94}$$

which is known as the *Thomson Equation* (after J. J. Thomson, elder brother of Lord Kelvin). It shows that the boiling point is lower the smaller the droplet. Thus in order to condense a vapor to droplets, the latter must be sub-cooled below the handbook value of the boiling point. A more detailed treatment of the effect of curvature on the thermodynamic properties of both pure and multicomponent systems is given by Defay *et al.*[70]

3. *Capillary condensation*

As illustrated in Fig. 2-58, the Kelvin effect leads to the condensation of vapor into finely porous solids wet by the condensate at partial pressures below the equilibrium vapor pressure. Such "capillary condensation" is often observed in the study of adsorption of vapors onto porous solids, as pictured in Fig. 2-59 for the case of nearly uniform sized pores. Assuming that the contact angle $\theta = 0°$ and that $Bo << 1$, so that the surface of the liquid is

---

[70] Defay, R., Prigogine, I., Bellemans, A, and Everett, D. H., **Surface Tension and Adsorption**, pp. 217-285, Longmans, London, 1966.

hemispherical with radius equal to that of the pores, r, vapor will begin to condense when its partial pressure reaches

$$p = p_\infty^{\mathrm{s}} \exp\left(-\frac{2\sigma v^{\mathrm{L}}}{rRT}\right). \tag{2.95}$$

Water vapor will start to condense into one-nm radius pores at a relative humidity of 0.34. At higher relative humidity, larger pores will start to fill, or when the pores fill to the top edge, further filling can occur as p is increased. All pores are completely filled only when p_∞^{s} is reached.

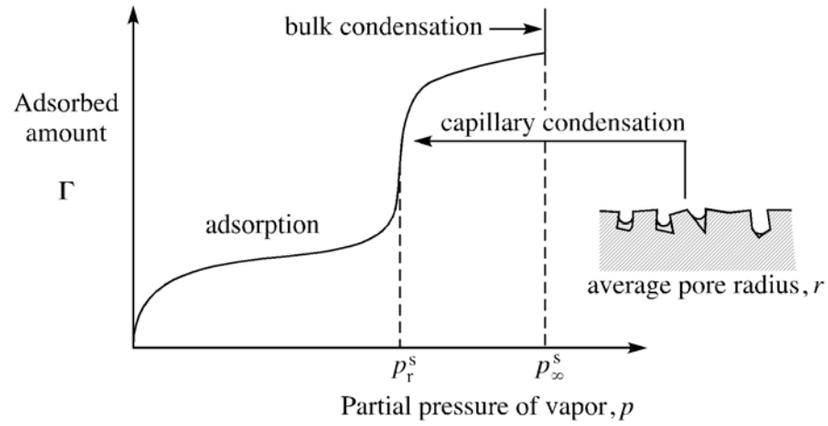

Fig. 2-59: Capillary condensation into a medium of approximately monodisperse pores.

Considerable hysteresis is nearly always found between adsorption and desorption, as shown in Fig. 2-60. One explanation may be contact angle hysteresis, discussed in Chap. 4.B, but a more generally satisfactory explanation is given in terms of pore geometry, specifically, the existence of so-called "ink bottle pores," *i.e.*, pores constricted at the top. They require

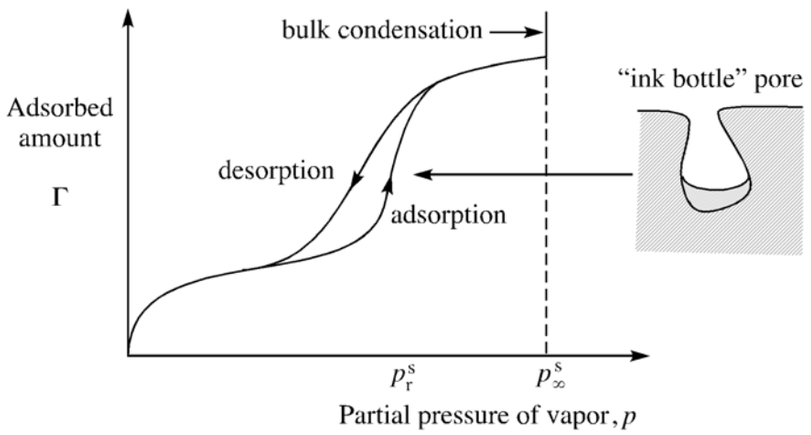

Fig. 2-60: Hysteresis associated with capillary condensation.

higher pressures to fill from the bottom up (for adsorption). For *desorption,* they start full so that the pressure must be reduced further to remove the

condensate from the smaller necks. This has received numerous qualitative confirmations by checking that the same back-calculated pore size and shape distribution is predicted for different liquids in the same solid and for the same liquid at different temperatures on the same solid specimen.

Capillary condensation shows promise for the safe storage of natural gas[71] or hydrogen[72] at reasonable pressures. Such technology is of particular currency in view of the need to provide these fuels for the operation of fuel cells. Thus major effort is currently under way to develop high porosity, high surface area materials, and a number of metal-organic framework (MOF) materials have been reported. Currently surface areas of the order of 4,500 m^2/g (!) and pore diameters of roughly 1 nm are being produced.[73]

Capillary condensation also occurs in powders (which are wettable by the condensate liquid) at the points of contact between the powder particles. The condensate then forms liquid bridges between the particles, "gluing" them together. It is thus often found that a powder that is freely flowing on a dry day may clump up and not flow evenly on a humid day. On the other hand, moisture may be introduced into the vapors surrounding the powder to induce their consolidation into clumps (called "spherical agglomeration"). The use of the Kelvin Equation, even though it is based on a macroscopic thermodynamic description of the meniscus, appears to be valid for menisci of nanoscale dimensions. Use of the surface forces apparatus (SFA) (described in Chap. 7.B.4) has revealed that it successfully describes condensate bridges of cyclohexane[74] as small as 4 nm, formed between approaching crossed mica cylinders. Monte Carlo simulations suggest that below this range, capillary condensation is preceded by accumulation of dense vapor between the surfaces, and that the snap-apart event is preceded by a gradual decrease in liquid density.[75] The liquid in the nano-meniscus is found to exist in a layered structure.

4. *Nucleation*

The phenomenon of phase change by *nucleation* and growth (binodal decomposition) is governed by the Kelvin effect.[76] Consider, for example, the condensation of liquid from a saturated vapor. For phase change to occur by this mechanism, clusters of molecules out of the vapor that subsequently grow into the new liquid phase must be formed. It is first of all clear that *supersaturation* will be required in order for this to happen. Any small cluster of molecules will have a very small radius and hence a very high

---

[71] Matranga, K. R., Myers, A. L., and Glandt, E. D., *Chem. Eng. Sci.*, **47**, 1569 (1992).

[72] Dillon, A. C., Jones, K. M., Bekkedahl, T. A., Klang, C. H., Bethune, D. S., and Heben, M. J., *Nature*, **386**, 377 (1997).

[73] Hee, K., Chae, H. K., Siberio-Pérez, D. Y., Kim, J., Go, Y., Eddaoudi, M., Matzger, A. J., O'Keefe, M., and Yaghi, O. M., *Nature*, **427**, 523 (2004).

[74] Fisher, L. R., and Israelachvili, J. N., *J. Colloid Interface Sci.*, **80**, 528 (1981).

[75] Stroud, W. J., Curry, J. E., and Cushman, J. H., *Langmuir*, **17**, 688 (2001).

[76] Zettlemoyer, A. C., (Ed.), **Nucleation**, Marcel Dekker, NY, 1969.

vapor pressure, causing it to rapidly re-evaporate. Once droplets of sufficient size do form, condensation occurs readily. Nucleation may be envisioned phenomenologically in the following way, as proposed by Becker and Döring.[77] At any degree of supersaturation, the vapor will contain a population of transitory clusters, as shown in Fig. 2-61, ranging from dimers up to nuclei whose size corresponds to the unstable equilibrium described by the Kelvin Equation. These are called *critical nuclei*, and there must be a

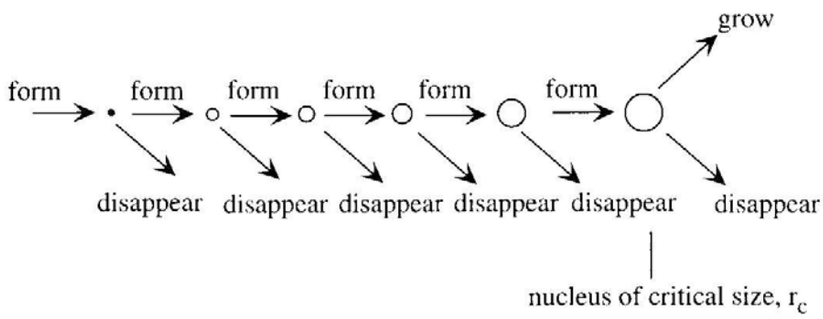

Fig. 2-61: Formation of critical nuclei leading to phase change.

sufficient number of them, *i.e.*, they must be produced at a sufficient rate, for phase change to occur at a finite rate. Only nuclei of this size or larger have a chance to grow under the prevailing conditions. The rate at which critical nuclei form is expressed by a rate equation of the Arrhenius type:

$$J(\text{nuclei/cm}^3\text{s}) = A e^{-E/kT}, \tag{2.96}$$

where E is the effective activation energy, and the pre-exponential factor A is dependent on the collision frequency of the vapor molecules. A is thus proportional to p^2, and the value given by simple kinetic theory is approximately: $A(\text{cm}^{-3}\text{s}^{-1}) \approx 10^{23} p^2(\text{mmHg}^2)$.

It is common to use as the activation energy, the change in Helmholtz free energy, ΔF, for the formation of the critical nucleus within a system at constant total volume and temperature. This is given by:

$$\begin{aligned}
\Delta F_{\text{form}} &= \Delta G_{\text{form}} - V_{\text{nuc}}\Delta p \\
&= \Delta G_{\text{phase change}} + \Delta G_{\text{area formation}} - V_{\text{nuc}}\Delta p \\
&= 0 + \sigma A_{\text{nuc}} - V_{\text{nuc}}\Delta p \\
&= 4\pi r^2\sigma - \frac{4}{3}\pi r^3\left(\frac{2\sigma}{r}\right) = \frac{4}{3}\pi r^2\sigma, \text{ so that,}
\end{aligned} \tag{2.97}$$

$$E \approx (\Delta F)_{\text{form}} = \frac{1}{3}\sigma A_{\text{nuc}} = \frac{4}{3}\pi r^2\sigma. \tag{2.98}$$

---

[77] Becker, R., and Döring, W., *Ann. Physik.*, **24**, 719 (1935).

The pressure of the vapor at a given T is p, while the equilibrium vapor pressure (over a flat surface) is p_∞^s. The degree of supersaturation is thus (p/p_∞^s), a quantity designated as x. The critical nucleus for these conditions is the one whose radius satisfies the Kelvin Equation, *i.e.*, the value of r for which $p = p_r^s$. Solving the Kelvin Equation for the radius of the critical nucleus gives

$$r = r_c = \frac{2v^L\sigma}{RT\ln x}, \tag{2.99}$$

and substituting into the expression for E:

$$E = \frac{16\pi}{3}\frac{(v^L)^2\sigma^3}{R^2T^2\ln^2 x}. \tag{2.100}$$

The presumption is that as the degree of supersaturation increases at a given T, J will increase until it reaches a value large enough to produce critical nuclei at a "sufficient rate," say one nucleus per cm^3 per second, such that $\ln J \approx 0$. (Alternatively, one may hold p constant and decrease T.) A numerical example is illustrative. Consider water vapor at 20°. The needed properties are: v^L = 18 cm^3/mole; σ = 72.7 dynes/cm; p_∞^s = 17.5 mmHg. For this situation:

$$\bullet\ A \approx 10^{23}p^2(\text{mmHg}^2) = 10^{23}(17.5)^2x^2 = 3\times10^{25}x^2 \tag{2.101}$$

$$\bullet\ E = \frac{16\pi}{3}\frac{(18)^2(72.7)^3}{(8.314\times10^7)^2(293.2)^2\ln^2 x} = \frac{3.51\times10^{-12}}{\ln^2 x}\ \text{(erg/nucleus)} \tag{2.102}$$

Then:

$$\ln J = \ln A \le \frac{E}{kT} = 58.7 + 2\ln x \le \frac{86.7}{\ln^2 x}. \tag{2.103}$$

A plot of this function is shown in Fig. 2-62, revealing that critical nuclei are formed at only a vanishingly low rate until the degree of supersaturation reaches about 3. This is in reasonable accord with experiment. It is of interest to note that the radius of the critical nucleus corresponding to these conditions is about one nm (entailing approximately 70 water molecules). The use of the continuum property of surface tension in the description of "droplets" so small would appear questionable, but the *a posteriori* agreement with experiment suggests its validity. One may similarly examine the situation in which the partial pressure of the vapor is held constant while the temperature is reduced, and similar results are found. For the above case of p = 17.5 mmHg, the temperature must be reduced to below 20°C before $\ln J \approx 0$, and condensation ensues. The degree of supersaturation required to boil a liquid, freeze a liquid or melt a solid are found by the same type of analysis. Interestingly, it is found that liquid water at atmospheric pressure may be reduced in temperature to below -30°C (!) before it freezes by the

above mechanism. A more detailed discussion of nucleation is given by Defay *et al.*[78] Numerous refinements to Becker-Döring theory have been made, but its essential features have been retained.

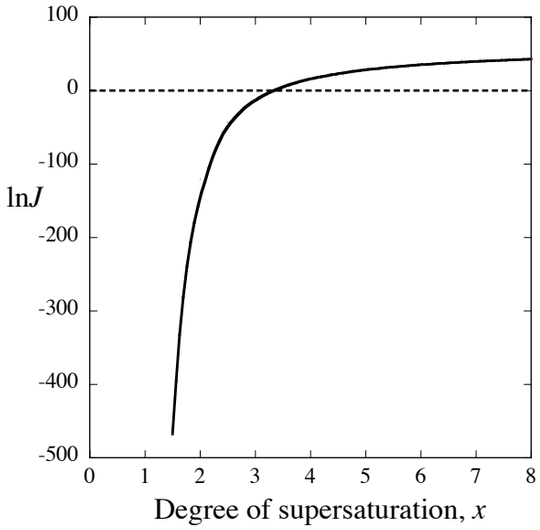

Fig. 2-62: Critical nucleus formation rate as a function of the degree of supersaturation.

What has been described above is *homogeneous nucleation*. Actual phase changes seldom occur in this way and seldom require the indicated degree of supersaturation. More likely, the initial nuclei are formed at imperfections (cracks, crevices, *etc.*) at solid surfaces that bound the system, yielding *heterogeneous nucleation*, as described further in Chap. 4. Not only is the energy required to produce a critical nucleus at such sites considerably less, but such sites may often permanently house nuclei of the new phase. Imperfections in solid surfaces, for example, are sometimes never completely evacuated of gas, so that when the system is heated, the trapped vapor pockets simply grow and are pinched off as bubbles. Boiling chips contain many of these imperfections and therefore provide smooth, even boiling (called *nucleate boiling*), as opposed to the "bumping" associated with higher degrees of superheat.

K. Thin liquid films

1. *Disjoining pressure and its measurement*

When fluids exist in the form of thin films, they are found to have properties differing from those of the same material in bulk, and such films are often unstable. To fix ideas, consider the examples shown in Fig. 2-63: (a) a foam lamella separating gas phases, (b) a liquid film between two flattened liquid droplets being drawn together, and (c) a liquid film supported on a smooth solid surface. (a) and (b) are examples of "free films," and (c) shows a "supported film." Thin films may also exist between

---

[78] Defay, R., Prigogine, I., Bellemans, A, and Everett, D. H., **Surface Tension and Adsorption**, pp. 310-348, Longmans, London, 1966.

solid surfaces ("confined films"), but discussion of such systems is deferred to Chap. 7, when the interaction between colloidal particles is discussed. Thin fluid films are often unstable in that they spontaneously seek to either thin or thicken themselves. This is because the equilibrium pressure within such a film, p_{film}, differs from the pressure that exists (or would exist) in an adjoining bulk phase of the same fluid under the same thermodynamic

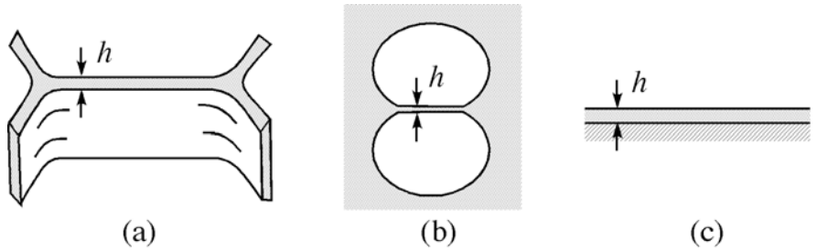

Fig. 2-63: Examples of thin films: (a) foam lamella; (b) liquid film between drops; (c) liquid film on a solid surface.

conditions (without regard to gravity). The difference is termed, originally by Derjaguin, the "disjoining pressure," $\Pi(h)$[79]:

$$\Pi(h) = p_{film} - p_{bulk}, \tag{2.104}$$

and, as indicated, is a function of the film thickness h. The function assumes different forms in different systems under different conditions, but in all cases Π tends to zero as h becomes sufficiently large (usually a few tens to hundreds of nanometers). Disjoining pressure quantifies the driving force for spontaneous thickening (if $\Pi > 0$) or thinning of a film (if $\Pi < 0$) in which, initially, $p_{film} = p_{bulk} = p$. The process of thickening is equivalent to separating (or "disjoining") its bounding surfaces; hence the name. A thermodynamically stable thin film may exist at a particular value (or values) of h in a given case, as described in more detail below, but more typically if a thin liquid film is found to exist over long periods of time (kinetic "stability") it is because free flow of the liquid between the film and an adjoining bulk phase (or potential bulk phase) of the same liquid is somehow impeded. In such cases, the disjoining pressure may be measured.

The immediate question is: what constitutes "thin?" For any particular case, one can distinguish between "bulk" films, for which h is sufficiently large that the film behaves the same as a bulk phase, and $\Pi = 0$, and "thin" films, for which $\Pi = \Pi(h) \neq 0$. Thin films may further be designated as either *thin* thin films or *thick* thin films. (These are designated in the Russian literature as α-films or β-films, respectively.) Thin thin films are adsorbed multilayers, monolayers or sub-monolayers, as examined in more detail in Chap. 3, whose thicknesses are of the order of a single nanometer or less, so that the zones of inhomogeneity of the bounding surfaces overlap. The

[79] Derjaguin, B.V., *Kolloid Zh.*, **17**, 205 (1955).

interfacial tensions of these bounding surfaces (generally not measurable properties) must be regarded as functions of film thickness for such films. Thin thin films are more usefully discussed as adsorbed layers, and their "effective thickness" is usually computed as the adsorbed amount Γ(moles/area) divided by the bulk molar density (moles/volume). For thick thin films, our major concern here, the interfacial zones do not overlap, and the interfacial tensions are the same as they would be for a bulk phase, but h is still within the reach of the integrated intermolecular forces. This generally puts thick thin films at a few hundred nm or less.

Extensive direct measurements of disjoining pressure have been reported, as in the classical work of Sheludko and coworkers,[80] who also provided an early perspective on the issue of thin liquid films. Figure 2-64 shows their technique applied to the study of free films (in which the disjoining pressure is generally negative, causing spontaneous thinning), consisting of a biconcave meniscus formed in a circular tube. A flat circular film is formed in the center, while the pressure in the bulk meniscus is

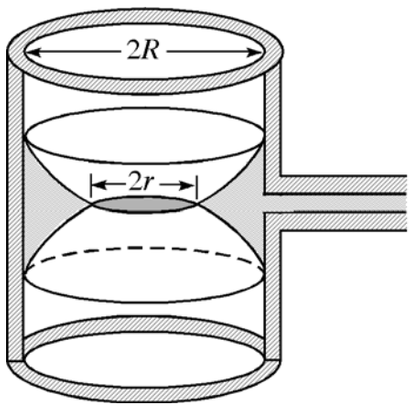

Fig. 2-64: Biconcave meniscus apparatus of Sheludko, *et al.* for measuring disjoining pressure in free thin films.

maintained at a value higher or lower (as needed to impede flow and maintain the film thickness at a desired value h) than the pressure in the film (which is the same as the ambient pressure) and accessed by means of a side port. The thickness of the film is usually measured interferometrically, and the pressure in the bulk liquid at the side required to maintain a given film thickness is recorded. Some results for $\Pi(h)$ obtained by Sheludko are shown in Fig. 2-65 for free films of aniline, and are seen to show that $\Pi(h)$ varies as $-1/h^3$. One of the ways of determining disjoining pressure in supported liquid films is by pushing a bubble of gas against the solid surface, as shown in Fig. 2-66, and monitoring the thickness of the film beneath the bubble as a function of the pressure applied to it by the bubble. This method is generally appropriate only if the disjoining pressure is positive. Reviews of relevant experimental techniques and their interpretation are given by Clunie *et al.*[81], and by Cazabat.[82]

---

[80] Sheludko, A., **Colloid Chemistry**, Elsevier, Amsterdam (1966).]

[81] Clunie, J. S., Goodman, J. F., and Ingram, B. T., "Thin Liquid Films," **Surface and Colloid**

2. *The molecular origin of disjoining pressure*

The origin of disjoining pressure can be traced to intermolecular and surface forces, integrated over finite distances, areas and volumes. As we have seen, it is a function of the film thickness h, and $\Pi(h)$, called the disjoining pressure isotherm (since it is usually obtained at constant temperature), depends on the makeup of the film, the adjoining bulk phases and the interfaces between them. If the film finds itself between two like

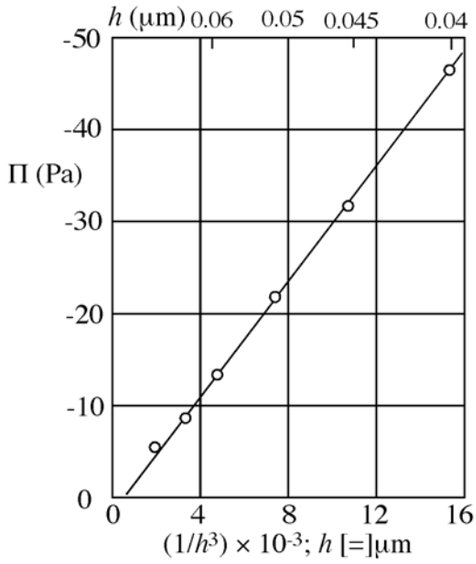

Fig. 2-65: Disjoining pressure isotherm $\Pi(h)$ in a free liquid film of aniline. After [Sheludko, A., **Colloid Chemistry**, pp. 173-207, Elsevier, Amsterdam (1966).]

phases, as in Fig. 2-64, it is usually (but not always) negative, whereas if it is between a condensed phase on one side and a gas on the other, as in Fig. 2-66, it is sometimes (but perhaps more often not) positive, and in other cases may be positive over some ranges of h and negative over others. Further discussion of the formation and properties of thin liquid films are given by Derjaguin *et al.*[83] and de Gennes.[84, 85]

As an example, consider the case of a thin supported film of non-volatile liquid on a smooth, horizontal solid surface, and a gas above it, as shown in Fig. 2-63(c). One may compute the disjoining pressure isotherm $\Pi(h)$ for the case when the origin of the disjoining pressure is the attractive van der Waals interaction of the molecules in the liquid film with the solid substrate, which can be regarded as a semi-infinite block. As seen earlier, the van der Waals interaction between a single molecule in the liquid L (a

---

Science, Vol. 3, E. Matijevic (Ed.), pp. 167-239, Wiley-Interscience, New York, 1971.

[82] Cazabat, A. M., in **Liquids at Interfaces**, J. Charvolin, J.F. Joanny and J. Zinn-Justin (Eds.), pp. 372-414, Elsevier, Amsterdam, 1990.

[83] Derjaguin, B. V., Churaev, N. V., and Muller, V. M., **Surface Forces**, V. I. Kisin, Trans., J. A. Kitchner (Ed.), Consultants Bureau, New York, 1989.

[84] de Gennes, P., *Rev. Mod. Phys.*, **57**, 827 (1985).

[85] de Gennes, P., in **Liquids at Interfaces**, J. Charvolin, J.F. Joanny and J. Zinn-Justin (Eds.), pp. 273-291, Elsevier, Amsterdam, 1990.

distance z from the solid surface) and the solid S half-space per unit area is, in accord with Eq. (2.11):

$$\Phi^{\sigma}_{\text{molec-solid}} = -\frac{\pi B_{\text{SL}}\rho_{\text{S}}}{6z^3}, \tag{2.105}$$

where the B_{SL} is the cross van der Waals interaction constant between the molecule of the liquid and the molecules of the solid, and ρ_{S} is the molecular density of the solid. To obtain an expression for the total interaction energy between all the molecules in the liquid film (per unit area) and the solid, $\Phi^{\sigma}_{\text{SL}(h)}$, one must integrate over all the molecules in the liquid (per unit area):

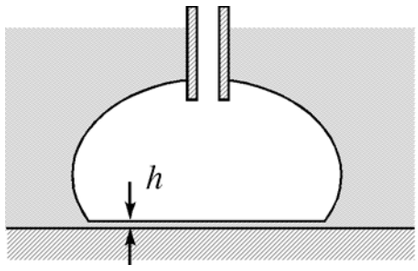

Fig. 2-66: Measurement of positive disjoining pressure in a supported liquid film.

$$\Phi^{\sigma}_{\text{SL}(h)} = -\frac{\pi B_{\text{SL}}\rho_{\text{S}}\rho_{\text{L}}}{6}\int_{D_0}^{h}\frac{\mathrm{d}z}{z^3} = \frac{\pi B_{\text{SL}}\rho_{\text{S}}\rho_{\text{L}}}{12}\left(\frac{1}{D_0^2}-\frac{1}{h^2}\right) \tag{2.106}$$

where "D_0", as before, is the distance of closest approach between the molecules of the liquid and the solid. It is evident that if h is large, $1/h^2 \rightarrow 0$, and $\Phi^{\sigma}_{\text{SL}(h)}$ is a constant with h. But for thin films, the second term is not negligible, *i.e.*, even the outermost molecules of the film "feel" the influence of the force field of the solid. The prefatory constant in Eq. (2.106) may be written in terms of the cross Hamaker constant, A_{SL} (see Eq. (2.23)) to give

$$\Phi^{\sigma}_{\text{SL}(h)} = \frac{A_{\text{SL}}}{12\pi}\left(\frac{1}{D_0^2}-\frac{1}{h^2}\right). \tag{2.107}$$

To obtain the *excess* energy of molecular interactions in the film resulting from its contact with the solid, one must subtract the energy of interactions within the film itself, $\Phi^{\sigma}_{\text{LL}(h)}$ to obtain

$$\Phi^{\sigma}_{\text{E}(h)} = \frac{(A_{\text{SL}}-A_{\text{LL}})}{12\pi}\left(\frac{1}{D_0^2}-\frac{1}{h^2}\right) = -\frac{A_{\text{eff}}}{12\pi}\left(\frac{1}{D_0^2}-\frac{1}{h^2}\right), \tag{2.108}$$

where $A_{\text{eff}} = (A_{\text{LL}} - A_{\text{SL}})$, the effective Hamaker constant for the system. Treating $\Phi^{\sigma}_{\text{L}(h)}$ as a free energy, the excess pressure in the film relative to that in a bulk layer, *i.e.*, Π, may be obtained for van der Waals materials as

$$\Pi(h) = -\frac{\partial(\Phi^{\sigma}_{\text{E}(h)}\cancel{\mathcal{A}})}{\partial V} \equiv -\frac{\cancel{\mathcal{A}}}{\cancel{\mathcal{A}}}\left(\frac{\partial\Phi^{\sigma}_{\text{E}(h)}}{\partial h}\right) = -\frac{A_{\text{eff}}}{6\pi h^3}, \tag{2.109}$$

where $\mathcal{A}$ is the surface area. The form of Eq. (2.109) is in agreement with the data shown in Fig. 2-65 for free films of aniline, but in this case, since no solid substrate is present, $A_{eff} = A_{LL}$. The Hamaker constant A_{LL} for a van der Waals liquid is always positive, so the disjoining pressure is negative for all h-values. Therefore a free film of van der Waals liquid will spontaneously thin.

As indicated in Eq. (2.108), for a liquid film supported on a solid substrate, the effective Hamaker constant of the film is given by

$$A_{eff} = A_{LL} - A_{SL}. \tag{2.110}$$

For van der Waals materials, A_{SL} is given by the geometric mean mixing rule:

$$A_{SL} = \sqrt{A_{SS} A_{LL}}\ , \text{ so that} \tag{2.111}$$

$$A_{eff} = \sqrt{A_{LL}}\left(\sqrt{A_{LL}} \le \sqrt{A_{SS}}\right). \tag{2.112}$$

Thus A_{eff} is either negative (if $A_{SS} > A_{LL}$), yielding a fully wetting film of finite thickness, or positive (if $A_{SS} < A_{LL}$), causing the film to spontaneously thin itself.

It has been argued that as the film thickness h approaches zero, $\Pi(h)$ should approach the spreading coefficient, $S_{L/S}$, as in Eq. (2.49), [86] *i.e.*,

$$\Pi(h)\big|_{h\to 0} = S_{L/S}. \tag{2.113}$$

It is useful here to digress briefly to consider the general situation in which a fluid film (1) is separated by phases of different materials (2) and (3). The latter may be gases, liquids immiscible with (1) or solids, or any combination thereof. The effective Hamaker constant of the film for computation of the disjoining pressure isotherm is given by[87]

$$A_{eff} = A_{23} + A_{11} - A_{21} - A_{31}. \tag{2.114}$$

The last two terms account for the interaction of the film with its adjoining phases, while the first two account for the interactions of the adjoining phases with each other and the film molecules with themselves. Applying the geometric mean mixing rule, Eq. (2.111), yields:

$$A_{eff} = \left(\sqrt{A_{33}} - \sqrt{A_{11}}\right)\left(\sqrt{A_{22}} - \sqrt{A_{11}}\right), \tag{2.115}$$

from which it is easy to see the various combinations that lead to either positive or negative values for A_{eff}. In applying Eq. (2.115), the Hamaker

---

[86] Brochard-Wyart, F., di Meglio, J.-M., Quéré, D., and de Gennes, P.-G., *Langmuir,* **7**, 335 (1991).

[87] Israelachvili, J. N., **Intermolecular & Surface Forces**, 2nd Ed., p. 200, Academic Press, London, 1992.

constant is generally taken to be zero for gas phases, due to the low molecular density in such media. Thus if the film is bound on both sides by gases, $A_{22} = A_{33} = 0$, and $A_{\text{eff}} = A_{11}$. If it is bound on one side by a condensed phase (2) and on the other by a gas (3), $A_{\text{eff}} = \sqrt{A_{11}}\left(\sqrt{A_{11}} - \sqrt{A_{22}}\right)$, as in Eq. (2.112).

In the above it has been tacitly assumed that only van der Waals interactions are relevant. Other intermolecular forces however (hydrogen bonds or other donor-acceptor interactions, solvent structuring effects, anomalous density profiles near the wall, *etc.*), may also contribute to the disjoining pressure, adding additional terms to the $\Pi(h)$ function. These may be especially important as $h \to 0$. Hydrogen bonding in water yields a term of the form

$$\Pi_{\text{H}}(h) = \frac{C_{\text{H}}}{h}, \tag{2.116}$$

where C_{H} is a constant. Solvent structuring effects are manifest near solid boundaries, in which there may be a strong, essentially chemical, affinity of the liquid for the solid surface. This is manifest at the boundary between water and strongly hydrophilic surfaces, such as quartz. The squeezing out of this final layer (often a monolayer) is strongly resisted, and has been approximated as[88]

$$\Pi_{\text{s}}(h) = K_{\text{s}} \exp(-h/\lambda_{\text{s}}), \tag{2.117}$$

where K_{s} is very large ($\approx 10^7$ N/m^2), and λ_{s} is of the order of a few Å (very short-ranged). In the absence of hydration, a strong "solvent structuring effect," for which $\lambda_{\text{s}} \to 0$, just a manifestation of Born repulsion, will be evident. Thus every disjoining pressure isotherm for a film bounded at least on one side by a solid will exhibit a steep positive branch as $h \to 0$. For a confined thin liquid film between two solid surfaces, successive layers of liquid must be squeezed out as the film thins. This may in principle lead to an oscillatory disjoining pressure, as shown in Fig. 2-67, in which the wavelength of the oscillation is the effective molecular diameter.

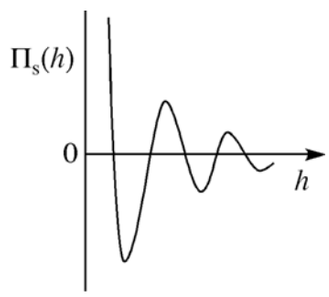

Fig. 2-67: Solvent structuring term of the disjoining pressure for a confined liquid film between smooth solid surfaces. The wavelength of the oscillations corresponds to the diameter of the solvent molecules.

[88] Derjaguin, B. V., and Churaev, N. V., *Langmuir*, **3**, 607 (1987).

Another possible contributor to the disjoining pressure is electrostatic forces. These may exist, for example, in an aqueous thin film containing an ionic surfactant adsorbed to both the bounding surfaces, as pictured in Fig. 2-68. Even a clean water surface against air possesses a negative surface charge. If the opposing surfaces possess diffuse electrical double layers (see Chap. 6), *i.e.*, adjacent clouds of ions opposite in charge to that of the surfaces, their overlap contributes to the total disjoining pressure with a term of the form:

$$\Pi_{el}(h) = K_{el} \exp(-\kappa h), \tag{2.118}$$

where K_{el} and κ are constants dependent primarily on the charge density at the surfaces and the ionic content and dielectric constant of the film. The bounding surfaces may also possess dissolved polymer adlayers, leading to

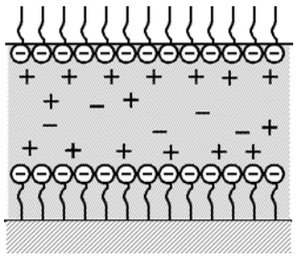

Fig. 2-68: Electrostatic forces due to presence of charges at the surfaces of the film. Here they are due to adsorbed ionic surfactant.

"steric" repulsive interactions as the adlayers overlap. Still other factors may contribute. For example, the Helfrich Equation for the free energy associated with the bending of an interface, Eq. (2.59), has been used to compute forces arising from the mutual undulation of opposing structured surfaces of thin films. Such undulation forces are found to be proportional to the Helfrich first modulus k_1, and inversely to the square of the film thickness. This bending force contribution, when relevant, must be added to the disjoining pressure expression.

3. *The disjoining pressure isotherm*

The disjoining pressure may be regarded as the sum of the various contributions to it, as described above.

$$\Pi_{tot}(h) = \Pi_{vdW}(h) + \Pi_{s}(h) + \Pi_{H}(h) + \Pi_{el}(h) + \Pi_{steric}(h) + \ldots \tag{2.119}$$

Depending on the various contributions to $\Pi(h)$, the function may take on a variety of different forms, but such isotherms are usually one of the four types shown in Fig. 2-69, with inserts shown for liquid films supported on a solid substrate. If the film is described entirely in terms of van der Waals interactions, the disjoining pressure curve takes the form shown in Fig. 2-69(a), Type I, if the effective Hamaker constant is negative, and (b), Type II, if it is positive. In the latter case, the steep repulsive force associated with squeezing out the last monolayer or so of the film is included. Even for a free film, there may be such repulsion as the final molecules in the film jockey for position. If not, the curve follows the dashed line. Type I isotherms are exemplified by supported films on solid substrates, if the

Hamaker constant for the solid is greater than that for the liquid, so that A_{eff} is negative, in accord with Eq. (2.112). Examples would be alkanes, for example octane, $A_{\text{LL}} = 4.50\times10^{-20}$ J, on fused silica, $A_{\text{SS}} = 6.55\times10^{-20}$ J, so $A_{\text{eff}} = \sqrt{4.50}\left(\sqrt{4.50} - \sqrt{6.55}\right)\times10^{-20} = -0.93\times10^{-20}$ J. Type II films are exemplified by free liquid films in air, such as the aniline film shown in Fig. 2-65, or supported films such as the case of octane on a Teflon substrate (with $A_{\text{ss}} = 3.80\times10^{-20}$ J).

For the case with both van der Waals (with a positive effective Hamaker constant) and electrostatic effects:

$$\Pi(h) = \Pi_{\text{s}}(h) + \Pi_{\text{vdW}}(h) + \Pi_{\text{el}}(h) = K_{\text{s}}\exp(-h/\lambda_{\text{s}}) - \frac{A_{\text{eff}}}{6\pi h^3} + K_{\text{el}}\exp(-\kappa h), \quad (2.120)$$

in which the ever-present solvent structuring term is included. This can lead to disjoining pressure curves of the type shown in Fig. 2-69 (c), Type III, or (d), Type IV, as exemplified by films of water on quartz.[89]

The fact that disjoining pressure isotherms of the type shown in Fig. 2-69 can be computed does not mean that the complete curves can all be observed in the laboratory. If a liquid film is in unimpeded contact with a reservoir of bulk liquid, it will spontaneously thicken or thin until it reaches a state of stable equilibrium. Such states correspond to local minima in the free energy of the system. The (Helmholtz) free energy of the thin film system, per unit area, may be written as

$$F^{\sigma}(h) = F_0^{\sigma} + \Phi^{\sigma}_{\text{E}(h)}(h), \quad (2.121)$$

where F_0^{σ} is a constant, and it is recalled from Eq. (2.108) that $\Phi^{\sigma}_{E(h)}(h)$ is the excess energy of the system due to its thin film status. In accord with Eq. (2.109), the disjoining pressure is obtained as the negative derivative, in this case, of $F^{\sigma}(h)$:

$$\Pi(h) = -\left[\frac{\partial F^{\sigma}(h)}{\partial h}\right]_{T,p}. \quad (2.122)$$

Equilibrium states are those for which the free energy derivative is zero, and hence disjoining pressure is zero. *Stability* then requires that the second derivative of the free energy be positive, *i.e.*,

$$\left[\frac{\partial^2 F^{\sigma}(h)}{\partial h^2}\right]_{T,p} = -\frac{d\Pi(h)}{dh} > 0, \text{ or } \frac{d\Pi(h)}{dh} < 0. \quad (2.123)$$

Thus thin film stable equilibrium states are limited to those where the disjoining pressure isotherm crosses or touches the $\Pi = 0$ line with a negative slope. These states are identified in Fig. 2-69.

---

[89] Derjaguin, B. V., and Churaev, N. V., "Properties of Water Layers Adjacent to Interfaces, " in **Fluid Interfacial Phenomena**, C. A. Croxton (Ed.), Chap. 15, Wiley, New York, 1986.

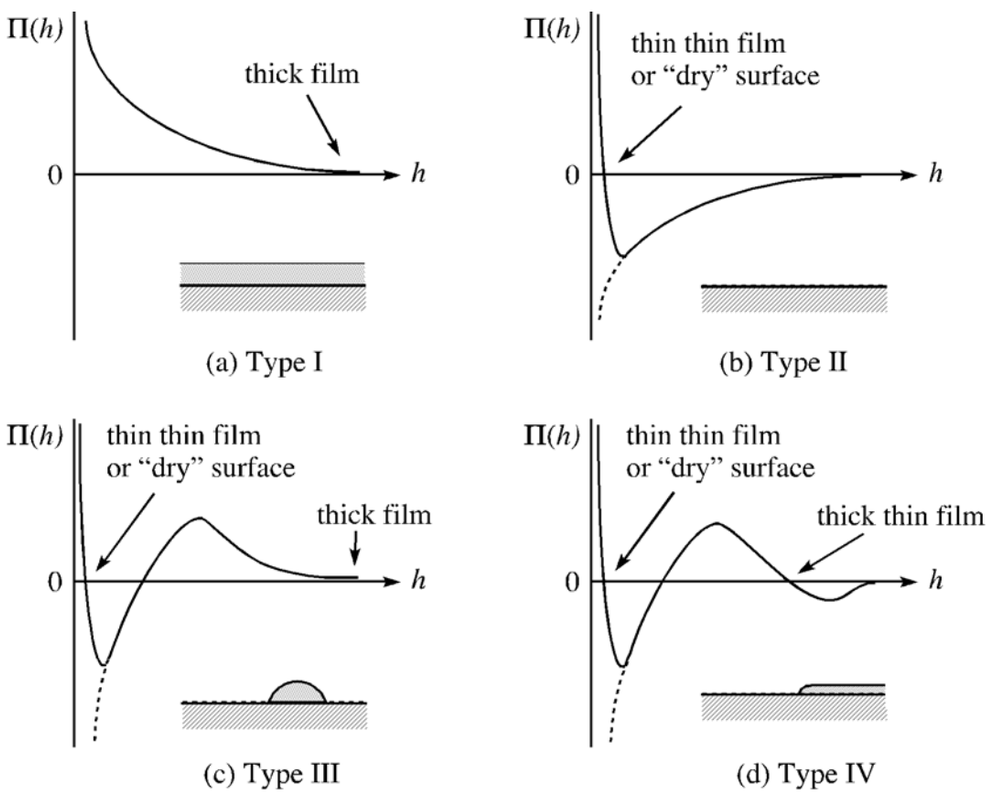

Fig. 2-69: Examples of disjoining pressure isotherms. (a) Type I: Spontaneously thickening film of van der Waals liquid on a solid or liquid substrate; (b) Type II: Spontaneously thinning film of van der Waals liquid on a solid or liquid substrate, or free liquid film; (c) Liquid film with both positive and negative contributions to the disjoining pressure, leading to possible coexistence of a thin thin film with bulk liquid; (d) Liquid film with both positive and negative contributions to the disjoining pressure, leading to possible coexistence of a thin thin and a thick thin film.

If the solid surface is finite in lateral extent, and the disjoining pressure is positive, as in Fig. 2-69 (a), the film will spontaneously thicken until $\Pi(h) \rightarrow 0$, and then level itself (even in the absence of gravity) due to surface tension, except at the edges of the solid. If $\Pi(h) < 0$, as in Fig. 2-69 (b), the film will *thin* itself until $\Pi(h) \rightarrow 0$ (essentially to $h \approx 0$), with any excess liquid left in the form of drops making a distinct contact angle with the "dry" solid. For the more complex disjoining pressure functions shown in Fig. 2-69 (c) and (d), it is possible to have an equilibrium, flat, horizontal thin film coexisting with bulk liquid, or even flat films of different thicknesses coexisting with each other.

In experiments such as those suggested in Figs. 2-64 and 2-66, as well as others,[90] particularly those in which a drop or bubble is pushed against a wetted solid substrate using the apparatus of atomic force microscopy,[91]

---

[90] Bergeron, V. B., Fagan, M. E., and Radke, C. J., *Langmuir*, **9**, 1704 (1993); Bergeron, V. B., and Radke, C. J., *Colloid Polym. Sci.*, **273**, 165 (1995).

[91] Basu, S., and Sharma, M. M., *J. Colloid Interface Sci.*, **181**, 443 (1996).

most of the isotherms of the type shown in Fig. 2-69 may in principle be observed and measured, either in a dynamic experiment or one in which the flow of liquid between the film and its adjacent bulk liquid is restricted or controlled. An interesting exception occurs for Types III or IV if one attempts to either reduce the thickness of the film or increase its internal capillary pressure beyond the point where the local maximum in disjoining pressure equilibrium exists, the film will undergo a spinodal decomposition to a thin thin film in coexistence with either bulk liquid droplets or thick thin films.

4. ***The augmented Young-Laplace Equation***

If one considers gravity in the case of a wetting film on a solid surface that is not horizontal, there may exist a final equilibrium situation in which a thin film coexists with bulk liquid, even for a Type I disjoining pressure isotherm. For example, consider the meniscus of a wetting liquid ($\theta = 0°$) against a vertical flat wall, as shown in Fig. 2-70. Considering disjoining pressure, this is somewhat more complicated than has been described earlier (in Fig. 2-31). In describing the meniscus shape, one must now write:

$$p_{\text{liq}} - p_{\text{vap}} \equiv \Delta p = +\sigma\kappa - \Pi(h), \tag{2.124}$$

which takes account of both the curvature and the disjoining pressure. First introduced by Derjaguin,[92] it is known as the *augmented* Young-Laplace Equation. For the case shown (for a wetting van der Waals liquid on a vertical substrate), it takes the form:

$$\rho g h = -\sigma \frac{y''}{\left[1 + (y')^2\right]^{3/2}} + \frac{A_{\text{eff}}}{6\pi x^3}, \tag{2.125}$$

The complete solution of this equation yields the detailed shape of the meniscus in the region of the nominal interline, but it is found to differ only microscopically from the solution obtained ignoring disjoining pressure, shown in Fig. 2-31 for a vertical surface. A thin film, however, extends far higher. In this region the meniscus becomes essentially flat so that the curvature term in the augmented Young-Laplace Equation may be neglected, leading to:

$$x = h \approx \left(\frac{A_{\text{eff}}}{6\pi \rho g y} \right)^{1/3}. \tag{2.126}$$

As an example, for octane against quartz, $A \approx 6 \times 10^{-20}$ J and $\rho = 0.7$ g/cm^3, so that at a distance of $y = 1$ cm above the flat liquid level, a film of thickness $h \approx 20$ nm exists. The boundary region between films of different

---

[92] Derjaguin, B. V., Churaev, N. V., and Muller, V. M., **Surface Forces**, Plenum Press, New York, 1987.

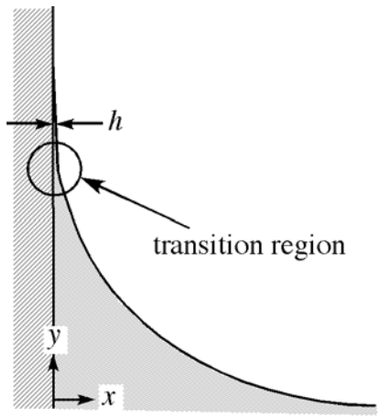

Fig. 2-70: Wetting film against a vertical wall.

thickness is in general described by the solution to the augmented Young-Laplace Equation. Further details are given in numerous references.[93,94,95]

Supported thin films are discussed further in the context of spreading phenomena in Chap. 4, and free thin films get more attention in Chap. 8 in the description of emulsions and foams. Confined films, *i.e.*, fluids between solid surfaces, are discussed further in the context of interactions between colloid particles in Chap. 7.

---

[93] Davis, H. T., **Statistical Mechanics of Phases, Interfaces, and Thin Films**, pp. 370-377, VCH, New York, 1996.

[94] Starov, V. M., Velarde, M. G., and Radke, C. J., **Wetting and Spreading Dynamics**, Chap. 2, CRC Press, Boca Raton, 2007.

[95] Hirasaki, G. J., *J. Adhesion Sci. Tech.*, **7**, 285 (1993).

Some fun things to do: Experiments and demonstrations for Chapter 2

At the end of this and the remaining Chapters, are suggestions for simple experiments to help illustrate the concepts of the chapter. Little or no instrumentation, or expensive or hard-to-get materials are required. Most experiments are suitable for classroom demonstration, either with direct observation or by projection onto a screen using an overhead projector or a camcorder connected to a video projector.

1. *The thinness of clean interfaces*

According to Fresnel's Law, light reflected at or near Brewster's angle (53° for water) from an interface *that is thin relative to its wavelength* (≈ 600 nm) will be plane polarized. This is why polarized sunglasses are able to block reflected glare from horizontal surfaces. The thinness of a clean water surface is demonstrated by reflecting the beam from a laser pointer from the surface of water in a shallow Petri dish. The laser beam from the pointer is plane polarized, so as it is rotated, an orientation will be obtained in which little or no reflection will occur.

Materials:

- laser pointer (A Class IIIa red laser pointer with output power 5 mW and beam diameter 4.5 mm at aperture is recommended. Care should be exercised not to shine this near anyone's eyes.)
- small Petri dish with a flat black piece of paper at the bottom (to avoid reflections from the bottom surface) and filled with clean water.
- small ring stand and clamp
- white cardboard screen

Procedure:

Mount the pointer in the ring stand clamp as shown in Fig. E2-1, and direct the beam at the surface at ≈ 50° and note the intensity of

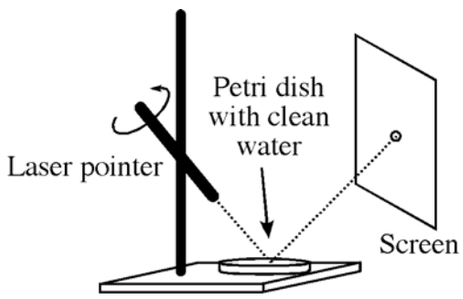

Fig. E2-1: Demonstration of Fresnel's Law for a clean water interface.

the reflected spot on the screen as the pointer is rotated. It may be necessary to use tape to keep the pointer turned on as this is done. Note the beam spot nearly disappears at a particular angle, showing the polarizing ability of the surface and hence its thinness.

2. *Soap bubbles and films*[96]

Soap films are layers of water stabilized by surfactant on each side. Their thickness is of the order of a few micrometers to two mm, small enough that structures composed of them are largely free of gravitational forces. They can therefore be used to produce surfaces of constant curvature.

Materials:

- 250 mL of soap solution: a 50/50 v/v solution of dishwashing detergent (*e.g.*, Joy®, Dawn®, Palmolive®) in a 250 mL beaker
- 3×3×1/4 in. glass plate (with edges smoothed)
- 4 in. piece of ½ in. Tygon® tubing
- 2 in. or larger diameter plastic ring (from a bubble toy kit)
- 10×5×1/8 in. plastic (Plexiglas®) sheet bent 180°, as shown in Fig. E2-2, to yield a spacing of $\approx$ 2 cm.
- cubical wire frame, about 2×2×2 in. This can be soldered together from bent pieces of wire. 16 AWG (American Wire Gauge) ($\approx$ 1.3 mm diameter) galvanized bailing wire is about right.
- capful of rubbing alcohol (70% isopropyl alcohol)

Procedure:

1) Dip the plastic ring in the beaker of soap solution and gently blow, as shown in Fig. 2-14, to demonstrate requirement of a pressure jump Δp required to sustain a non-zero curvature.

2) Pre-moisten the surface of the glass plate with the soap solution; then use the Tygon® tube to blow a bubble onto the glass surface. It will create a perfect hemisphere, as shown in Fig. E2-2.

3) Pre-moisten the inside surfaces of the bent plastic sheet, and use the Tygon® tube to blow a bubble that spans the gap between the plate surface to create a perfect cylindrical bubble, as shown in Fig. E2-2. Multiple bubbles can be blown into this space to create a variety of right cylindrical surfaces.

4) Dip the cubical wire frame in the beaker of soap solution. If carefully withdrawn, it produces a pattern of soap films as shown in Fig. 2-37. These can be selectively broken carefully using your fingers or using a sharpened pencil tip dipped in the capful of rubbing alcohol

---

[96] A wealth of additional experiments on soap films and bubbles can be found in:
1) Boys, C. V., **Soap Bubbles, Their Colours and the Forces Which Mould Them**, Dover Pub., New York, 1959.
2) Mysels, K. J., Shinoda, K., and Frankel, S., **Soap Films: Studies of their Thinning**, Pergamon Press, New York, 1959.
3) Isenberg, C., **The Science of Soap Films and Soap Bubbles**, Dover Pub., New York, 1992.

to produce a variety of compound and single saddle shaped surfaces of zero mean curvature, illustrating solutions to Plateau's problem.

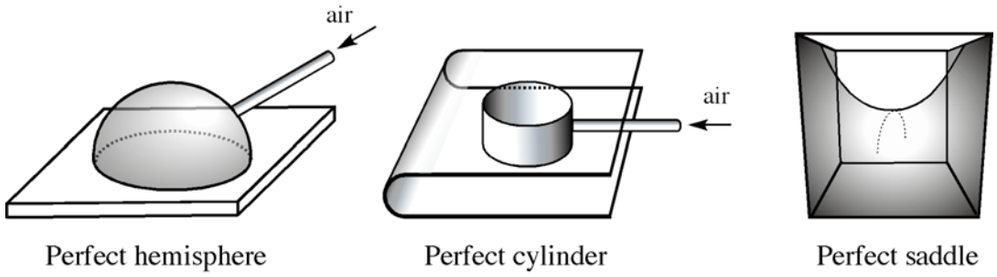

Fig. E2-2: Some soap film structures.

3. *Liquid bridges*

A small liquid drop may exert a considerable adhesive force between solid objects that it wets, as shown schematically in Fig. 2-51 for a pair of flat plates. Equation (2.76) shows that the principal force of attraction depends directly on the cosine of the contact angle, θ. For water on glass, $\theta \to 0°$, the force is maximum. A single drop of water will produce an adhesive force that makes the plates difficult to pull apart. (It must be noted that part of the attractive force is the viscous resistance to thickening of the water film.) For water on Teflon®, $\theta \approx 110°$, $\cos\theta < 0$ so the adhesive force has a negative pressure component and only a weak positive interline force, and a net value near zero. For a fair test, make sure the Teflon® surfaces are as smooth as possible. The water bridge between glass and Teflon has a zero pressure component and only a very weak attractive interline force.

Materials:

- two clean glass plates, 3×3×1/4 in. (with edges smoothed)
- two smooth Teflon® plates, 3×3×1/4 in.
- small container of water, with drop-dispensing tip

Procedure:

Place a single drop of water at the center of one of the glass plates, and place the second plate on top. Try to pull them apart, as in Fig. E2-3. Do the same thing with the Teflon® plates, as well as one glass and one Teflon plate. The differences will be very noticeable. More interesting results can

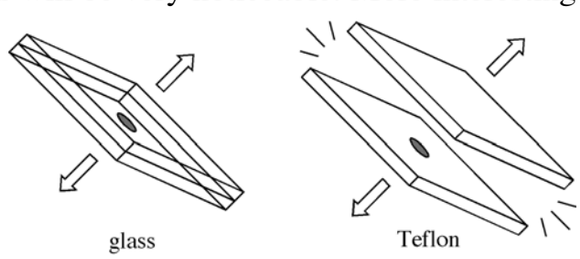

Fig. E2-3: Liquid bridge adhesion of water between glass *vs.* Teflon® plates.

be obtained by substituting rubbing alcohol (70% isopropyl alcohol in water) for water.

4. *Shared menisci*

Equation (2.88) suggests that solid objects of like wettability, either wet or non-wet, will be attracted to one another by capillary forces when they share a liquid meniscus. Thus particles of the same type floating or suspended at a water surface should be drawn together and stick. Particles of opposite wettability characteristics will be repelled from one another. Particles will also be either attracted or repelled from the meniscus at the container wall depending on whether the meniscus at the wall shows the same shape, *i.e.* concave upward or downward, as it does against the particles.

Materials:

- small Petri dish half filled with clean water.
- cork particles, approximately 2-4 mm diameter
- Teflon® shavings, approximately 2-4 mm diameter
- forceps
- plastic water bottle with delivery tube.
- overhead projector

Procedure:

Gently place a few cork particles on the surface of water in the Petri dish at least several mm apart from one another. This can be done with the Petri dish placed on an overhead projector focused on the particles and projected on the screen. Then gently blow on the surface to bring the particles close to one another, and watch them snap together. Note also how they are drawn to the wetted glass edge of the dish. Then gently place a few Teflon particles on the surface. (This must be done carefully as Teflon® is heavier than water and will sink if submerged.) These particles also clump together, but are seen to repel the cork particles and to stay away from the glass meniscus. Next, gently increase the water level in the dish until it bulges over the rim, creating a concave downward meniscus. Observe the cork particles leaving the meniscus and the Teflon particles moving into it, as shown in Fig. 2-56 and Fig. E2-4.

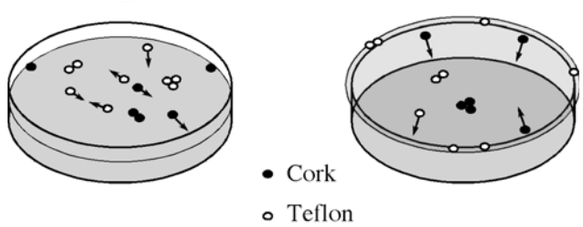

Fig. E2-4: Wettable (cork) and unwettable (Teflon) particles on a water surface.